Quantifying water use and rainfall partitioning of dominant tree species in a post-mined landscape in the Athabasca Oil Sands Region, Alberta

by
Sarah Fettah

A thesis
presented to the University of Waterloo
in fulfillment of the
thesis requirement for the degree of
Master of Science
in
Geography (Water)

Waterloo, Ontario, Canada, 2020

Author's Declaration

I hereby declare that I am the sole author of this thesis. This is a true copy of the thesis, including any required final revisions, as accepted by my examiners.

I understand that my thesis may be made electronically available to the public.

Abstract

Large-scale oil sands mining has caused significant disturbances to forest and wetland ecosystems in the Western Boreal Plains of Northeastern Alberta. Provincial and federal laws mandate restoration of these systems in an attempt to return the landscape to pre-disturbed conditions. Reclaiming these important ecosystems has faced many challenges including re-vegetation of uplands to a state of self-sustainability and productivity. The Nikanotee Fen Watershed in Fort McMurray, Alberta, is a post-mined landscape consisting of a constructed upland-fen peatland connected through runoff and groundwater. The design of these systems' impacts many components of the ecosystem, including vegetation growth and productivity. Changes in soil moisture dynamics at the site have been attributed to the development in soil and vegetation cover in the upland, leading to significant changes in the ecosystem. The trajectory of reclaimed sites depends on the population of tree species, such as conifers or broadleaf. Development of the tree canopy will lead to increases in precipitation interception and transpiration, ultimately reducing water available for recharge to the adjacent wetland. Characterizing vegetation distribution and composition and their impacts on the water balance may help improve reclamation techniques for future projects. Understanding the functioning of constructed ecosystems and the controls of tree communities on water use will feedback to influence soil moisture dynamics. Soil moisture dynamics dictate water availability for tree growth, recharge and system function, ultimately influencing the uplands ability to support low-lying systems. The objectives of the study are to assess the trends in transpiration of dominant tree species throughout the growing season; quantify throughfall, stemflow and interception of dominant tree species and understand the role they play in intercepting precipitation and its impact on near-surface soil moisture regime and tree water use.

The study used a variety of meteorological, hydrological and biometric methods to assess the suitability of dominant tree species used in reclamation projects. To examine the variability in tree water use across the upland, vegetation surveys were completed, and several dominant tree species were instrumented with Stem Heat Balance sap flow sensors to determine individual species' transpiration rates. Rainfall was partitioned into interception, throughfall and stemflow alongside monitoring soil moisture dynamics and soil water potential to determine the plant available water. Results indicate that tree transpiration is a dominant control on water use at the site averaging 51% of total evapotranspiration and is controlled by water availability. Canopy interception is beginning to play an important role in partitioning growing season rainfall with broadleaf tree species, *Populus balsamifera* and *Populus tremuloides*, averaging 25.7% and 28.5%, respectively. Coniferous tree species, *Picea mariana* and *Pinus banksiana,* averaged 34.5% and 31.5%, respectively. While vegetation is currently in the early stages of development, rainfall redistribution may become an important consideration when selecting tree communities in reclamation projects.

Acknowledgements

Most importantly, I would like to send my greatest appreciation to my supervisor Dr. Richard Petrone for giving me this opportunity to complete my master's thesis and for his endless support throughout this process. I am thankful to have had the opportunity to work with you and the Hydrometeorology Research Group for the last three years.

The last two years have been challenging, exciting, stressful, but most importantly successful and there are many people who have contributed to my experience. Rebecca and Karisa, I am grateful for that first drive to Fort McMurray, where we were thrown into a truck to drive with people we had never met. I could not have completed these last two years without your friendship and support. I am glad we had the opportunity to go through this experience together.

I would like to thank members of the Waterloo Hydrometeorology Lab Group for their guidance and support throughout this entire process. I am appreciative of having the opportunity to have worked alongside members of the Wetland Hydrology and GHG Exchange Lab both during field seasons and laboratory data analysis. Especially, a special thank you to Adam and Eric for answering my numerous phone calls all summer and for all their help and guidance throughout the data analysis and writing processes. This work could not have been completed without the collaboration and help of Suncor's Field Services and Reclamation team. Thank you to the Bear Scare team for allowing us to continue our work safely and helping in the field.

Lastly, I would like to thank my friends and family for their endless support throughout my entire education. Thank you for listening to me talk about my work despite never completing knowing what I was actually doing. Thank you for uplifting me when I would stress out and encouraging me to continue to work. I could not have done this without you guys by my side.

Table of Contents

List of Figures

List of Tables

Chapter 1: Introduction

1.1. Background and rationale for research

The Athabasca Oil Sands Region (AOSR) is located in the Western Boreal Plain (WBP) in Northeastern Alberta, covering approximately 142,200 km^2 (Government of Alberta, 2017). Northeastern Alberta contains some of the largest oil sand reserves in the world, consisting of approximately 4,800 km^2 of surface mineable area (Government of Alberta, 2017). The process of open-pit mining leads to landscape degradation, impacting the overall functioning and loss of many ecosystems (Rooney *et al.* 2012). The pre-disturbed landscape consisted of 64% wetlands, of which 90% were fen peatlands, and 23% upland forests (Rooney *et al.* 2012; Daly *et al.* 2012). Wetlands and forests provide many important ecosystem services; specifically, they act as important carbon sinks, stores and conveyors of water (Johnson & Miyanishi, 2008). However, processes involved in resource extraction have led to the clearing and drainage of wetland and forest ecosystems. As a response to landscape disturbances, the Alberta Government mandates oil companies to return land to equivalent function of pre-disturbed landscapes. Therefore, to mitigate the impacts of oil sands activities, post-mined landscapes are reclaimed in an attempt to create functionally equivalent systems.

While, pre-disturbed landscapes consisted primarily of peatlands, reclamation has generally involved the conversion to upland forests (Rooney *et al.* 2012). Reclamation of upland forests has been preferred due to the complexities of peatland formation, in respect to peat accumulation and maintaining hydrological function in Alberta's sub-humid climate (Price *et al.* 2010). The recognition of the importance of peatlands to the AOSR has encouraged their integration in recent reclamation projects. Natural peatland systems are characterized by their hydrological connectivity to adjacent uplands through the redistribution of groundwater during

moisture deficits, encouraging the use of integrative upland-fen systems in constructed post-mined landscapes (Dimitrov *et al.* 2014; Ketcheson *et al.* 2016; Price *et al.* 2010). Combined efforts of peatland restoration strategies (Quinty & Rochefort, 2003) and salvaged peat material are believed to sustain hydrological conditions, making peatland reclamation possible (Price *et al.* 2010). However, predicting the trajectory of upland systems becomes increasingly important when addressing the connectivity to low-lying peatlands. That is, vegetation development will lead to increases in precipitation interception and transpiration, ultimately reducing water available for recharge to the adjacent peatland (Sutton & Price, 2020). Water partitioning by vegetation explains the processes by which vegetation redistributes water resources throughout the landscape. Characterizing the impacts of vegetation distribution and composition on the water balance may help improve reclamation techniques for future projects. Improving reclamation techniques is essential when addressing concerns of climate change, as predictions suggest that parts of the Canadian Boreal Forest will likely become drier, especially in the summer, due to warming temperatures and/or decreasing precipitation (Price *et al.* 2013).

1.2. Research objectives

Upland reclamation in the oil sands region requires improved understanding of the re-establishment of vegetation communities. The trajectory of vegetation on site is critical to the success of reclamation projects, particularly its potential to influence hydrological regimes and movement of water to the adjacent fen peatland. The objectives of the study are designed to determine the role of dominant tree species in partitioning water, and influence moisture recharge and groundwater contributions to the adjacent fen. Trees used in re-vegetation strategies encompass predominant trees in the WBP and range in their water use and partitioning abilities. Specifically, the research objectives are to:

I) quantify rainfall partitioning components of throughfall, stemflow and interception of dominant tree species

II) assess trends in transpiration of dominant tree species used in upland reclamation throughout the growing season

III) understand the effectiveness of tree rainfall partitioning and its significance on near-surface soil moisture regime and tree water use.

Chapter 2: Literature review

2.1. Introduction

Canada's WBP plays an important role in the country's landscape and natural environment, providing many important ecological services, such as creating habitats for several species, water filtration, carbon storage, and climate regulation (Marshal *et al.* 2015). In Alberta, the WBP covers 381,000 km^2, or 57% of the province (Alberta Wilderness Association, 2015). However, while its importance is widely recognized, the Government of Alberta protects only 13.2% of the WBP (Alberta Wilderness Association, 2015). As a result of industrialization, natural and anthropogenic disturbances have altered and changed this landscape, leading to the disappearance of many ecosystems. Wildfires and timber harvesting are common disturbances causing large-scale loss of vegetation communities in the WBP. Currently, the dominant anthropogenic disturbances in Alberta are related to resource extraction concentrated mainly in the AOSR, having consequences on wildlife and vegetation communities (Marshall *et al*. 2015). While, surface mining disturbances currently represent only a small fraction of Alberta's WBP, the expansion of mining activities following increasing demand will further modify our natural landscapes, highlighting the need for successful large-scale mitigation strategies (Audet *et al.* 2015).

2.2. Oil sands mining in the AOSR

Beginning in 1967, the development of oil resources has provided thousands of Canadians with jobs and contributed significantly to its national wealth and trade balance (Bott, 2007). Although the oil sands industry has provided considerably to economic growth in Canada, expansion of oil sands development leads to increases in greenhouse gas emissions (GHG), along with several impacts to land and water resources (Jordaan, 2012). In 2013, 4700 km^2 of land in Alberta has been leased for oil sands development and led to a disturbance footprint of 700 km^2 (Audet *et al.* 2015). According to Alberta Biodiversity Monitoring Institute (2018), the total human footprint in 2016 in the AOSR reached 8,086 km^2, equivalent to 2.5% of the land area.

The region of Fort McMurray, Alberta is one of the prime locations for oil extraction (Price *et al.* 2010). Many of the large-scale oil deposits are recovered using surface mining processes, which cause significant disturbances to the landscape (Leatherdale *et al.* 2012). During the mining process of bitumen extraction, landscapes are completely stripped, permanently altering ecosystems and their natural hydrologic and nutrient cycles (Leatherdale *et al*. 2012; Rowland *et al.* 2009). Stripping includes removing all vegetation, soil, glacial tills, clay and Cretaceous clay shale, which is stockpiled and used in future reclamation (Rooney *et al.* 2012). Erosion, weathering and high pH are common during removal processes, rendering these materials unsuitable for reclamation, thereby promoting the use of non-saline overburden to cap the soil surface below (Rowland *et al.* 2009). The last step is placing an appropriate cover soil to stimulate the establishment of forest communities (Huang *et al.* 2015; Leatherdale *et al.* 2012).

2.3. Reclamation of post mined landscapes in the AOSR

Future mining activities have the potential to further disturb Alberta's natural landscape, emphasizing the importance of effective reclamation of disturbed areas (Vitt & Bhatti, 2012).

Considering large-scale disturbances, restoration solutions are not adequate, requiring the engineering of new ecosystems (Johnson & Mayashimi, 2008). Reclamation entails the recovery of ecosystem services following disturbances through revegetation strategies, in hopes of creating equivalent land capabilities to pre-disturbed conditions (Lima *et al.* 2016; Stefani *et al.* 2018). One of the first attempts at peatland reclamation in the WBP was conducted at the Suncor Energy Inc. pilot fen, incorporating an upland to fen transition (Daly *et al.* 2012). The sub-humid climate characteristic of the AOSR make the creation of peatlands difficult, due to the long-term water deficit resulting from high potential evapotranspiration (PET) and minimal rainfall (Brown *et al.* 2010; Devito *et al.* 2015).

The limitation in moisture availability promoted the use of uplands to supply groundwater and runoff to the adjacent peatland and maintain sustainable moisture conditions (Price *et al.* 2010). However, runoff generation in the WBP is highly variable between wet and dry years, stressing the importance of high available water storage capacity of uplands (Ketcheson *et al.* 2016). A large proportion of annual precipitation occurs during the growing season (May to September) in the form of rainfall, while precipitation during the non-growing season is minimal and dominated by snowfall (Brown *et al.* 2012). If properly managed, excess water from winter snowmelt is stored and made readily available during limiting moisture conditions (Ketcheson *et al.* 2016; Sutton & Price, 2019).

In natural WBP systems, a flow reversal in groundwater flow is observed where peatlands supply uplands when PET demand is high (Devito *et al.* 1997; Johnson & Miyanishi, 2008). This generally occurs during dry years, as water is moved from peatlands to the upland through capillary action and root water uptake (Nicholls *et al.* 2016; Ferone & Devito, 2004; Depante *et al.* 2018). The success of the constructed fen peatland is reliant on the trajectory of upland vegetation and its

ability to supply adequate moisture to support vegetation water use and fen functioning. Obstacles of newly reclaimed uplands include variations in topography from pre-excavated landscapes. Prior to mining, sands are compressed from past glaciation events creating low-relief characteristic of the WBP (Devito *et al.* 2005; Rowland *et al.* 2008). Following oil sand mining, remaining sand is used to fill pits and occupies a greater volume. Using the remaining sand to fill pits, resulting in topographical differences to pre-disturbed landscapes, ultimately altering natural water dynamics (Rowland *et al.* 2009; Leatherdale *et al.* 2012). Thus, site-specific topographical differences must be considered to understand the hydrological connectivity between land units (Elshorbagy *et al.* 2005, Gingras-Hill *et al.* 2018, Sutton *et al.* 2019).

2.3.1. Nikanotee Fen Watershed upland reclamation

Upland reclamation has been successful in the past, developing productive self-sustaining systems and performing ecosystem functions. However, these systems differ significantly from their natural analogues with respect to vegetation and tree communities, hydrology and soil conditions (Audet *et al.* 2015). The reconstruction of post-mined landscapes has faced many challenges including the establishment of successional vegetation communities to a state of self-sustainability and productivity. The design of the constructed system plays an important role in the trajectory of the site, specifically vegetation growth. In a region with high rates of evapotranspiration (ET), moisture depletion in the rooting zone is common (Strilesky *et al.* 2017). Capillary barriers are often used in engineered systems and play an important role in vegetation development by restricting water from percolating deeper into the soil profile (Macdonald *et al.* 2015a; Naeth *et al.* 2010). Additionally, as tree cover establishes and moisture partitioning is altered, it is expected that roots will benefit from increased water availability created at the capillary barrier (Sutton *et al.* 2019).

Studies have assessed the importance of cover soil used during reclamation for the establishment and development of tree communities (Macdonald *et al.* 2015b; Stefani *et al.* 2018; Huang *et al.* 2015). Cover soil was found to have strong controls on ET rates, varying spatially and temporally (Strilesky *et al.* 2017; Brown *et al*. 2014). While the selection of an appropriate cover soil is important to yield adequate moisture for vegetation growth, it is equally important in its ability to minimize movement of saline water into the rooting zone (Carey, 2008; Huang *et al.* 2015). Movement of saline water into the rooting zone is initiated by high ET rates characteristic of the WBP, which promotes depletion of near-surface soil moisture stores when water is limiting, restricting vegetation growth (Strilesky *et al.* 2017). Low infiltration abilities and high soil erodibility are common characteristics of newly reclaimed soils, displaying variability in hydrologic behaviour and emphasizing the importance of early vegetation establishment (Moreno-de las Heras *et al.* 2009). Forest-Floor Material (FFM) and Peat-Mineral Mix (PMM) are two cover soils commonly used in the AOSR (Macdonald *et al.* 2015). In literature, FFM is identified by many terms and most frequently referred to as LFH (Macdonald *et al.* 2015b). The LFH capping layer is comprised of overstripped organic soil horizons L (Litter), F (Fibric), and H (Humic) and was selected as a vegetation growth substrate (Price *et al.* 2010). PMM generally has high moisture holding capacity and organic matter content, indicating its suitability for tree seedling establishment (Errington & Pinno, 2015). The high-water holding capacity of PMM make them suitable to enhance water availability and sustain upland vegetation growth. While LFH may have lower water holding capacity, it would promote greater recharge (Tremblay *et al.* 2019). The use of LFH cover soils is preferred in upland reclamation due to its similarities to natural WBP in pH and texture, as well as its potential as a source of native vegetation propagules (Mackenzie & Naeth, 2010).

Understanding tree canopy development is of primary importance to the management of constructed systems, and sets the groundwork for effective future reclamation projects. Upland forests are complex systems, requiring careful consideration of optimal conditions. Over time, soil and vegetation cover will develop, leading to significant changes in the ecosystem (Moreno-de las Heras *et al.* 2008). Water availability is a primary driver in tree growth and productivity (Elliot *et al.* 1997; Huang *et al.* 2011), creating feedback systems as the establishment of tree cover is dependent on moisture availability, which ultimately results from the interactions of vegetation with soil water (D'Odorico *et al.* 2007). Increasing tree cover will exhibit higher rates of transpiration and root uptake, which will increase water table depth, affect vegetation growth and productivity (Wang *et al.* 2019). Topography, soil texture, depth to water table, meteorological conditions and vegetation are all factors influencing soil water dynamics (Benegas Negri, 2018; Asbjornsen *et al.* 2011). Vegetation has the ability to control moisture conditions by partitioning rainfall (Lishman, 2015; Spencer & Van Meerveld, 2016; Marin *et al.* 2000). The change in water use dynamics with developing canopy will control hydrologic conditions of adjacent peatlands by altering moisture downslope (Strilesky *et al.* 2017). Early stages of reclamation show evidence of dynamic hydrologic regimes, which are expected to stabilize as soil and vegetation establishes (Leatherdale *et al.* 2012). Dynamics in tree water use are dependent on tree colonization in the upland and will differ in magnitude throughout the growing season (Cienciella *et al.* 1997).

2.4. Vegetation dynamics

Tree population in natural upland WBP systems consisting of mineral soils are dominated by a coniferous-deciduous mix of *Pinus banksiana* (jack pine), *Populus tremuloides* (trembling aspen) and *Populus balsamifera* (balsam poplar) (Audet *et al.* 2014). Low-lying areas, consisting of organic soils within the WBP, are typically dominated by coniferous *Picea mariana* (black spruce)

(Leatherdale, 2012). As a result of slow vegetation regeneration on oil sands reclamation sites, additional planting is often required (Dhar *et al.* 2018). In current reclamation projects, *Populus tremuloides* trees are the target species to re-establish due to their ability to promote colonization of other species by influencing soil conditions, and their ability to naturally colonise quickly (Carrera-Hernández *et al.* 2011; Dhar *et al.* 2018; Stefani *et al.* 2018).

Vegetation colonization plays an important role in stabilizing disturbed systems by reducing soil erosion and increasing infiltration rates. Therefore, reclamation requires re-establishment of native tree communities characteristic of natural forests in the region (Errington & Pinno, 2015). Natural and constructed systems are classified into specific ecosites using the Land Capability Classification System (LCCS) for Forest Ecosystems, which integrates soil and landscape characteristics fundamental to ecosystem productivity (Cumulative Environmental Management Association, 2006). Moisture regimes of ecosites are identified by the Available Water Holding Capacity (AWHC), by means of the difference between field capacity (FC) and wilting point (WP) in the rooting zone (Huang *et al.* 2015). Determining ecosites is important when considering potential re-vegetation strategies, as soil moisture regimes will influence success of tree establishment (Mackenzie, 2013). Conversely, vegetation selected for reclamation will impact moisture regimes through physiological processes and promote growth of specific ground vegetation type, which will elicit different soil water use (Huang *et al.* 2011; Barbier *et al.* 2007).

Interactions between vegetation and hydrological processes are complex. Trees uptake soil water through roots and recycle back to the atmosphere through the process of Transpiration (T) (Naeth *et al.* 2011). ET is a significant component in the hydrological cycle, in which tree T makes up a large proportion of its water fluxes and is a major pathway for energy loss in forested ecosystems, especially in the AOSR (Lagergren & Lindroth, 2002; Petrone *et al.* 2015; Tfwala *et*

al. 2019). Specifically, in a region experiencing soil water deficits, monitoring ET and T of developing canopies becomes increasingly important to validate current upland reclamation procedures and ensure sufficient water supply recharges adjacent peatlands. Periodic water deficits result in T relying on growing season rainfall events and excess snowmelt stored during the non-growing season (Ogle & Reynolds, 2004; Potts *et al*. 2006; Raz Yaseef *et al*. 2012). While current studies have focused on the impacts of growing vegetation on ET rates following landscape disturbances (Macdonald *et al.* 2015a; Strilesky *et al.* 2017), less focus has been on the role specific tree communities play in partitioning water resources and their suitability in upland reclamation, which is important to understand the impact successional development will have on a systems hydrology.

Selecting appropriate trees to populate uplands depends on their abilities to effectively use and partition water resources throughout the landscape. Trees partition water through T, rainfall interception and root water movement in the soil profile (Strilesky *et al.* 2017). Sap flow techniques are useful for measuring total single tree water use (Lagergren & Lindroth, 2002), in which T is generally controlled by atmospheric conditions and water availability by regulating stomata behaviour (Whitehead, 1998; Buckley *et al.* 2003; Wang *et al.* 2014). Single tree water use measured from sap flow instrumentation is often scaled-up to obtain stand-level T (Asbjornsen *et al.* 2011). The ability to assess trends in tree water use across different scales is important to evaluate the role of trees in the hydrologic cycle, though scaling from tree-level remains a challenge in ecohydrology (Clulow *et al.* 2012; Clulow *et al.* 2014; Mackay *et al.* 2010; Asbjornsen *et al.* 2011).

To better understand the hydrological effects of a developing forest canopy in a constructed upland landscape, rainfall partitioning and the interaction with near-surface soil moisture must be

studied. A large quantity of precipitation, which falls to a watershed does not reach the soil surface to become available for plant growth or moisture recharge (Livesley *et al.* 2014; Johnson & Lehmann, 2016). Redistribution of rainfall by vegetation canopies will increase the spatial variability of moisture stores in soil (Swaffer *et al.* 2014) but may also reduce water reaching adjacent peatlands. Trees have the ability to partition rainfall through three main pathways: I) throughfall (TF) – the proportion of gross precipitation (GP) passing through the canopy or dripping from foliage and wood components (Schooling & Carlyle-Moses, 2015); II) stemflow (SF) – the proportion of GP entrained by the canopy and channelled down trunks and stems (Crockford & Richardson, 2000; Siegert & Levia, 2014); and III) interception (INT) – proportion of GP that remains on the tree canopy and subsequently evaporated back to the atmosphere (Crockford & Richardson, 2000; Swaffer *et al.* 2014). The outcome of these interactions with the canopy depends on the type and characteristics of both the vegetation and precipitation (Tobón Marin *et al.* 2000; Crockford & Richardson, 2000).

Current research on rainfall partitioning has focused on canopy INT and TF, whilst SF is often neglected due to its minor volumetric significance (Aboal *et al.* 1999, Levia & Frost, 2003; Levia & Herwitz, 2005; Staelens *et al.* 2008). Despite its lower volumetric contributions to rainfall partitioning, SF represents a spatially localized point source of water and nutrients to the bole of the tree and will vary depending on species type (Carlyle-Moses & Price, 2006; Levia & Herwitz, 2005). With delivery concentrated at the base of the tree, SF yields are important point sources of water for soil moisture and groundwater recharge (Mckee, 2011). Additionally, tree diameter at breast height (DBH), basal area (BA) and height will impact stemflow volumes, but the magnitude of their impacts will depend on tree species (Spencer & Van Meerveld, 2016). For instance, studies have found approximately 2% of GP can be channeled as SF in coniferous trees, whereas broadleaf

species are approximately 6% (Barbier *et al.* 2009). Overall, Barbier *et al.* (2009) recorded higher SF volumes with broadleaved than coniferous species, due to differences in bark morphology (Levia & Herwitz, 2005). Interspecific differences in SF among tree species have been attributed to bark roughness and branch angles (Aboal *et al.* 1999; Barbier *et al.* 2009; Siegert & Levia, 2014). Smoothed bark trees, characteristic of broadleaf trees, are known to produce higher stemflow volumes than rough bark trees, typical of coniferous trees (Tate, 1995). Additionally, lower SF channeled by conifers can be attributed to the SF reducing "funnel crown" (Barbier *et al.* 2009; Otto, 1998). The base of the tree is characterized by macropores and tree roots creating pathways for funneled SF to infiltrate rapidly and deeply into the soil profile following rainfall events (Spencer & Van Meerveld, 2016).

TF accounts for the majority of rainfall partitioned by a tree canopy and has been studied extensively in literature (Crockford & Richardson, 2000; Livesley *et al.* 2013; Swaffer *et al.* 2014). TF contributions are critical sources of soil moisture to vegetated systems, with the potential to determine productivity and increase water availability for recharge (Su *et al.* 2019). Similar to SF, TF varies with tree type, and characteristics (density, LAI, leaf orientation), as well as precipitation characteristics (Reynolds & Henderson, 1967; Rutter, 1963; Williams, 2004). In a review of literature, Barbier *et al.* (2009) reported high TF for broadleaf species than coniferous, as a result of differences in LAI. Intensity and depth will determine the proportion of precipitation partitioned as TF by a canopy, where low intensity precipitation will promote INT, reducing TF and SF (Levia & Frost, 2003; Williams, 2004). During intense precipitation events, contributions from TF will increase as canopy storage capacity is reached and conducting channels to the stem are saturated (Williams, 2004).

The process of INT prevents precipitation from reaching the surface, generally increasing with developing canopy cover (Kermavnar & Vilhar, 2017). INT becomes an important concept to consider in reclamation consisting of an upland-fen peatland design, as a developing canopy will reduce water available to recharge the adjacent peatland. INT percentages on an individual plant level will vary depending on tree species, seasonal characteristics, canopy density, canopy age and LAI (Tate, 1995, Staelens *et al.* 2007). Annually, conifers will intercept higher proportions of precipitation than broadleaf, since they retain needles during the non-growing season. Broadleaf trees will have high INT rates at peak growing season, when foliage reaches full expansion. Overall, needles have large total surface area yielding higher total interception contributions than broadleaf trees (Tate, 1995).

2.5. Summary

The overall goal of reclamation is creating a self-sustaining system with equivalent function to the pre-disturbed landscape of the natural WBP (MacKenzie *et al.* 2011). A major challenge faced with reclamation in the AOSR involves the sub-humid regional climate with limited moisture availability. It is important to provide sufficient soil moisture to sustain upland forest, while delivering adequate moisture to the adjacent peatland. More specifically, broadleaf stands require higher proportions of water availability to maintain productivity, while coniferous stands are less dependent on high moisture conditions. Understanding how these proportions compare to seasonal precipitation is important, as the difference represents the recharge water available. Current literature demonstrates the dependence of rainfall partitioning and tree water use on vegetation cover, which in turn will control soil moisture regimes. It is anticipated that with a developing tree canopy, interception will increase reducing moisture available for recharge. However, rainfall partitioning and tree water use depend on tree species and characteristics necessitating the

characterization of the impacts of vegetation distribution and composition on the water balance to improve reclamation techniques for future projects.

Chapter 3: Methods

3.1. Study site

The study area is located approximately 40 km north of Fort McMurray, Alberta on a post-mined landscape consisting of a constructed upland-fen system. The Nikanotee Fen Watershed (NFW) design comprises an upland aquifer (~7.7 ha) connected to a fen peatland (~2.2 ha) through surface and groundwater (Ketcheson *et al.* 2017). Located within the sub-humid WBP, NFW experiences short summers and long winters where PET often exceeds precipitation, resulting in periods of water deficit. Mean annual temperature of the region is 1^{o}C, with a peak in July of 17.1^{o}C, from the thirty-year climate normal data (1981 - 2010) (Environment Canada, 2015). The AOSR loses on average approximately 520 mm to PET, which slightly exceeds annual average precipitation of 455 mm. Precipitation is dominated by high-intensity convective rainfall during the summer growing season and dominated by snowfall during the winter months (Carey, 2008).

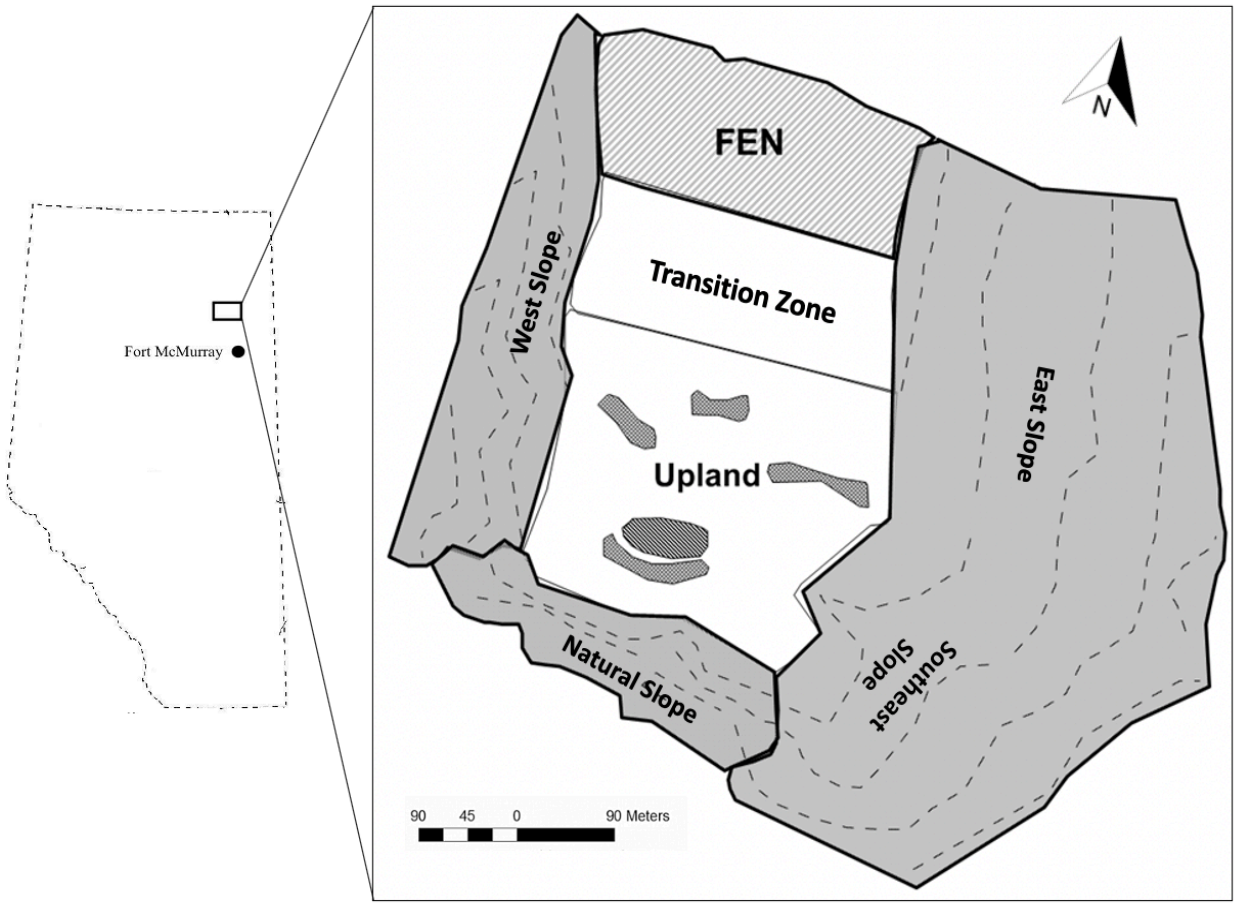

Figure 1: Map of the Nikanotee constructed upland-fen system, including three adjacent reclaimed hillslopes and natural slope.

Data for this study were collected from the upland of the system during the 2019 growing season (May to September). Specifically, data were collected from day of year (DOY) 145 to 267 (25 May to 24 September 2019). The upland system was constructed with coarse tailing sands material, overlain with a 30 - 50 cm thick layer of LFH mineral soil reclamation cover in 2013 (Ketcheson *et al.* 2017). Tailing sands material was placed above an impermeable engineered geotextile clay liner, which was implemented to promote lateral groundwater movement between the upland and fen system (Price *et al.* 2010). When the upland was constructed in 2013, large precipitation events led to periods of intense overland flow out of the system (Sutton & Price, 2019). Thus, to improve the system hydrologically and increase infiltration rates, the upland was

scoured in an east to west direction creating a series of ridges and furrows (Ketcheson, 2015). Presently, the upland is characterized by its deep-water table, which is generally 2 to 3 m below the ground surface, and its relatively low surface infiltration rates (Irving, 2020).

The largest area of the watershed is comprised of three previously reclaimed hillslopes, East Slope, West Slope, Southeast Slope and Natural Slope, which are described in detail in Ketcheson & Price (2016) (Figure 1). The East Slope was constructed in 2007 and was planted in 2008, which has developed into a well-established, robust vegetation layer comprised of *Picea glauca* (white spruce), *Populus tremuloides* (trembling aspen), *Betula papyrifera* (white birch), *Populus balsamifera* (balsam poplar), *Alnus viridis* (green alder) and an assortment of shrub species. The West and Southeast slopes were reclaimed in 2011 and planted in 2012, resulting in a much less developed vegetation layer at this time. The west slope was planted as a moist-rich site, consisting primarily of *Picea glauca* and *Populus tremuloides*. Whereas, the Southeast slope was planted as a dry site consisting primarily of *Pinus banksiana* (jack pine). The natural slope located in the southern upslope region of the system is comprised of natural soil and vegetation layers, which are characteristic of the AOSR. The role of these reclaimed hillslopes on the hydrology of the constructed system is to provide significant amounts of water to the downstream ecosystems, and in turn help address any issues of water availability (Ketcheson & Price, 2016). However, as vegetation continues to develop on the hillslopes, increased percolation and water storage along with water uptake by an ever-growing vegetation layer will reduce their hydrologic contributions to adjacent low-lying systems.

Planting prescriptions on the upland of the constructed site followed procedures developed by the Cumulative Environmental Management Association revegetation manual (Alberta Environment, 2010). Planting prescriptions were selected based on site type, location and soil

characteristics, which are ultimately used to predict moisture and nutrient regimes (Daly *et al.* 2012). The upland was classified as two distinct ecosites, hereafter referred to as the transition zone and upland. The transition zone, low-slope region of the upland, extends approximately 100 m from the fen peatland and makes up 2.3 ha. This zone was distinctly identified from the upland due to the underlying petroleum coke underdrain which extended 100 m from the fen. The transition zone was planted in 2013 as a treed rich fen ecosite (k1.1), consisting of *Picea mariana* (black spruce), *Rhododendron groenlandicum* (labrador tea), *Betula nana* (dwarf birch), *Salix spp.* (willow), *Vaccinium oxycoccos* (bog cranberry), *Calamagrostis lacustris* (northern reed grass), and *Carex aquatilis* (water sedges) (Alberta Environment, 2010). In 2014, *Larix laricina* (tamarack) were additionally planted in the Transition Zone. The upland consists of the remaining area, totaling 6 ha and contains the mid and upper slope regions of the upland. The upland was planted as a moist poor ecosite (c1.1); planting in this area included *Picea mariana*, *Pinus banksiana*, *Rhododendron groenlandicum*, *Vaccinium oxycoccos*, *Vaccinium myrtilloides* (blueberry), *Rosa acicularis* (prickly rose) and *Cornus canadensis* (bunchberry) (Alberta Environment, 2010). In moist poor ecosites, the forest is usually comprised of a two-layered canopy with an upper layer dominated by fast-growing *Populus tremuloides* and *Populus balsamifera* species, and a secondary layer dominated by slow growing *Pinus banksiana* and *Picea mariana* species (Millennium EMS Solutions Ltd. 2011).

3.1.1. Forest inventory surveys

Vegetation surveys were conducted in the upland to determine forest stand characteristics. Surveys were completed once towards the end of the field season on DOY 205 (24 July 2019), to capture maximum foliage expansion during the growing season. Nine 5 m radius (78.5 m^2) plots were established along 3 transects in a west to east direction across the upland (Figure 2). Within each

5 m radius plot was a smaller 1 m radius plot created for groundcover surveys, selected to capture adequate spatial coverage and shifts in dominant tree species populations from the transition zone to the drier upslope regions of the upland. At each sampling plot, tree surveys were conducted to determine species identification, DBH, height and BA of each tree. Tree heights were measured using a PVC pole delineated with measurements and recording height of tree relative to the pole. When necessary, a clinometer was used to measure trees taller than the vegetation stick. DBH was measured using a flexible measuring tape, recording the circumference of the trees, which were later converted to a diameter. DBH was recorded at 1.37 m above ground surface and trees smaller than this height were considered saplings for which only the height was recorded.

At the nine sampling plots, two 1 m x 1 m quadrats were established beneath dominant tree species to determine understory vegetation. A total of 16 plots were sampled across the upland. Within each plot, a visual estimate of groundcover classification was completed using the quadrat method to determine species type and percent ground cover. Ground vegetation was classified as either bare ground, grass, weeds, alfalfa or shrubs.

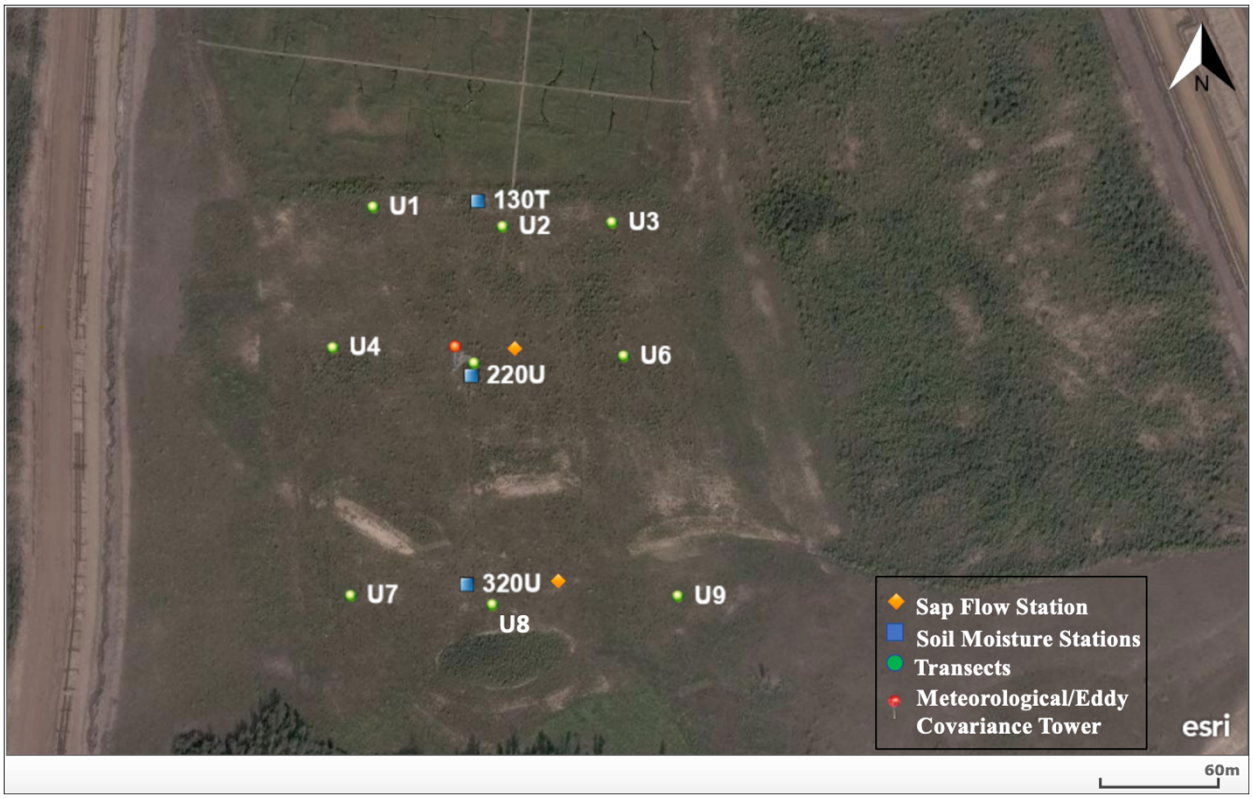

Figure 2: Map of Nikanotee Fen Watershed (NFW), showing instrumentation and sampling transects in the upland (3 transects, 9 plots).

Leaf area index (LAI) was measured using a LAI-2200 plant canopy hand analyzer (LI-COR, Lincoln Nebraska, USA). Measurements were taken using the 180° view cap, following the most suitable method for isolated trees (LI-COR, 2012). LAI was taken once a month, for a total of 4 measurements throughout the growing season. Measurements were taken on 12 trees of each of the dominant tree species distributed randomly across the 9 plots in the upland. The sparse nature of the canopy makes it difficult to measure LAI without large uncertainty and error. Therefore, a more useful measure is that of foliage density of individual trees. The foliage density is a measure of the foliage area (m^2) divided by the canopy volume (m^3), resulting in units of inverse length (m^{-1}) (LI-COR, 2012). The FV-2200 software (version 2.1; LI-COR, Lincoln Nebraska, USA) was used to process values obtained in the field and apply a sun-scattering correction. The software uses simple tree measurements to calculate the volume of the crown and

determines its foliage density (Pu, 2017). Additionally, a conifer correction was applied to the *Picea mariana* and *Pinus banksiana* species measurements to account for the non-random spatial distribution of foliage and clumping of needles (Chen *et al.* 1997). Corrections were calculated using,

$$LAI = (1-\alpha)L_e / \left(\frac{\Upsilon E}{\Omega E}\right) \quad (1)$$

where L_e is the effective LAI derived from gap fraction measurements by the optical instrument, $(1-\alpha)$ is a factor which removes contributions from non-leafy materials, Y_E is the needle-to-shoot ratio, Ω_E indicates the foliage clumping at scales larger than the shoot (Chen *et al.* 1997). Conversion factors of 1.8 (Y_E = 1.4, $(1-\alpha)$ = 0.84; Chen *et al.* 1997) and 1.3 (Y_E = 1.45, $(1-\alpha)$ = 0.69; Chen *et al.* 1997) were used for corrections after being determined in literature as being suitable for *Picea mariana* and *Pinus banksiana* species, respectively (Chen *et al.* 1997).

3.1.2. Soil properties

Soil cores were collected using PVC pipe under trees instrumented with sap flow sensors, along with trees instrumented with TF and SF collectors. Collected cores were 10 cm in diameter and 10 cm in height, driven into the ground and wrapped in polyethylene film. Cores were frozen until transported back to the University of Waterloo, where they were analyzed for bulk density and porosity (Freeze & Cherry, 1979). Soil texture analysis was run on sub-samples, which were dried and sieved through a 2 mm sieve. Particle size distribution was measured for samples using a laser scattering particle size analyser (Horiba LA – 950V2; Kyoto, Japan).

Soil infiltration rates were measured at the 9 sampling plots using a single ring infiltrometer test. A minimum of 6 replicates were run at each sampling location and runs were distributed between both ridges and furrows. Rings were inserted into the surface at a depth of approximately

1 cm and test were run until steady state was achieved (determined by a minimum of 4 consecutive measurements within ± 15%) (Ketcheson & Price, 2016). Field measurements were corrected and converted to an infiltration rate ($mm\ hr^{-1}$).

3.2. Hydrometeorological data measurements

Hydrometeorological data were collected using Eddy Covariance (EC) and meteorological (MET) systems located on a tower in the upland from DOY 121 to 266 (1 May 2019 to 25 September 2019). Measurements were taken 3 m above the surface with average canopy height referenced at 2 m. The MET system measured relative humidity (%) and air temperature (°C) above the canopy (Rotronic HC2S; Bassersdorf, Switzerland), along with the four components of net radiation (Q^*) (CNR4 Net Radiometer; Kipp & Zonen; VA, USA). Ground heat flux (Q_g) was measured using soil heat flux plates (HFT3 Soil Heat flux Plates, Campbell Scientific Inc. UT, USA) inserted horizontally at a depth of 5 cm below the ground surface. Plates were placed a few meters apart from each other, facing in a southern direction. Precipitation was measured using a tipping bucket rain gauge (HOBO U23 Pro v2, Onset Computer Corporation, Bourne, MA) and placed within a clearing near the tower to avoid influences from the canopy layer and MET tower. All data were collected on a CR1000 (Campbell Scientific: Logan, Utah, USA) datalogger at a sampling frequency of 10 seconds and averaged every half-hour.

The EC system was used to derive the remaining energy fluxes at the site and estimate ecosystem-scale ET. The system was instrumented with a 3-dimensional sonic anemometer (CSAT3; Campbell Scientific Inc. UT, USA), and an open-path infrared gas (CO_2/H_2O) analyzer (LI-7500; LI-COR, Lincoln, NE) sampling at 20 hz and logged on a CR3000 data logger (Campbell Scientific: Logan, Utah, USA), which processed the high frequency data and computed half-hourly averaged fluxes (Petrone *et al.* 2015), while also correcting for vapour density, sensor

separation and double coordinate rotation following common Fluxnet protocols (Webb *et al*. 1980; Kaimal and Finnigan, 1994; Leuning and Judd, 1996; Foken and Leclerc, 2004; Aubinet et al., 2012; Burba et al., 2012). The following half-hour fluxes were then filtered to ensure that at least 80% of the high-frequency records were collected and that there was no potential for dew formation on the IRGA lenses by either precipitation or by comparing the dew point temperature to Ta. Additional filtering removed values that were greater than ±3 standard deviations of a moving average, which consisted of 10 half-hour neighbouring values; further filtering was completed to check for physically improbable values. The Kljun et al. (2015) footprint analysis was used to constrain the measured fluxes to be within 80% of the desired site boundaries. Thereafter, fluxes with a friction velocity (u*) of u* < 0.1 m s^{-1} were removed from the dataset to ensure significant turbulent mixing.

ET was estimated using a radiation balance approach. The MET and EC systems were used to determine components of the energy balance,

$$Q^* = Q_H + Q_E + Q_G \quad (2)$$

where Q^* is total net radiation, Q_H is sensible heat flux, Q_E is latent heat flux and Q_G is ground heat flux. Final flux corrections and gap-filling followed the methods used in Petrone *et al*. (2001), Wilson *et al.* (2001) and Brown *et al.* (2010) where energy balance closure was completed by subtracting the turbulent fluxes (Q_H + Q_E) from the available energy (Q^*- Q_g) and partitioning the residual by the Bowen ratio ($\beta = Q_H / Q_E$) back into the sensible (Q_H) and latent (Q_E) heat fluxes, respectively (Barr *et al*. 2006). The Penman Monteith method was used to calculate PET,

$$PET = \frac{\Delta(Q^* - Q_G) + \rho_a c_p \frac{(e_s - e_a)}{r_a}}{(\Delta + \Upsilon) r_a} \quad (3)$$

where Δ ($kPa\ °C^{-1}$) is the slope of the saturated vapour pressure curve, Q^* is the total net radiation ($MJ\ m^{-2}\ 30\ min^{-1}$), Q_G is the ground heat flux ($MJ\ m^{-2}\ 30\ min^{-1}$), ρ_a is the mean air density ($kg\ m^{-}$

^{3}), C_p is the specific heat of the air ($MJ\ kg^{-1}\ K^{-1}$), (e_s - e_a) is the vapour pressure deficit (kPa), r_a is the aerodynamic resistance (1 s m^{-1}) and γ is the psychrometric constant ($kPa\ ^{o}C^{-1}$) (Allen *et al.* 1998). PET was used for gap-filling during periods when Actual Evapotranspiration (AET) were missing. The equation was adjusted to calculate ET by removing stomatal conductance (r_s) and having aerodynamic resistance (r_a) to equal 1 s m^{-1}. The relationship between PET and AET is expressed through a coefficient α,

$$\alpha\ (0.86) = PET/AET \tag{4}$$

where PET ($W\ m^{-2}$) is the evaporation that would occur in non-limiting water conditions and AET ($W\ m^{-2}$) is the actual amount of water lost from a surface (Petrone *et al.* 2007).

Continuous measurements of Volumetric Water Content (VWC) were collected using dielectric impedance reflectometry soil moisture probes (Stevens Hydra Probe II) at 3 locations along a north to south transect across the upland, SAF 130T, SAF 220U and SAF 320U (Figure 2). SAF 130T, located in the upland-fen transition zone in the lower slope region of the upland, recorded VWC at depths of 5, 10, 15, 30, 40, 60, 100 and 150 cm. Instrumentation issues at this location led to a 10-day data gap, between DOY 199 (18 July 2019) and 209 (28 July 2019). SAF 220U recorded VWC at the same depths and was located in close proximity to the EC/MET tower in the mid slope region of the upland (Figure 2). SAF 320U is located in the upper slope region of the upland and measured VWC at depths of 10, 20, 32 and 38 cm. Data were sampled every minute, and averaged at hourly and daily intervals. VWC was averaged from 0-60 cm at each station to capture entire rooting depth of trees.

Additionally, manual measurements of soil moisture were taken throughout the field season surrounding trees instrumented with SF and TF collectors to determine the impact of vegetation on the volume of rainfall reaching the surface and identify the rate at which isolated

trees deplete near-surface soil moisture. Manual measurements were taken using the handheld Stevens Hydra Probe II and recorded VWC within the top 10 cm of the soil at a frequency based on major rainfall events and extended periods without rainfall in an attempt to capture a range of soil moisture conditions. Continuous recording soil tensiometers (UMS T4 Tensiometer GmbH München; Munich, Germany) were installed adjacent to trees monitored with sap flow sensors and measured from DOY 161 (10 June 2019) to 266 (24 September 2019). Two tensiometers at depths of 30 cm and 50 cm were installed in proximity of two trees of each species (2 *Populus tremuloides*, 2 *Populus balsamifera*, 2 *Pinus banksiana*, 2 *Picea mariana*) with data being logged on a CR1000 data logger (Campbell Scientific: Logan, Utah, USA). Due to a limited number of continuously measuring tensiometers, these were coupled with additional tensiometers (Soil Measurement Systems Tensiometer; AZ, USA) measured manually. Tensiometers at 50 cm are placed close to the LFH-tailing sand interface and therefore may potentially measure soil water pressure within the tailing sand layer.

3.3. Rainfall partitioning

3.3.1. Interception

Rainfall partitioning was measured for isolated trees due to the sparse nature of the canopy. Species-specific INT was determined by collecting TF and SF volumes following major precipitation events throughout the field season. A total of 19 events were measured between DOY 145 and 266 (25 May 2019 and 25 September 2019). Data collected in the field were reviewed, and events in which clogging was apparent or gauge volumes were exceeded were removed. Canopy interception was calculated based on a simple mass balance equation, which is often used to describe precipitation partitioning and is described by (Kermavnar & Vilhar, 2017),

$$Interception = Gross\ Precipitation - (Throughfall + Stemflow) \quad (5)$$

3.3.2. Throughfall

TF was measured using v-shaped aluminum troughs cut to varying sizes, depending on tree size and area. Each sampled tree was instrumented with 2 troughs funneling into 18.9 l buckets, covered with lids to avoid evaporation from collectors (Figure 3A). Collectors were distributed across the 9 sampling plots and included 4 trees of each dominant tree species, for a total of 16 trees. After each rainfall event, bucket weights were collected, and converted to a volume of TF. TF depth in millimetres (*mm*) were calculated by dividing by the trough projection area (m^2),

$$Throughfall\ (mm) = \frac{Volume\ of\ rainfall\ collected\ during\ event\ (mm^3)}{Trough\ projection\ area\ (mm^2)} \quad (6)$$

All measurements were converted to millimeters (mm) to be comparable with precipitation data collected from the tipping rain gauge.

3.3.3. Stemflow

SF was measured on the same trees instrumented with TF collectors, using plastic funnels cut to fit the diameter of the tree trunks (Figure 3B). Funnels included a 0.5 cm polyvinyl chloride (PVC) tubing directing SF collected in the funnel to a 250 ml sampling bottle. Funnels were sealed using silicone and were continuously tested throughout the study period for potential leaks and repaired if needed. Window mesh was placed over funnels to avoid canopy litter from falling into funnels and influencing water flow through tubing. A layer of tape covered the mesh to avoid capturing direct TF through the canopy. Tape was placed about 2 cm from the trunk of the tree as to not inhibit flow down the stem but to limit drops from branches and leafy material. After each rainfall event, sample bottle volumes were weighed and converted to a depth (*mm*) of precipitation by

dividing by the tree BA (m^2). Measurements were converted to a depth (mm) to be comparable with precipitation data collected from the tipping rain gauge,

$$Stemflow\ (mm) = \frac{Volume\ of\ rainfall\ collected\ during\ event\ (mm^3)}{Canopy\ basal\ area\ (mm^2)} \quad (7)$$

Figure 3: A) V-shaped throughfall collector capturing beneath canopy rainfall of an isolated *Picea mariana* tree, B) stemflow collector on an isolated *Pinus banksiana* tree.

SF funneling ratios (FR) were calculated to analyze SF water flux. FR is a measure of the contribution from outlying parts of the tree canopy to SF volumes (Herwitz, 1986). FR is also used to determine the efficiency with which tree species are able to generate SF from incoming rainfall. This relationship is expressed as,

$$Funneling\ Ratio\ (FR) = Stemflow\ (l)/(Gross\ Precipitation\ (mm) \cdot Basal\ area\ (m^2)) \quad (8)$$

The product of GP and BA determines the amount of rainfall that would have been collected by a rain gauge of the same area of the tree trunk. FR greater than 1 indicates that the depth of SF

received at the surface of the tree is greater than the depth of precipitation received by a rain gauge (Carlyle-Moses *et al.* 2018), suggesting outlying portions of the canopy are contributing to SF production.

3.4. Upland transpiration measurements

3.4.1. Stem Heat Balance Theory

The Stem Heat Balance (SHB) method was used to measure sap flow in dominant tree species of the upland. Sensors provided by Dynamax Inc. are flexible insulating sensors that wrap around the stem of trees and avoids invasive procedures, such as the heat pulse velocity method (Burgess *et al*. 2001). These sensors provide a direct measurement of the water use of specific plants based on its movement through the stem. Sensors must be sealed and insulated to reduce changes and contributions of heat exchange from the environment. A detailed review of the SHB theory is described by Sakuratani (1981). In brief, the SHB approach consist of measuring the energy balance of the stem, which is supplied by an external continuous heating energy source. Once constant heat is supplied to the stem, the theory assumes there is no heat storage and the energy balance is expressed as,

$$Q_{in} = Q_r + Q_v + Q_f\ (W) \tag{9}$$

$$P_{in} = V^2/R \tag{10}$$

where Q_{in} is the energy input into the stem, Q_r is the radial heat conducted away from the stem into the gauge, Q_v is the vertical heat conduction through the stem and Q_f is the heat convection carried by the sap (Figure 4). Equation (10) follows Ohm's law, where V is the heater voltage and R is the heater resistance. From Equation (9), Q_v consist of two components, Q_u and Q_d, which represent the upstream and downstream fluxes of energy respectively by thermal conduction along

the stem. Broken down into upstream and downstream components, the equation can be expressed as,

$$Q_{in} = Q_r + Q_f + Q_u + Q_d\,(W) \tag{11}$$

$$Q_v = Q_u + Q_d \tag{12}$$

$$Q_u = (K_{st} \cdot A \cdot dT_u) \,/\, dX \tag{13}$$

$$Q_d = (K_{st} \cdot A \cdot dT_d)/dX \tag{14}$$

Fourier's Law is used to explain the vertical fluxes within the stem (Q_r and Q_d), using pairs of thermocouples located above and below the heating source. In Equations (13) and (14), K_{st} is the thermal conductivity of the stem, A is the cross-sectional area (m^2), dT_u/dX and dT_d/dX represent the temperature gradients and dX is the distance between the thermocouples. To compute sap flow as a mass flow rate per unit time, Q_f is calculated using the residual components of the energy balance from Equation (9). The residual components of the energy balance are then divided by the product of heat capacity of water (4.186 $J\ g^{-1}\ {}^oC^{-1}$) and the temperature increase of sap (^oC) (Dynamax Inc. 2007b),

$$F = Q_{in} - Q_v - Q_r/C_p \cdot dT \tag{15}$$

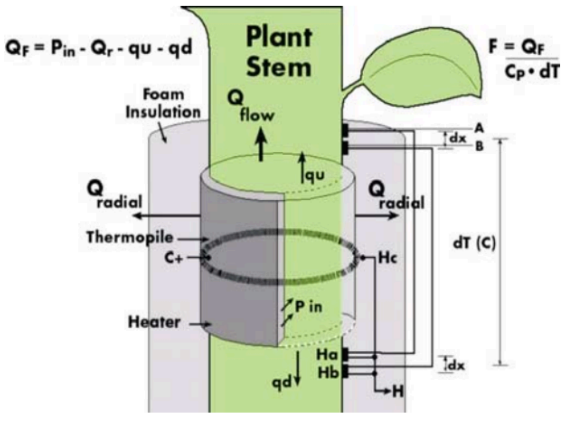

Figure 4: Diagram representing the conductive fluxes of a heated tree stem, where Q_f is the heat convection carried by the sap, Q_u and Q_d are the upstream and downstream fluxes of energy respectively by thermal conduction along the stem, and Q_s is energy lost by convection to the surrounding air (Dynamax Inc. 2007).

It is important to understand sources of errors, especially when considering assumptions with measurement methods. Accuracy of the steady-state SHB method has been estimated at approximately ± 10% (Sakuratani, 1981). However, accuracy has been found to decrease at low and high flow rates, in which low flows are common in conifers (Groot & King, 1992). Accuracy decreases at high flow rates due to the inability to adequately represent the temperature distribution within the stem by measurements at the stem surface (Groot & King, 1992). Errors in high flow rates were negligible within this study due to the exclusion of high flows beyond a specific threshold (Dynamax Inc. 2007), as well as the small tree sizes resulting in lower flow rates. Inaccuracies at low flow rates may be a result of the exclusion of the heat storage within the sap flow calculation (Grime *et al.* 1995), and the size of the error will increase with increasing tree size (Smith & Allen, 1996). However, when scaling T to daily stand measurements, the change in heat storage is generally zero (Weibel & Boersma, 1995).

3.4.2. Scaling Sap flow measurements

Stand T was estimated by up-scaling sap flow measurements collected from individual trees using tree surveys completed in the 2019 field season. Two sap flow systems were installed at the site. The first system was installed in proximity to the EC and MET tower, and the second towards the southern region of the upland. The systems collected data from DOY 145 (25 May 2019) until 266 (24 September 2019), capturing the 2019 growing season. Continuous measurements of sap flow were recorded and stored on a CR1000 Campbell Scientific data logger (Campbell Scientific; Logan, Utah, USA) installed at each site. Each system was equipped with 8 sensors, which were allocated based on dominant species in the upland. At each system, 2 *Pinus banksiana*, 2 *Picea mariana*, 2 *Populus tremuloides* and 2 *Populus balsamifera* were instrumented with sap flow sensors (Table 1), for a total of 4 trees of each species. To accurately estimate stand T, a range of

species of varying size must be sampled to capture stand heterogeneity. Due to sensor availability, trees were selected based on average size, and therefore DBH of instrumented trees ranged from 1.2 cm to 3.8 cm (Table 1). Instrumenting trees based on average size raises uncertainty in scaling processes, as measurements are not capturing the entire range in tree size and therefore not accounting for the heterogeneity in the stand.

Table 1: Sap flow sensor installation characteristics including location, sensor number, sensor type and size, species, DBH (cm) and height (m).

Location	Sensor Number	Sensor Type/Size	Species	DBH (cm)	Height (m)
System 1 (220U – EC/MET Tower)	1	SGB25	*Pinus banksiana*	3.34	2.22
	2	SGB25	*Pinus banksiana*	2.87	1.94
	3	SGA10	*Picea mariana*	1.66	0.98
	4	SGEX13	*Picea mariana*	1.43	1.06
	5	SGEX16	*Populus tremuloides*	1.59	2.47
	6	SGB25	*Populus tremuloides*	1.59	1.90
	7	SGEX13	*Populus balsamifera*	1.50	1.67
	8	SGEX13	*Populus balsamifera*	1.88	2.01
System 2 (320U – Soil moisture station)	1	SGB25	*Pinus banksiana*	3.82	2.08
	2	SGB25	*Pinus banksiana*	3.66	1.90
	3	SGEX10	*Picea mariana*	1.18	1.02
	4	SGEX10	*Picea mariana*	1.27	1.01
	5	SGEX13	*Populus tremuloides*	1.94	2.33
	6	SGEX13	*Populus tremuloides*	1.43	1.84
	7	SGA10	*Populus balsamifera*	1.43	2.07
	8	SGEX16	*Populus balsamifera*	1.97	1.91

Raw data was reported as hourly sap flux measurements ($g\ hour^{-1}$) and quality controlled by correcting for gaps, faulty sensor measurements, and broken sensors. After processing, all 16 sensors had quality data to be used in the scaling process. Scaling from single tree to stand

measurements is based on the relationship between daily sap flow and a specific biometric parameter, typically tree DBH or BA are used (Čermák *et al.* 2004). Daily sap flow sums were calculated for each instrumented tree and used to develop daily regression equations. Daily sums per species were obtained to preserve daily dynamics in sap flow (Cienciala *et al.* 1997). Linear regression equations were created for each of the 4 dominant tree species (*Pinus banksiana, Picea mariana, Populus balsamifera, Populus tremuloides*) between modelled total daily flow and DBH for each day between DOY 145 and 266 (25 May 2019 and 24 September 2019). Daily regression equations were applied to the 2019 tree survey using the estimated sapwood area (cm^2) and daily flows per plot were determined. A major limitation is found in scaling from tree to stand-level measurements, due to difficulties in determination of sapwood area (Kool *et al.* 2014). The inability to conduct destructive sampling on site led to the use of an estimate of sapwood area. Potential errors may arise, as using an estimated value of sapwood area may not be representative of all trees used in the scaling measurement. Existing literature discusses the relationship between DBH and sapwood area for mature boreal tree species, however there is little research done on juvenile trees. Bond-Lamberty *et al.* (2002), determined a relationship between DBH and sapwood area for Canadian boreal tree saplings for *Pinus banksiana*, *Picea mariana* and *Populus tremuloides*. This relationship was determined using linear regression and a logarithmic transformation to correct for heterogenous variation of the independent diameter variable (Bond-Lamberty *et al.* 2002),

$$Sapwood\ Area\ (cm^2) = a + b\ (Log_{10}DBH) + c(AGE) + d\ (Log_{10}DBH \cdot AGE) \quad (16)$$

where *a, b, c*, and *d* are species-specific parameters determined from destructive sampling procedures by Bond-Lamberty *et al.* (2002) (Table 2), DBH (*cm*) of trees with height of 1.37 m and greater, AGE is the age of trees in years. The age of trees was determined to be 6 years, as this

is when the site was planted, and all trees are of similar size and age. Total cumulative volume of water use per species (*l*) was summed for each subplot and converted to mm day^{-1} following a series of conversions similar to what was done by Langs (2019) and Gabrielli (2016). In brief, once the daily regressions are applied to the tree survey and daily flows are summed (*l day^{-1}*), T is then converted to ground-area by dividing by the total sampled area of the tree survey (*m^2*) (Santos *et al.* 2012). This conversion results in a depth in m day^{-1}, which is subsequently converted to mm day^{-1}. Total daily T as a depth (*mm day^{-1}*) was averaged per plot and then across the study area. Potential errors may arise due to omitting radial variability in stem sap flow, where not accounting for radial variability may result in overestimation of sap fluxes (Ford *et al.* 2007). Ford *et al.* (2007) found that errors in scaling to stand-level may be minimized by obtaining stand-scale LAI measurements, which were not possible in the sparse canopy at NFW.

Table 2: Species-specific parameters for relationship between diameter at breast height (DBH) and sapwood area determined from destructive sampling procedures (Bond-Lamberty *et al.* 2002).

Species	DBH Range (cm)	*a*	*b*	*c*	*d*	R^2
Populus tremuloides	0.4 – 23.7	0.000	2.015	-0.014	0.008	0.995
Picea mariana	0.3 – 14.8	-0.451	2.442	0.002	-0.007	0.961
Pinus banksiana	0.7 – 17.0	-0.221	2.145	-0.004	0.000	0.984
Populus balsamifera	0.4 – 23.7	0.000	2.015	-0.014	0.008	0.995

Chapter 4: Results

4.1. Climate and vegetation dynamics

The study was conducted throughout the 2019 growing season, which generally extends from mid-May to early September. Specifically, data collection occurred between DOY 145 to 267 (25 May to 24 September, 2019). Over the study period, the upland received 287.5 mm of rainfall, slightly exceeding the Fort McMurray thirty-year climate normal (1981-2010) of 283.4 mm (Environment Canada, 2015). Maximum rainfall of 38.1 mm occurred on DOY 228 (16 August 2019), with other notable events occurring on DOY 179 (28 June 2019; 28.8 mm) and DOY 215 (3 August 2019; 22.3 mm) (Figure 5A). Majority of precipitation fell throughout the early and end of the growing season, specifically in June and August with 78.1 mm and 125.5 mm, respectively. PET at the site surpassed precipitation, reaching 428.3 mm over the growing season.

Average air temperature at NFW from DOY 145 to 267 (25 May to 24 September 2019) was 15.6ºC (Figure 5B). Monthly average temperatures were 12.5ºC, 16.97 ºC, 18.8 ºC, 15.6 ºC and 13.6 ºC, respectively, higher than Fort McMurray thirty-year climate normal data (1981-2010) of 9.9ºC, 14.6ºC, 17.1ºC, 15.4ºC and 9.5ºC (Environment and Climate Change Canada, 2015). Relative humidity (RH) followed similar patterns as air temperature, increasing throughout peak growing season and decreasing during the month of August with the onset of senescence (Figure 5C). Seasonal mean RH was approximately 65%, with spikes occurring during large precipitation events, and minimums occurring several consecutive days of no rainfall.

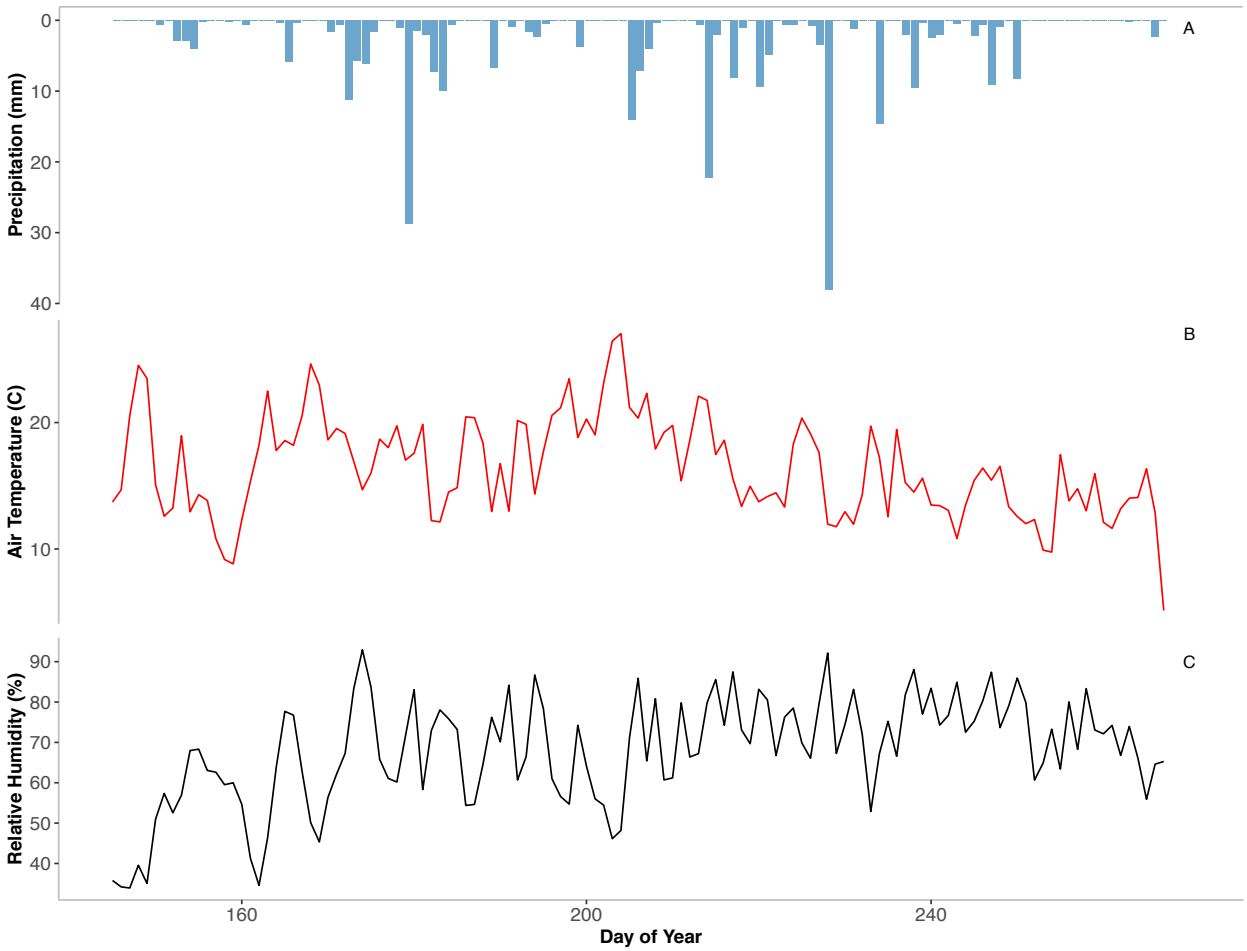

Figure 5: Growing season (25 May – 24 September 2019) time series of (A) total daily precipitation (mm), (B) daily average air temperature (°C), and (C) daily average relative humidity (%) at the Nikanotee Fen Watershed (NFW), Fort McMurray, Alberta.

Monthly average VPD ranged between 0.57 to 1.67 kPa at the NFW, fluctuating throughout the study period (Figure 6). Fluctuations were large in the early and middle stages of the growing season, decreasing moving into the month of August when precipitation was high. VPD and Q^* follow similar trends, increasing slightly until August and then decreasing for the remainder of the season (Figure 6). Q^* averaged 112.8 W m^{-2} during the growing season, reaching daily average maximum of 190.3 W m^{-2} on DOY 176 (25 June 2019).

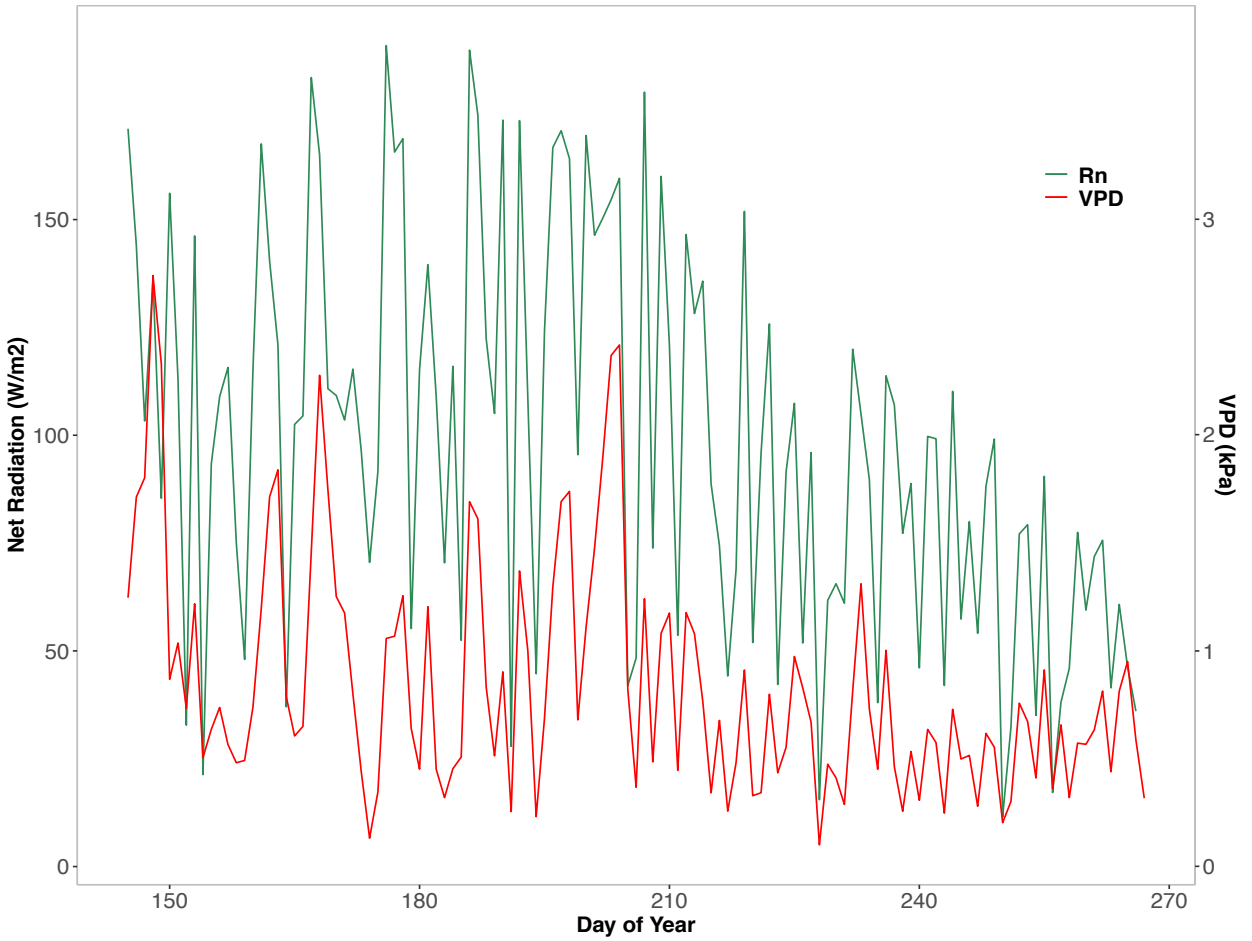

Figure 6: Daily average daytime vapour pressure deficit (VPD) (kPa) and net radiation (Q*) (W m^{-2}) at Nikanotee Fen Watershed (NFW), Fort McMurray, Alberta, 2019.

Dominant tree population in the upland includes conifer tree species *Picea mariana*, *Pinus banksiana*, and broadleaf deciduous species *Populus balsamifera* and *Populus tremuloides* trees. Additional trees populating the site include *Larix laricina* (tamarack) and *Alnus tenuifolia* (river alder), which constitute only 3% of the total tree population and were not considered for this study. Overall, tree population in the study area consisted primarily of *Populus balsamifera* which make up 72%, followed by *Picea mariana*, *Populus tremuloides* and *Pinus banksiana* at 13%, 8.4% and 8.3%, respectively (Table 3). Variability in tree height and DBH was large for *Populus balsamifera* due to the significant abundance of tree saplings (Figure 6). Average height and DBH were 1.4 m (± 0.28) and 5.23 cm (± 2.55) for *Populus balsamifera*, 1.14 m (± 1) and 3.12 cm (± 0.60) for

Picea mariana, 2.40 m (± 0.29) and 8.0 cm (±1.27) for *Pinus banksiana* and 1.87 m (± 0.88) and 4.20 cm (± 2) for *Populus tremuloides* (Table 3). *Picea mariana* trees were generally smaller than the other species, with the largest tree measuring 1.85 m in height and a corresponding DBH of 1.4 cm. Population composition of prevalent tree species differed significantly along transects moving upslope from the fen peatland. Although not planted, *Populus tremuloides* and *Populus balsamifera* tree species have dominated the transition zone with 96% of the tree population, while *Picea mariana* consisted of only 4%. The middle transect starts a transition towards a growing presence of conifer trees, as *Pinus banksiana* and *Picea mariana* make up 20% collectively. The final transect, approximately 130 m south of the middle transect and in the upper slope region furthest from the fen peatland, was dominated by conifer species consisting of 71% of total tree population. *Populus tremuloides* and *Populus balsamifera* represented only 29% of the tree population within this transect. Tree planting density in the upland was 6001 stems per hectare.

Table 3: Characteristics of Nikanotee Fen Watershed (NFW), Fort McMurray, Alberta, upland tree survey of dominant tree species including total tree count, percent coverage (%), mean diameter at breast height (DBH) (cm), mean height (m) and average foliage densities (m^{-1}). (± value represent standard deviations)

Species	Number of trees	Percent cover (%)	Mean DBH (cm)	Mean Height (m)	Average Foliage Density (m^{-1})
Picea mariana	52	12.26	3.12 (± 0.60)	1.14 (± 0.28)	3.20 (± 1.09)
Pinus banksiana	33	7.78	8.00 (± 1.27)	2.40 (± 0.29)	2.62 (± 0.72)
Populus balsamifera	304	71.70	5.23 (± 2.55)	1.14 (± 1)	1.69 (± 0.51)
Populus tremuloides	35	8.25	4.20 (± 2)	1.87 (± 0.88)	1.26 (± 0.50)

Foliage density (Table 3) is the total leaf surface area per unit volume of space (m^2 m^{-3}) and is a good measure of vegetation structure, specifically for isolated canopies (Jain *et al.* 2010). Coniferous tree species averaged greater foliage densities than deciduous species (Table 3). *Picea*

mariana reported the highest densities averaging 3.20 m^{-1} (± 1.09 m^{-1}), despite their relatively low average heights and DBH (Figure 7). DBH averages were collected from a smaller population, as a majority of *Picea mariana* trees were below a height of 1.37 m and omitted from average measurements. *Pinus banksiana* followed with an average foliage density of 2.62 m^{-1} (± 0.72 m^{-1}), while *Populus balsamifera* and *Populus tremuloides* reported averages of 1.69 m^{-1} (± 0.51 m^{-1}) and 1.26 m^{-1} (± 0.50 m^{-1}), respectively. Foliage densities for all dominant species peaked in July during peak growth period and declined significantly in August with the onset of senescence. Foliage densities decreased most during senescence for deciduous tree species which lose their leaves.

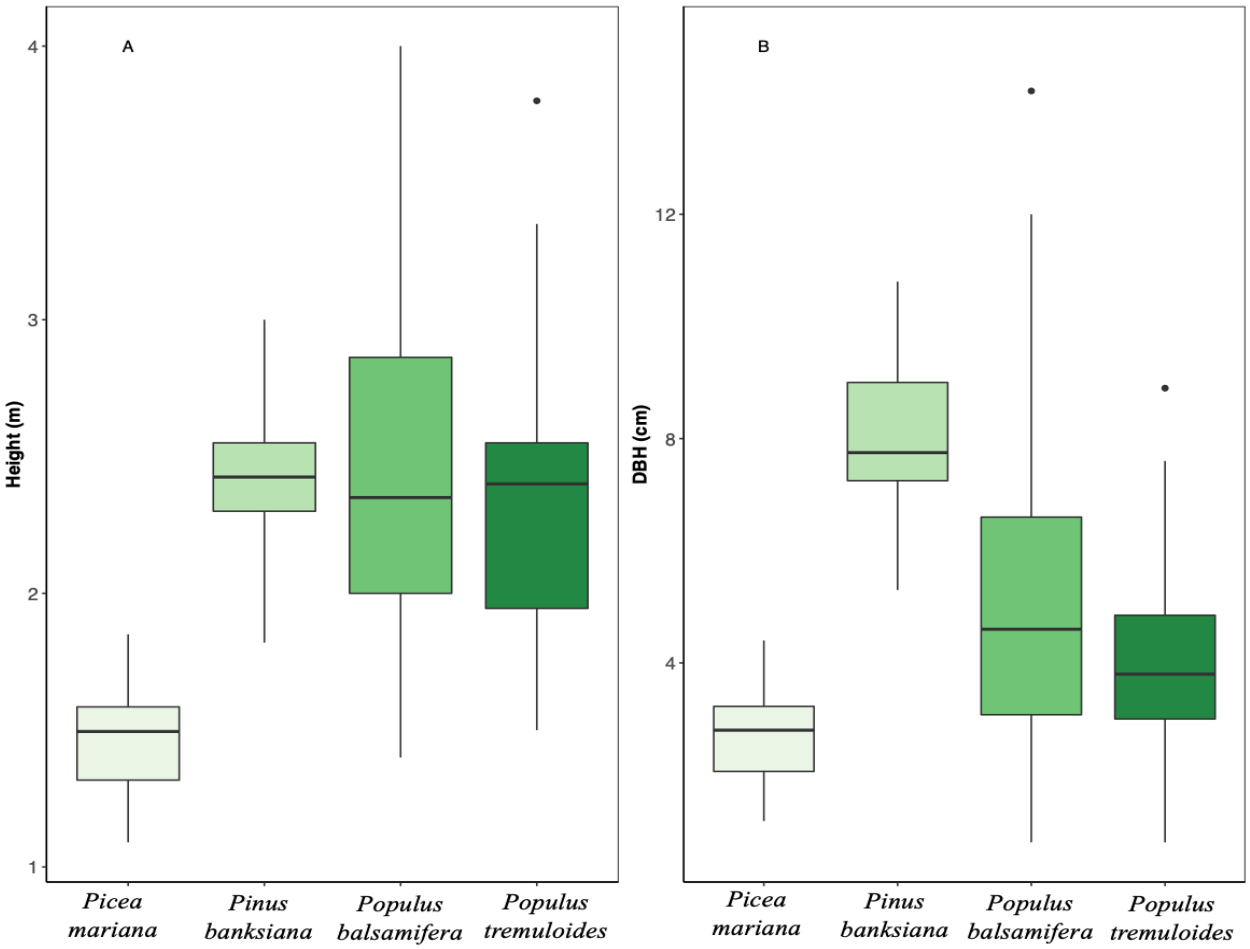

Figure 7: Average tree height (m) and diameter at breast height (DBH) (cm) measured from tree surveys for dominant upland tree species at the Nikanotee Fen Watershed (NFW), Fort McMurray, Alberta, 2019.

4.2. Rainfall partitioning

4.2.1. Throughfall

During the study period, 18 rainfall events were measured, which yielded a total of 258.8 mm, accounting for approximately 90% of total growing season rainfall. Individual measured events ranged from 1 mm to 43.8 mm, with the largest occurring towards the end of the growing season on DOY 229 (17 August 2019). Few measurements were removed due to obstruction or damage to the gauge, such as blocking of the tubes from falling litter. Partitioning averages between TF, SF and INT per species are summarized in Table 4.

Table 4: Rainfall partitioning contributions (%) and average stemflow funnelling ratios of studied dominant tree species at the Nikanotee Fen Watershed (NFW), Fort McMurray, Alberta, 2019.

Tree Species	Throughfall (%)	Stemflow (%)	Interception (%)	Average Stemflow Funnelling Ratios
Picea mariana	51.8	13.7	34.5	19.3
Pinus banksiana	66.2	2.3	31.5	4.8
Populus tremuloides	67.3	4.2	28.5	5.0
Populus balsamifera	70.4	3.9	25.7	6.6

TF was the largest rainfall partitioning pathway of the measured tree species. Strong linear relationships were found between TF (mm) and gross precipitation (mm) for all measured trees, with TF increasing with increasing rainfall (Figure 8). All trees (*Picea mariana*, *Populus balsamifera, Pinus banksiana* and *Populus tremuloides*) had linear correlations of $r^2 = 0.97$ (p-value <0.001) (Figure 8). The intercept of the regression equations indicates the interception capacity of the tree, in which *Populus balsamifera* had the largest of the 4 species. For larger rainfall events (> 40 mm), Figure 8 shows that approximately 20-30 mm is partitioned as TF.

While SF consists of a small proportion of incoming rainfall and trees have small interception capacities, the differences are accounted by rainfall falling without interacting with vegetation. When considering all TF gauges, cumulative TF ranged between 89.0 mm (34.4% of total cumulative TF) to 167.2 mm (64.6% of total cumulative TF) with considerable variability between tree species. On average, cumulative TF depths were higher for broadleaf trees (*Populus tremuloides* and *Populus balsamifera*) than coniferous (*Picea mariana* and *Pinus banksiana*) (Table 5). On an event scale, TF ranged from 0.1 mm to 41.3 mm, once again with significant variability between tree species. During most events, broadleaf species contributed most to total TF depths (Table 5). Variability in event scale TF was observed for broadleaf species over the course of the growing season, where events of the same scale and intensity resulted in a decrease in TF as the growing season progressed and leaf expansion developed. Similar trends were observed for coniferous species, but less evident due to minimal needle growth throughout the growing year. The relationship between percentage of gross precipitation partitioned into TF and gross precipitation (mm) showed an initial increase in TF percentages until a certain precipitation threshold after which TF percentage begins to plateau (Figure 11).

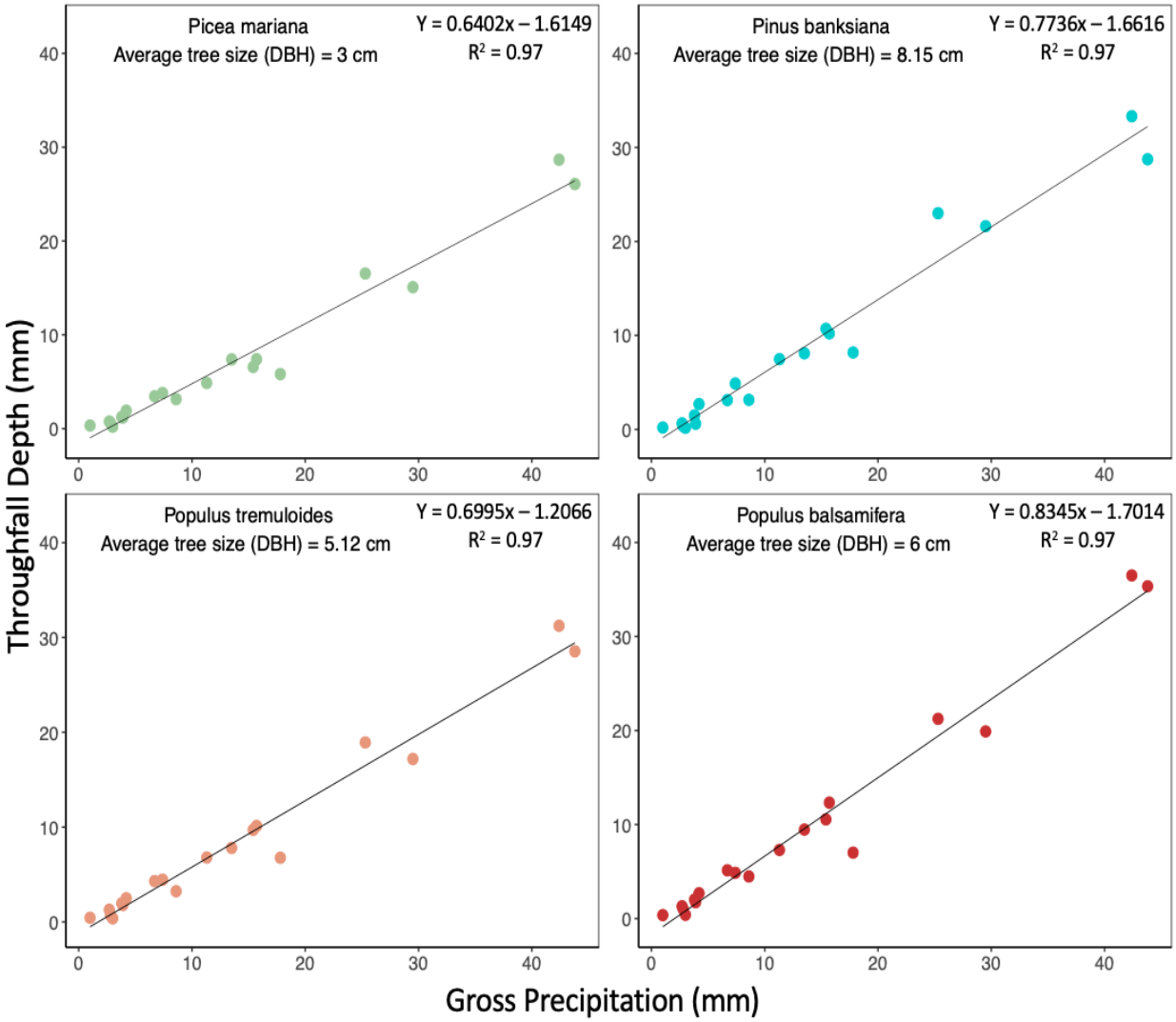

Figure 8: Average event scale throughfall depth (mm) of dominant tree species in relation to event gross precipitation (mm) during the growing season at the Nikanotee Fen Watershed (NFW), Fort McMurray, Alberta, 2019.

4.2.2. Stemflow

SF production by all tree species were volumetrically smaller than INT and TF, ranging between <1% to 50.6%, and varying considerably within and between species. An average of 13.7% of incoming rainfall was partitioned as SF by *Picea mariana* trees (Table 4), which was the largest contribution of the tree species measured. Contrarily, *Pinus banksiana* had the lowest SF contribution with an average of 2.3% of gross precipitation (Table 4). The variability between broadleaf species of *Populus tremuloides* and *Populus balsamifera* were minimal as they yielded

averages of 4.2% and 3.9%, respectively (Table 4). SF generation was initiated by *Picea mariana, Populus tremuloides* and *Populus balsamifera* for all rainfall events, while *Pinus banksiana* did not initiate substantial SF until a rainfall magnitude of approximately 3 mm.

Table 5: Average growing season cumulative rainfall partitioning depths (mm) and rainfall partitioning pathways as a percentage of total precipitation for the growing season at the Nikanotee Fen Watershed (NFW), Fort McMurray, Alberta, 2019.

Growing	Throughfall		Stemflow		Interception	
Season	mm	%	mm	%	mm	%
Broadleaf	170.8	66	13.1	5.1	74.8	28.9
Coniferous	151.9	58.7	19.7	7.6	87.2	33.7

Bark roughness has been determined to have a strong impact on SF production, as rougher bark surfaces have a higher storage capacity ultimately reducing SF (Siegert & Levia, 2014; Barbier *et al*. 2009). Coniferous and broadleaf tree species differed significantly in their respective bark roughness. Results showed that broadleaf trees contributed more to TF (%) averaging 66% of total rainfall, while INT and SF were greater for coniferous trees throughout the growing season (Table 5). Broadleaf trees (*Populus tremuloides* and *Populus balsamifera*) have smooth bark surfaces while coniferous trees (*Picea mariana* and *Pinus banksiana*) have characteristically rougher bark surfaces (Carlyle & Price, 2006; Barbier *et al.* 2009; Levia & Herwitz, 2005; Livesley *et al.* 2014). These characteristics resulted in *Pinus banksiana* producing lower SF depths with rougher barks than the broadleaf tree species (Figure 9). However, *Picea mariana* differed from this hypothesis as it yielded a significantly higher average SF (Table 4) and overall was most efficient at partitioning rainfall into SF. Figure 9 shows the event scale variability in SF production, for all measured species. As leaf and needles developed over the growing season, SF production decreased for events of similar size and intensity, due to a higher percentage of rainfall being

intercepted by the canopy. The relationship between SF depth (mm) and gross precipitation (mm) was similar for all species, with SF depth reaching a plateau within a rainfall range of 15 mm to 17 mm (Figure 9). During a rainfall event of 13.5 mm on DOY 175 (24 June 2019), *Populus balsamifera* and *Populus tremuloides* experienced maximum SF depths above 2 mm, representing an outlier greater than the rest of the data points measured.

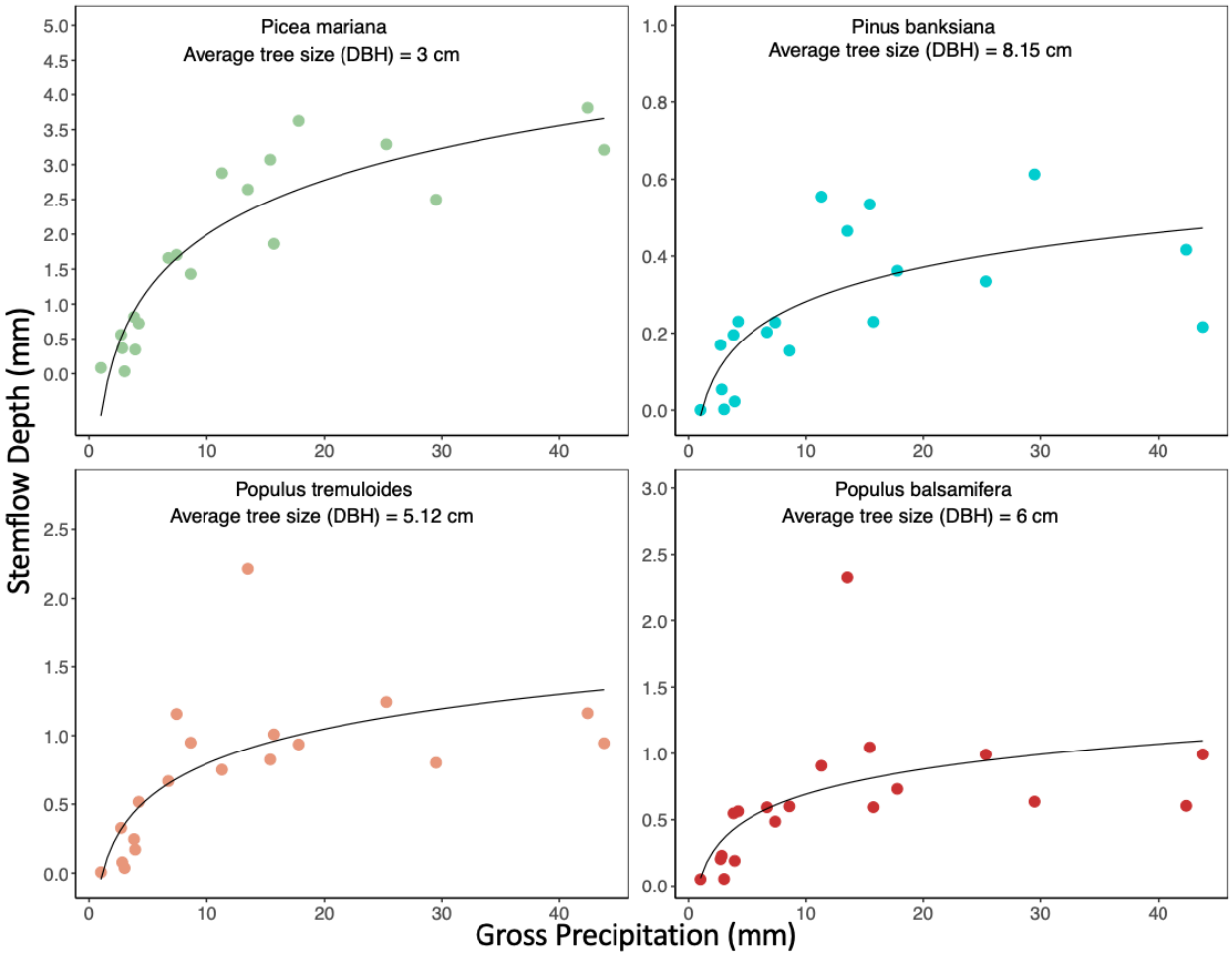

Figure 9: Average event scale stemflow depth (mm) of dominant tree species in relation to event gross precipitation (mm) during the growing season at the Nikanotee Fen Watershed (NFW), Fort McMurray, Alberta, 2019.

SF funneling ratios were variable within and between species, initially increasing with increasing rainfall depth until reaching a peak, after which ratios began decreasing with increasing rainfall (Figure 10). This depth differed for each species, with ratios reaching a maximum at 11.3

mm for *Picea mariana*, 4.2 mm for *Pinus banksiana* and *Populus balsamifera*, and 2.7 mm for *Populus tremuloides* (Figure 10). Few trees yielded low FR relative to findings in existing literature (Lishman, 2015; Swaffer *et al.* 2014). Low FR (FR < 1) suggesting that these trees (*Pinus banksiana* and *Populus tremuloides*) are inefficient at generating SF during small magnitude rainfall events. Most trees remained above a ratio of 1 (FR > 1) indicating they are having contributions from outlying parts of the canopy and highlight the impacts of meteorological conditions on SF production (Siegert & Levia, 2014). Event scale FR ranged between 0.15 and 71.5 throughout the growing season, while demonstrating clear differences in funneling capabilities between species. Average species funneling ratios were 19.3 (*Picea mariana*), 4.8 (*Pinus banksiana*), 5.0 (*Populus tremuloides*) and 6.6 (*Populus balsamifera*) (Table 4). Results show that SF funnelling ratios are greater for smaller trees such as *Picea mariana*, which have a greater ability to funnel SF per unit BA (Figure 10). While following similar trends with increasing precipitation, ratios were generally smaller for trees of greater average DBH, such as *Pinus banksiana.* Angles of needles and leaves, as well as geometric orientation of branches played a role in each trees ability to partition SF, which was ultimately shown through SF FR.

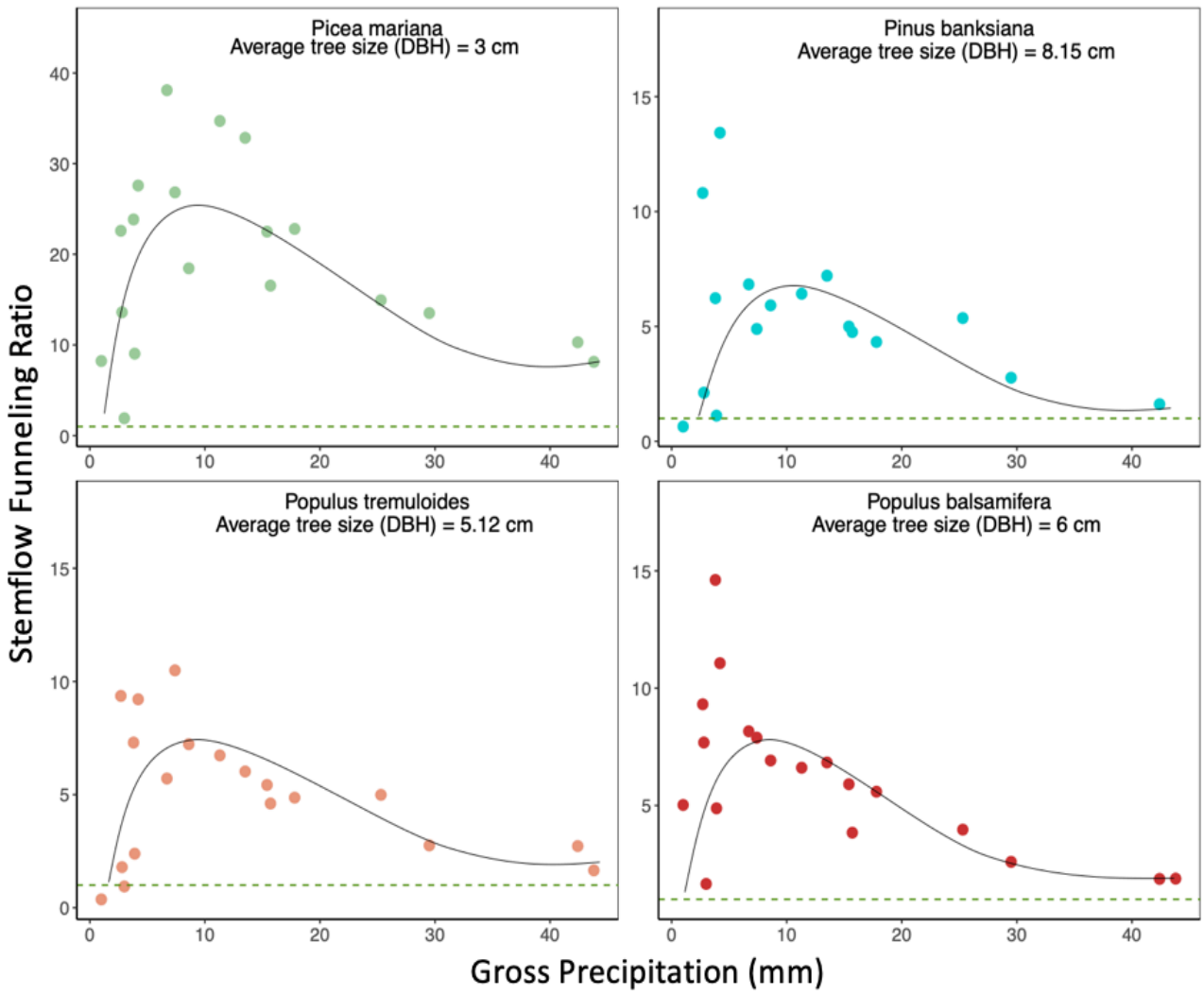

Figure 10: Average event scale stemflow depth (mm) of dominant tree species in relation to event gross precipitation (mm) during the growing season at the Nikanotee Fen Watershed (NFW), Fort McMurray, Alberta, 2019. Dashed line indicates a stemflow funneling ratio of 1.

4.2.3. Interception

Canopy INT was the second largest rainfall partition, ranging between 1.9% to 96.7% depending on tree and rainfall characteristics (Figure 11). Pooling all tree species measured at the site, INT differed between conifer and broadleaf trees, with coniferous trees 4.8% greater than broadleaf trees (Table 5). On an individual species scale, *Picea mariana* yielded greater INT percentages (34.5%) as a result of high foliage densities (Table 4). Similarly, *Pinus banksiana* had a greater

INT percentage (31.5%; Table 4) than broadleaf tree species, however, it was slightly lower than *Picea mariana* due to its sparser canopy and lower density needle distribution. *Populus tremuloides* and *Populus balsamifera* both had similar ranges in intercepted rainfall with overall seasonal average percentages of 28.5% and 25.7%, respectively (Table 4). Similar to trends in TF and SF, INT of measured trees varied on an event scale throughout the growing season. Both coniferous and broadleaf species experienced increases in INT depths as the growing season progressed and leaf and needle growth were enhanced. The relationship between interception depth (mm) and gross precipitation (mm) was linear, with INT increasing with event size. Figure 11 shows INT as a percentage of gross precipitation (mm) for events measured throughout the growing season and followed a hyperbolic decay relationship. Initially, INT percentages decreased rapidly with minor increases in rainfall magnitude. At approximately a rainfall size of 10 mm, the difference in average interception percentages with increasing rainfall began to decrease for all measured trees.

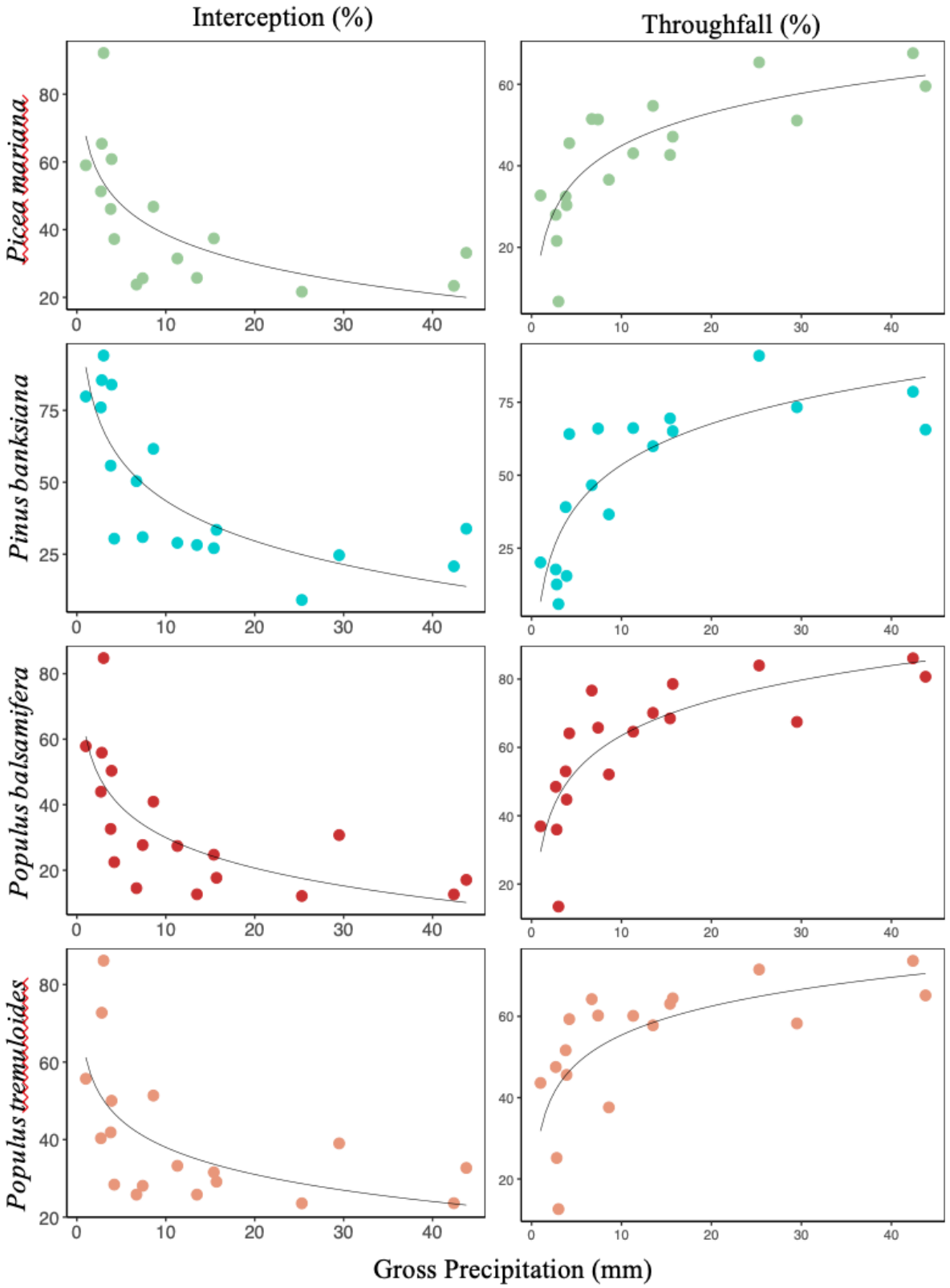

Figure 11: Analysis of throughfall (%) and interception (%) as a function of gross precipitation (mm) for all studied tree species at the Nikanotee Fen Watershed (NFW), Fort McMurray, Alberta, 2019.

Manual soil moisture measurements recorded at the base of instrumented trees highlighted the impacts of tree rainfall partitioning on near-surface soil moisture regimes. Measurements were taken away from the base of the tree to avoid roots and therefore might miss some impacts from SF. After days of minimal precipitation and soil drying, *Picea mariana* had higher VWC within the top 10 cm than the other tree species. Greater VWC by *Picea mariana* corresponded with low water use by this species and minimal root water uptake, reducing depletion of water storage. Following rainfall events, VWC around the base of *Populus balsamifera* and *Populus tremuloides* trees was greater than coniferous trees, as a result of high TF and low INT by broadleaf species, increasing water distribution to the base of the tree. Coniferous trees had lower VWC than broadleaf trees due to low TF and high INT, which minimized the depth of water reaching the base of the tree. Almost all tree species were responsive to rainfall events, as tensiometers show an increase in soil water pressure almost instantaneously with increasing VWC. However, *Picea mariana* tensiometers do not respond quickly to rainfall events and experience a slight delay in the response due to low TF and despite having high SF volumes.

4.3. Transpiration and Evapotranspiration

Sap flow sensors and vegetation survey data were used to derive stand level transpiration between DOY 145 and 267 (25 May to 24 September 2019) through the use of linear regression models (Cienciala *et al.* 2000; Quiñonez-Piñón, 2007). Up-scaling transpiration to dominant tree species resulted in a total T of 122.1 mm for the growing season. Average growing season stand T was approximately 1 mm day^{-1}, with a range from 0.15 mm day^{-1} on DOY 174 (23 June 2019) to 3.45 mm day^{-1} on DOY 207 (26 July 2019). The greatest water depths transpired by the stand, amounting to 36.2% of total T, occurred in the month of July during periods of greatest leaf expansion with a measured total depth of 44.2 mm. T was lowest for the month of May, with a

total of 5.8 mm, accounting for only 4.7% of total T. T rates at NFW varied throughout the growing season remaining relatively low until DOY 177 (26 June 2019), when it spiked significantly from 0.77 mm day^{-1} to 2.65 mm day^{-1} (Figure 7). This was followed by a moderately high and consistent trend for the duration of July and August, during the aforementioned period when leaves were fully developed. High T rates in July (36.2%, 44.2 mm) and August (30.9%, 37.8 mm) were associated with a period of large rainfall events, in which 65% of total growing season rainfall occurred. T rates responded quickly to large rainfall events, as noteworthy spikes were observed. This is evident on DOY 207 (26 July 2019) when daily T rates peaked at 3.45 mm day^{-1} following 3 consecutive days of rainfall, totalling a depth of 25.3 mm of precipitation. This was also seen on DOY 216 (4 August 2019), when daily T rates spiked once again at 2.65 mm day^{-1} following 3 days (1 August to 4 August 2019) of precipitation (25.1 mm).

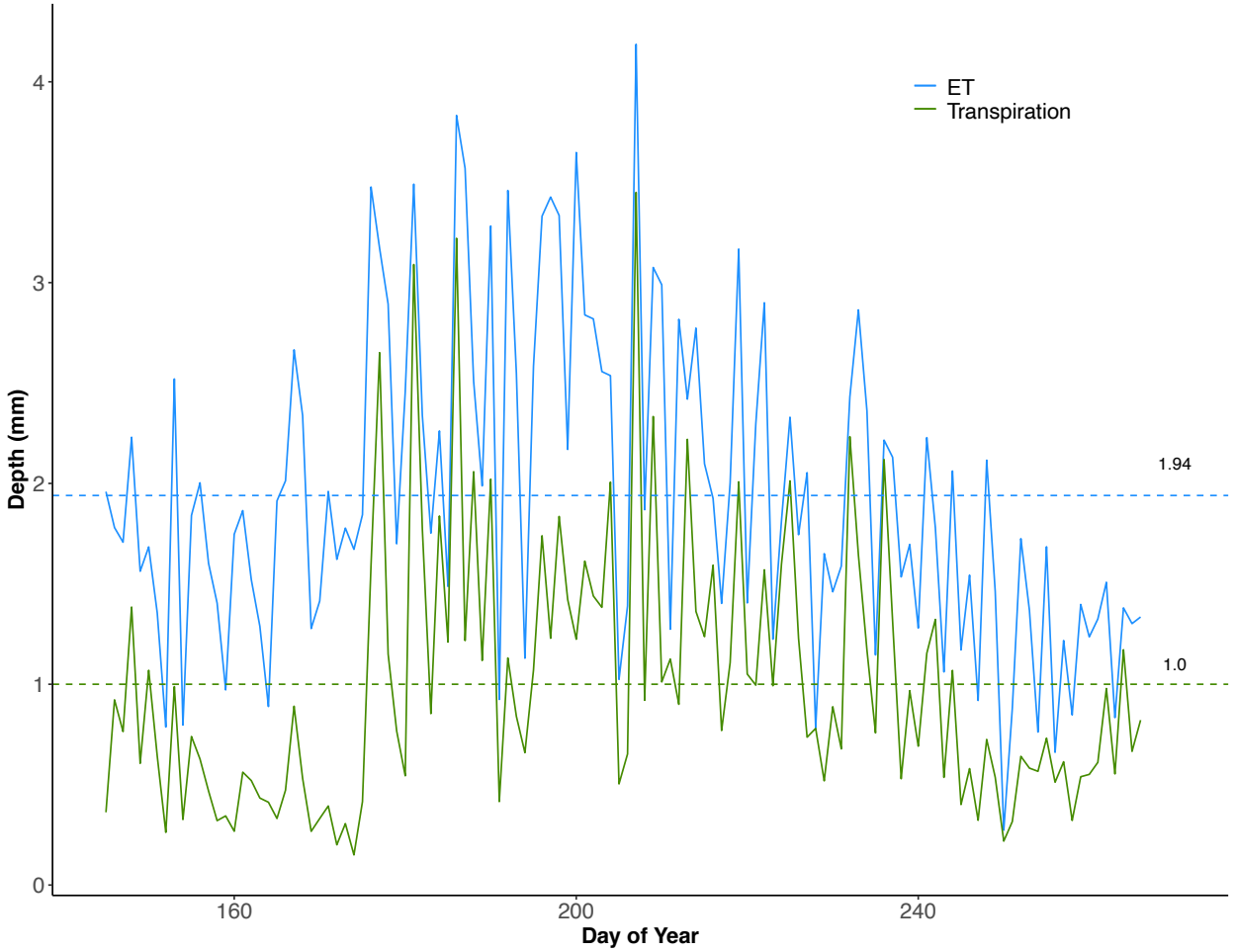

Figure 12: Scaled stand level transpiration (mm day-1) and evapotranspiration (mm day-1) for the 2019 growing season at the Nikanotee Fen Watershed (NFW), Fort McMurray, Alberta.

ET was obtained from an EC tower for the same time period as T data. Seasonal mean ET was 1.94 mm day^{-1}, ranging from 0.66 mm day^{-1} to 4.19 mm day^{-1} (Figure 12). ET exceeded precipitation in May, July and September, whereas precipitation exceeded ET in June and August. ET followed similar trends to T throughout the growing season, both reaching maximums on DOY 207 (26 July 2019). Total ET during the growing season was 236.9 mm, with T accounting for 52%. Both followed similar seasonality, with higher depths of water lost through ET throughout the months of July and August, and declining into September when senescence begins, and T is reduced. T and ET in the month of September accounted for 11.5% (14.0 mm) and 12.2% (29

mm), respectively. There were 3 occurrences during the growing season when T was considerably lower than ET. The first occurred between DOY 154 to 174, which was marked as a period with minimal leaf development and a time of heavy rainfall (37.2 mm). Between DOY 225 to 232, 43.7 mm of rain fell resulting in T lagging behind ET rates. Both periods are distinguishable by heavy rainfall events where evaporation of intercepted water outweighed T rates. The large differences amid T and ET between DOY 191 and 204 result from low water availability, limiting root water uptake.

Species contributions to overall upland T are summarized in Table 6. *Populus balsamifera* tree species had the greatest contribution to T, accounting for 57% as a result of its large tree population. There was low variability between *Picea mariana*, *Pinus banksiana* and *Populus tremuloides* contributing 16%, 13% and 14%, respectively. T peaked for all species in July, except *Populus balsamifera* which had its highest monthly total T depth in August (Table 6). Beginning in September, T of broadleaved species began decreasing as trees moved into senescence, while conifer trees continued to consistently transpire until the end of the growing season.

Table 6: Summary of species characteristics (Number of Trees, Percentage Cover (%)) and contributions to upland T (%) and their respective average daily T (mm) throughout the 2019 growing season at the Nikanotee Fen Watershed (NFW), Fort McMurray, Alberta.

Species	Number of Trees	Percentage Cover (%)	Percentage of Total T (%)	Average Species Daily T (mm day^{-1})
Picea mariana	53	23	16	0.62
Pinus banksiana	33	14	13	0.54
Populus tremuloides	32	13	14	0.53
Populus balsamifera	116	50	57	2.33

4.4. Seasonal trends in water availability and tree water use

Sap mass fluxes (g hour^{-1}) were measured on dominant tree species in the upland from DOY 145 to 267 during the 2019 growing season. A 26-day period from DOY 205 to 231 (24 July to 19 August 2019) was used to analyse species specific sap fluxes (Figure 13 & 14). This period was selected due to the occurrence of large precipitation events, ultimately to observe species response to water availability.

Early growing season sap velocity increased with a period of rapid leaf expansion. Diurnal patterns in sap flow were also evident over the study period, with exception of rainy days where sap fluxes were suppressed, and VPD remained below 1 kPa. On DOY 228 (16 August 2019) the site received 38.1 mm of rain with a rainfall intensity of 3.7 mm hour^{-1}, resulting in suppressed sap fluxes for all species. Figures 13 and 14 highlight a delay in the increases in sap fluxes following rainfall events, where increases occur a day or two following the event. During days with little or no rainfall, there are spikes in sap fluxes for *Populus tremuloides*, *Populus balsamifera* and *Pinus banksiana* species, while *Picea mariana* remained reasonably low and consistent (Figure 13 & 14). There was a steady increase in VWC throughout the month of August, as the site received a total of 125.5 mm (43.7%) of rain. The late summer increase in VWC was accompanied by increases in sap fluxes for all measured trees. Along with the large rainfall period in August, there are reasonably low sap fluxes moving into September as vegetation begins to transition into senescence. Rapid changes in sap fluxes observed for all species, which were especially evident for Pinus banksiana, indicate the presence of clouds reducing Q* and VPD.

Sap flow measurements presented significant variability in water uptake rates among different tree species. Instrumented dominant tree species experienced an increase in sap fluxes approaching the end of June into July, coinciding with a period of rapid leaf expansion observed

through LAI measurements. Magnitude in tree water use varied in response to tree size (DBH), as trees with larger DBH had greater water use. Overall, *Pinus banksiana* trees have the highest water use among all species transpiring as much as 463.7 g hour^{-1} throughout the growing season and coincided with the large tree size relative to other species measured at the site. Contributions are followed by *Populus tremuloides*, *Populus balsamifera* and *Picea mariana,* respectively. *Populus tremuloides* trees had general trends of high sap fluxes in the early growing season until approximately DOY 213 (1 August 2019), where sap fluxes decreased for the remainder of the season (Figure 13 & 14). Variations between broadleaf tree species were minimal, following comparable trends and having similar daily magnitudes in water use. *Populus tremuloides* and *Populus balsamifera* transpired as much as 451.4 g hour^{-1} and 427.4 g hour^{-1}, respectively, on days of high evaporative demand. *Picea mariana* sap fluxes were considerably lower and remained consistent throughout the measurement period, resulting in the lowest average growing season tree water use. *Picea mariana* magnitudes amounted to approximately a third of *Pinus banksiana*, *Populus tremuloides* and *Populus balsamifera* water use, peaking at 168.3 g hour^{-1} on DOY 174 (23 June 2019). Figures 13 and 14 show a spatial variation in tree water use and water availability at the site, with a transition from dryer VWC conditions and less variability at station 320U further away from the transition zone (Figure 14) to higher VWC and more variability at station 220U closer to the upland-fen transition zone (Figure 13).

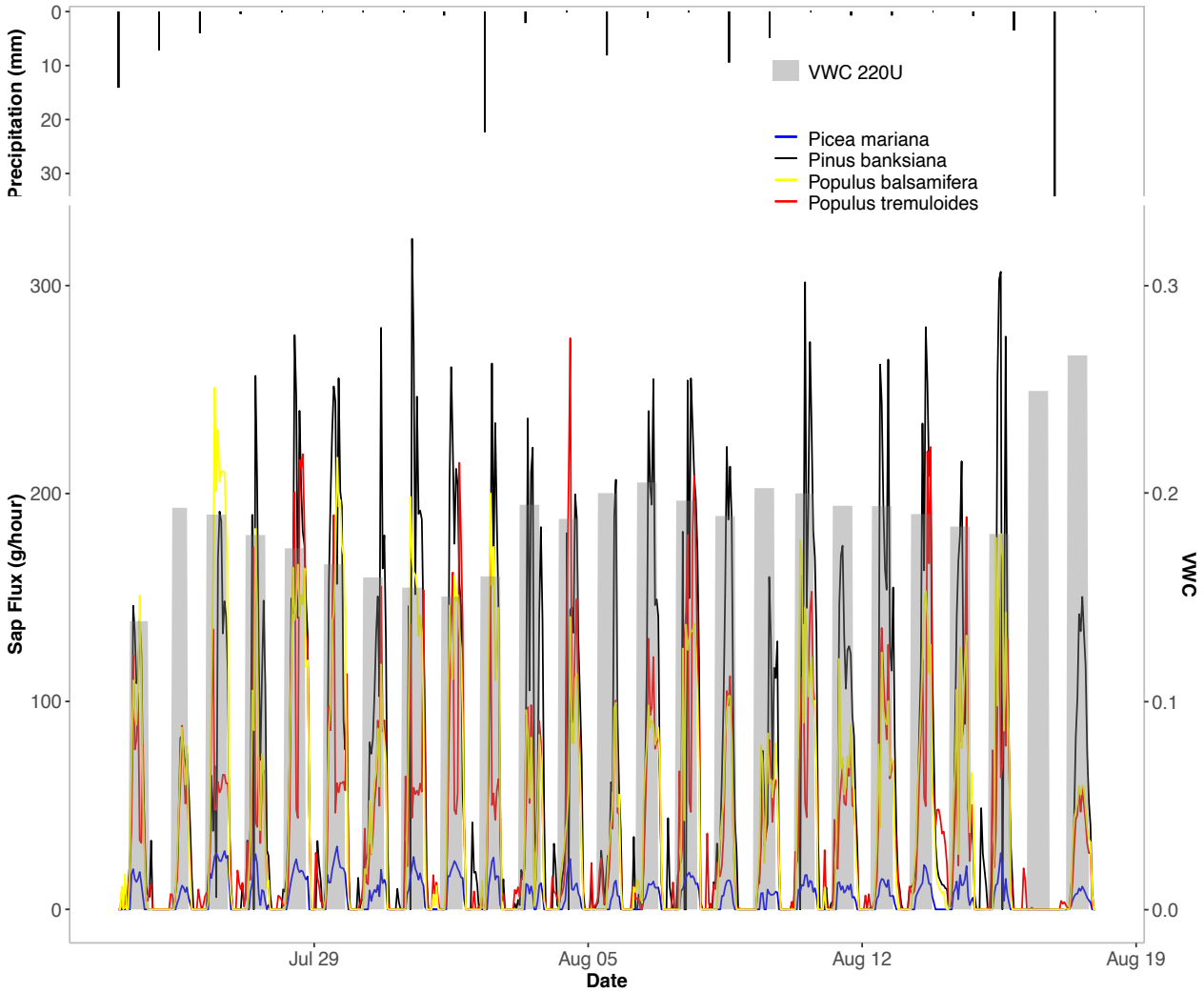

Figure 13: 26-day trend (DOY 205 to 231; 24 July to 19 August 2019) in sap fluxes (g hour-1) of dominant tree species at (A) station 220U in the upland of the Nikanotee Fen Watershed (NFW), Fort McMurray, Alberta.

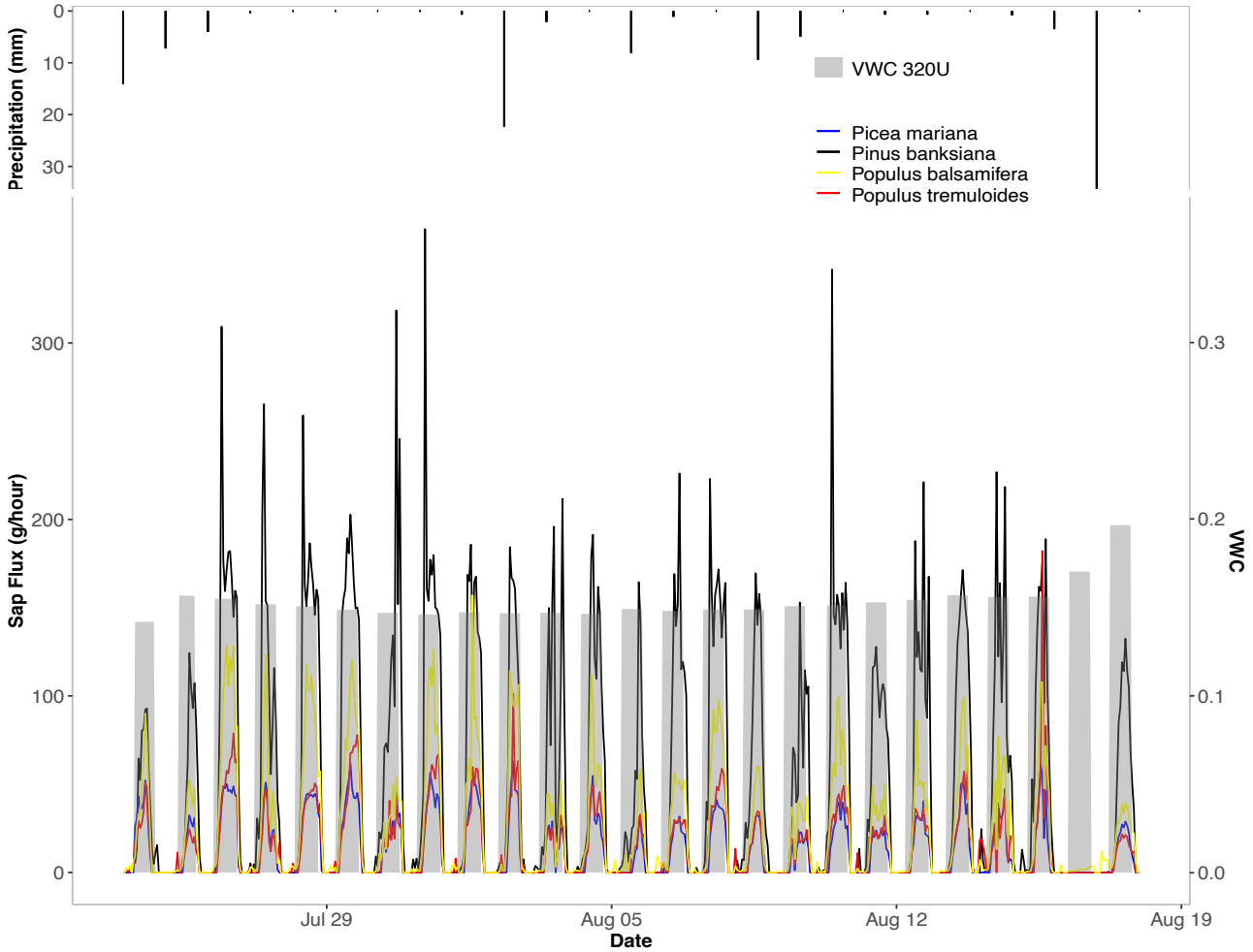

Figure 14: 26-day trend (DOY 205 to 231; 24 July to 19 August 2019) in sap fluxes (g hour-1) of dominant tree species at station 320U in the upland of the Nikanotee Fen Watershed (NFW), Fort McMurray, Alberta.

In order to assess the trends in canopy T, variables such as VPD and Q^* were measured and compared for each species (Figure 6). To test the relationship between T and different variables, regression analysis was carried out (Figure 15). Relationships between VPD and *Picea mariana, Pinus banksiana and Populus tremuloides* were strong and statistically significant. A positive relationship exists until a certain threshold, at which T begins to plateau. Thresholds are similar for each species with T rates reaching a plateau within the range of 1 - 1.5 kPa. Beyond the threshold of >1.5 kPa, T rates were insensitive to changes in VPD. These species also showed positive relationships with Q*, with T increasing in response to increasing Q*. *Populus*

balsamifera trees did not show strong relationships between T and both VPD and Q*. Weak relationships between climatic variables and T rates indicate the reliance on soil water availability for tree water use. Additionally, the relationship between T of *Populus balsamifera* and environmental variables (VPD and Q*) showed slight hysteresis behaviour (Figure 15).

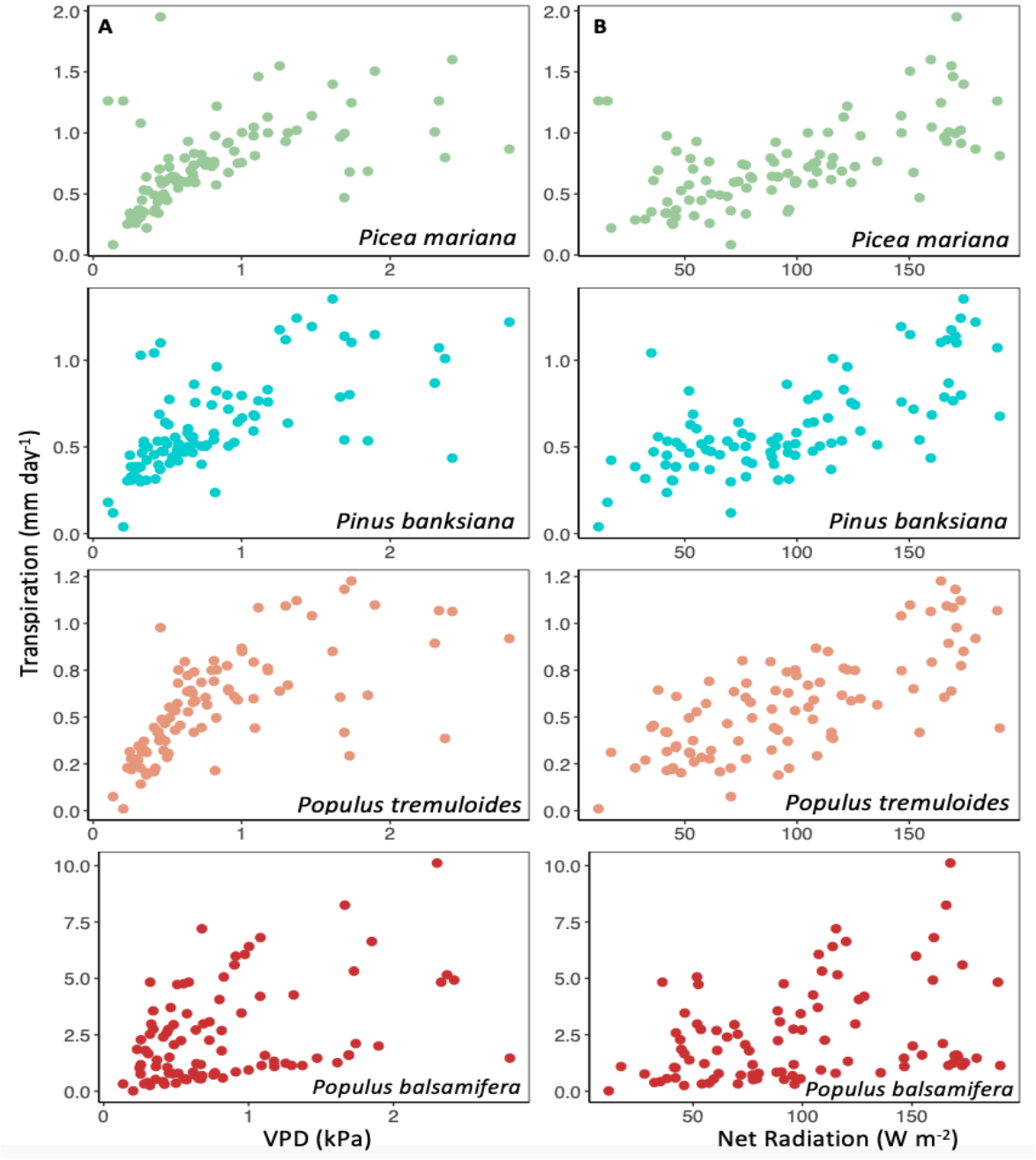

Figure 15: Relationships between species T (y-axis) and (A) vapour pressure deficit (VPD) and, (B) net radiation (Q*) in the upland of the Nikanotee Fen Watershed, Fort McMurray, Alberta.

Trends in VWC, T, ET and soil water potential throughout the growing season are presented in Figure 16. A general drying trend in VWC was observed moving from the transition zone to the southern region of the upland. VWC at 130T was consistently higher than 220U and 320U, as the transition zone is at the foot of the upland and experienced wetter conditions. At stations 220U and 320U, VWC began the season relatively low, fluctuating between 0.1 and 0.2 from DOY 145 to 179 (25 May – 24 September 2019). VWC at all stations was within the range of AWHC, remaining below FC (0.37) and above WP (0.07) throughout the growing season, which were determined by Irving (2020) using ROSETTA to estimate the van Genuchten parameters for the upland during the 2018 growing season. Stations recorded sharp increases immediately following the first large rainfall event of 28.8 mm on DOY 179 (28 June 2019). This was followed by a period of soil drying from DOY 185 to 205 (4 July – 24 July 2019), complemented by increases in soil water potential (more negative). VWC increased into August and remained high for the remainder of the growing season following large rainfall inputs to the surface. A positive relationship was observed between VWC and soil water potential ($R^2 \geq 0.54$ - 0.82 at 30 cm and $R^2 \geq 0.44$ - 0.78 at 50 cm), as lower soil moisture corresponds with lower soil water potential. Infiltration rates indicate that water received at the surface from rainfall infiltrated the upper soil horizons quickly and no ponding occurred. This is supported by the quick response of VWC and soil water potential to rainfall events, with an instantaneous increase in VWC and higher soil water potential (less negative). All tensiometers displayed seasonally inclined patterns of decreasing soil water potential (more negative) during peak growing season when temperatures and evaporative demands are high. At 50 cm, tensiometers located in proximity to the *Populus tremuloides* tree type experienced a dramatic response to soil drying (DOY 186; 5 July 2019) leading to reduced sap fluxes, while the response from the remaining tensiometers was gradual. On DOY 205 (24

July 2019), tensiometers at *Populus tremuloides* (30 cm) and *Pinus banksiana* (50 cm) were responsive to a 14.1 mm precipitation event while *Pinus banksiana* (30 cm) has a delayed response.

There is an observable relationship between T and water availability. At times when water availability was high (high soil water potential and high VWC), T rates were also high. These trends were also accompanied by periods of heavy rainfall. When rainfall was minimal, there was a drying of the 60 cm soil profile (low soil water potential and low VWC) resulting in decreasing T rates (Figure 16). Three notable rainfall events occurred throughout the growing season (P > 20 mm). The events occurred on DOY 179 (28 June 2019), 214 (2 August 2019) and 228 (16 August 2019) with 28.8 mm, 22.3 mm and 38.1 mm, respectively. On days of rainfall events, T decreased sharply as a result of suppressed sap fluxes despite high VWC and high soil water potential. The day following each event resulted in a spike in VWC and increasing soil water potential at both depths (30 cm and 50 cm). This was also accompanied by an increase in individual species sap fluxes and overall T rates, as high T rates were reached during non-limiting soil moisture conditions. Limited precipitation and decreasing water availability (decreasing soil moisture and decreasing soil water potential) led to a period of low transpiration rates from DOY 196 to 204 (15 July to 23 July 2019). Despite high water availability beginning from DOY 216 (4 August 2019), there was a decreasing trend in T and ET. Decreasing T could be explained by the combination of trees transitioning to senescence and a lack of soil aeration stemming from high water content and subsequently limiting root respiration.

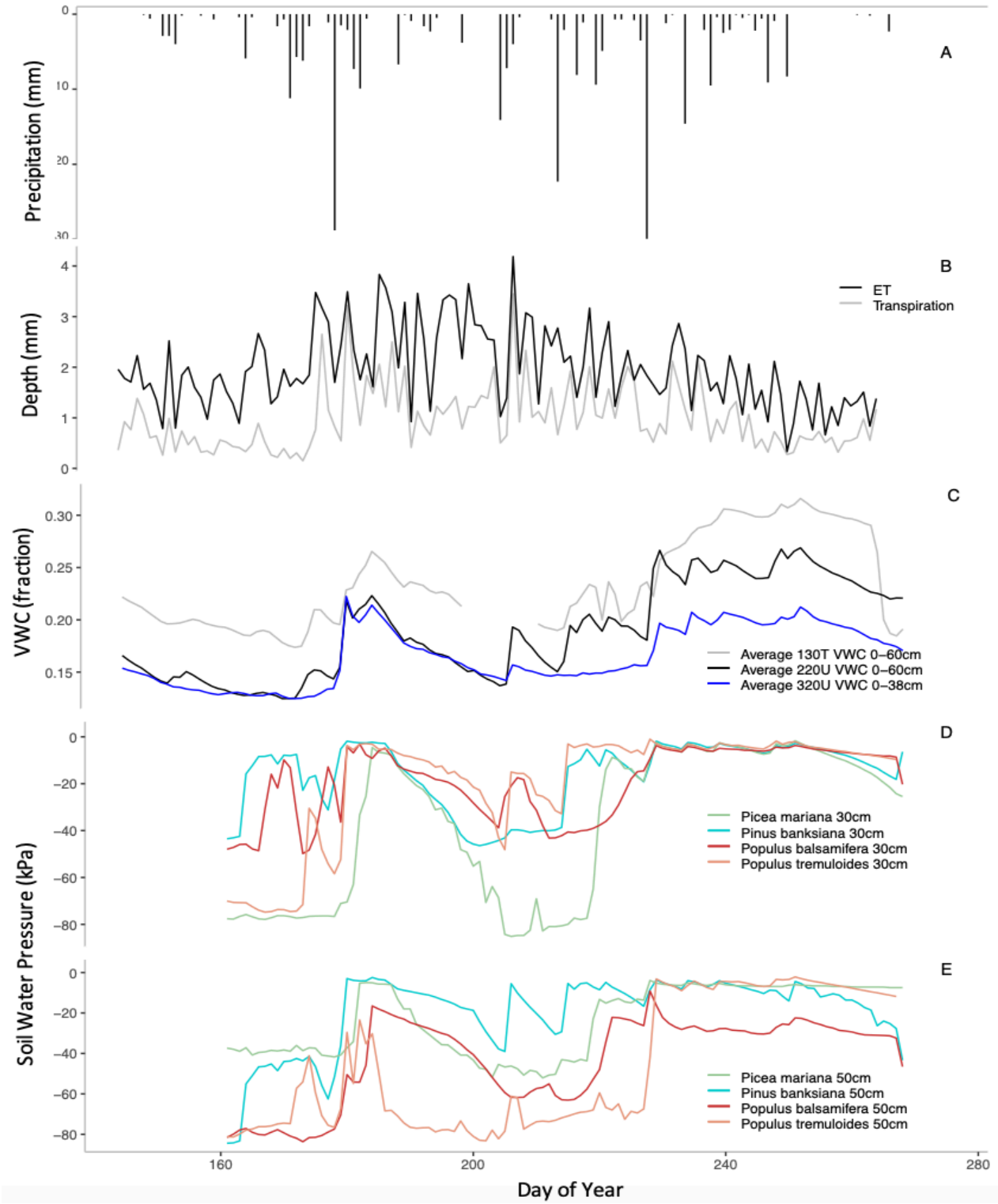

Figure 16: Variation in environmental variables during the 2019 growing season at the Nikanotee Fen Watershed (NFW), Fort McMurray, Alberta. (A) Daily precipitation, (B) Daily tree T and ecosystem-scale ET, (C) Soil VWC at station 130T, 220U and 320U averaged between depths of 0-60 cm, (D) Average daily soil water pressure at 30 cm and (E) Average daily soil water pressure at 50 cm.

Chapter 5: Discussion

5.1. Vegetation dynamics at NFW

In the first 7 years since reclamation, vegetation and hydrological regimes at NFW have changed substantially. Ground vegetation and tree communities have grown, which are beginning to play a significant role in the hydrological cycle, especially vadose zone dynamics. In 2015, vegetation diversity was low, dominated by a variety of forbs (28 species, 50%), whereas only 7% consisted of 3 species of tree saplings (Gringas-Hill, 2017). Findings by Gringas-Hill (2017) coincide with what has been observed in other newly disturbed areas, as Pinno & Hawkes (2015) determined that major plant communities are generally characterised by forbs and graminoids in the early stages following construction. In 2019, results of this study show that tree communities have established and comprise a large fraction of vegetation cover in the upland, with a tree density of 6001 stems per hectare. *Picea mariana, Pinus banksiana, Populus balsamifera, Populus tremuloides* are the dominant tree species at the site, resembling natural WBP. Spatial patterns have been observed following planting procedures, leading to a shift from deciduous broadleaf trees (*Populus tremuloides* and *Populus balsamifera*) at the upland-fen transition zone in the low slope regions, to a strong presence of coniferous trees (*Pinus banksiana* and *Picea mariana*) in the upper slope regions further away from the fen. The upper and low slope regions of the upland dominated by broadleaf and coniferous species consist of isolated and scattered trees, with fairly low density that create an open stand. The mid-slope region of the upland consists of a mix between broadleaf and coniferous trees, having a much higher density and beginning to create a closed canopy.

Spatial patterns at the site arose due to favorable conditions for growth of specific species. Tree growth in the WBP is often limited by nutrient and moisture availability, which will differ

between soil cover type (Pinno & Hawkes, 2015). However, Gingras-Hill (2017) concluded that sapling growth at NFW was limited mostly by moisture availability, and less likely limited by nutrient availability. For instance, broadleaf trees require adequate moisture supply to promote successful growth in disturbed environments (Errington & Pinno, 2015), which therefore along with planting prescriptions, explained their large presence in the upland-fen transition zone where moisture conditions are generally higher throughout the growing season. *Populus tremuloides* and *Populus balsamifera* are early successional and fast-growing species, able to respond rapidly following disturbance and making it a focus of many reclamation strategies (Errington & Pinno, 2015; Jean *et al.* 2019). Productivity of tree communities is often assessed by measuring height growth over a period of time (Pinno & Hawkes, 2015). As such, measurements of average height and DBH (Table 3) of *Populus tremuloides* and *Populus balsamifera* here highlight their rapid and early growth compared to coniferous species in this young constructed system.

Growth of *Populus tremuloides* and *Populus balsamifera* can be successful on a variety of different substrates including mineral upland soils, if moisture conditions can meet their water demands (Errington & Pinno, 2015; Depante *et al*. 2018). More specifically, studies have found that growth of *Populus tremuloides* on peat substrates has outperformed growth on LFH cover soil due to enhanced moisture retaining abilities, greater nutrient availability and decreased competition from other vegetation (Jean *et al.* 2019; Gingras-Hill, 2017; Errington & Pinno, 2015; Tremblay, 2017). Particle size distribution varied across the upland, with an overall mean loam soil classification (38% sands, 45% silt, 17% clay). Results from this study show similar patterns, as *Populus tremuloides* and *Populus balsamifera* had greater success in the lower slope regions of the upland, which were overlain with peat substrates and experienced greater moisture availability. Success of these species declined in the upper slope regions of the upland, where moisture

conditions were less desirable. Rather, *Populus balsamifera* shows a greater response to growing conditions with a greater tree abundance across the site and having a greater ability to grow in the drier high slope regions likely attributed to the greater opportunity for vegetative reproductivity (Frerichs *et al.* 2017; Peterson & Peterson, 1992). Contrarily, *Populus tremuloides* appeared to be less successful in the first 6 years following construction as overall, they were outperformed by *Populus balsamifera* in terms of size and distribution across the site (Figure 7). Wolken *et al.* (2010) found similar results with *Populus tremuloides* performing poorly in soils that were too dry and attributing the success of *Populus balsamifera* to its lower nutrient requirements.

Conditions favorable for successful growth of conifer species are similar, in that they can tolerate a wide range of moisture conditions in their early growing stages (LeBarron, 1944; Heinselman, 1965; Arnup *et al.* 1988). There were few differences observed in measured growth between the two coniferous species, which is likely due to differences in optimal growing conditions. In 2013, *Pinus* banksiana were planted in the high slope regions of the upland following characterisation of a dry ecosite and the presence of well drained soils. *Pinus banksiana* are known to grow in dry sandy and shallow soils, with low nutrient availability (Elliot-Frisk, 1988; Farrar, 2003; Quiñonez-piñón, 2007; Viereck & Johnston 1990; Sims *et al.* 1990). Today, their development at NFW emphasises their success within these soil conditions as they were capable of growing large trees rapidly following disturbances (Table 3), while they are not present in downslope areas of the upland, where moisture conditions are greater. Although moisture and nutrient availability have not been found to limit development, a critical requirement for successful growth of *Pinus banksiana* is access to sufficient light resources (Hu, 2000; LeBarron, 1944; Bell *et al.* 2000). Since NFW upland consists of isolated and scattered trees, conditions are favorable for their rapid growth as sufficient light is received by the canopy throughout the growing season.

After a few years, fast growing species *Populus tremuloides* and *Populus balsamifera* may reduce conifer growth by restricting access to light resources (Petrone *et al*. 2015). Conversely, *Picea mariana* are slow growing species capable of growing in a wide range of conditions (Bell, 1991), often considered an opportunistic species due to their ability to regenerate and easily populate sites with poor environmental conditions (Quiñonez-piñón, 2007). At NFW, *Picea mariana* were planted in the lower, mid and high slope regions of the upland due to its aforementioned abilities to tolerate a wide range of soil conditions. Results of this study show that growth was successful on both mineral and organic soils, which is consistent with what has been reported by Bell (1991). However, as found by Hu (2000) and Quiñonez-piñón (2007), higher productivity is associated with trees growing in the upper slope region of the upland consisting of mineral soils. Nonetheless, it is difficult to predict potential competition in a highly dynamic site, and the poor success of broadleaf trees in the upper slope regions of the upland suggest conifers may be capable of sustaining optimal light conditions for successful growth.

5.2. Seasonal trends in rainfall partitioning

There are many different factors that influence the partitioning of rainfall into TF, SF and INT. Most importantly, rainfall partitioning is affected by vegetation structure and rainfall event characteristics promoting interspecific and intraspecific differences in partitioning abilities (Swaffer *et al.* 2014; Johnson & Lehmann, 2006). Species-specific measurements of rainfall partitioning among young dominant tree species of the WBP are scarce in literature (Barbier *et al.* 2009). Studies have focused on developed overstory canopies (Price *et al.* 1997; Levia *et al.* 2011), which may have different characteristics than juvenile trees (Lishman, 2015). TF was the largest partitioning pathway for coniferous and broadleaf tree species in the NFW upland throughout the 2019 growing season, followed by INT and SF, respectively. Contributions by each water flow

pathway are similar to what has been observed in other studies assessing rainfall partitioning of WBP trees (Barbier *et al.* 2009; Levia *et al.* 2014). In a review of 28 papers assessing the influence of tree traits on rainfall partitioning, Barbier *et al.* (2009) found that TF during the growing season of trees in the Boreal Forest accounted for 71% of total precipitation in broadleaf trees and 64% in coniferous. These findings are slightly higher than measurements obtained at NFW, where TF of broadleaf trees accounted for 66% of total precipitation, while coniferous trees accounted for 58.7% (Table 5). Variations in TF between coniferous and broadleaf tree species are a result of differences in canopy foliage densities and canopy structure (Barbier *et al.* 2009; Quiñonez-piñón, 2007; Crockford & Richardson, 2000). Specifically, *Picea mariana* (3.20 m^{-1}) and *Pinus banksiana* (2.62 m^{-1}) had foliage densities greater than *Populus balsamifera* (1.69 m^{-1}) and *Populus tremuloides* (1.26 m^{-1}), resulting in lower TF proportions per event size class.

Differences in measured proportions of rainfall partitioning pathways at NFW to current literature (Barbier *et al.* 2009; Crockford & Richardson, 2000; Levia *et al.* 2014; Mckee, 2011; Levia & Herwitz, 2005) arise due to the current state of the site, which is dominated by juvenile, isolated and scattered trees. These characteristics lead to large spatial variability in TF (Lishman, 2015), allowing for more direct rainfall to reach the upland surface and recharge the adjacent fen peatland. However, with development in tree canopy the future state of the site will create large differences in partitioning abilities as LAI will increase with shifts in species abundance, transitioning towards higher contributions of canopy interception (Levia *et al.* 2011). Increases in LAI and foliage densities are often associated with increases in interception capabilities (Benyon & Doody, 2015; Barbier *et al.* 2009; Kermavnar & Vilhar, 2017; Elliot *et al.* 1998), suggesting that as vegetation develops at NFW, a larger proportion of rainfall will be intercepted by the canopy and reduce partitioning into TF, ultimately affecting soil water dynamics (Marin *et al.*

2000; Spence & Van Meerveld, 2016). A study on the effects of forest harvesting on soil water dynamics by Elliot *et al.* (1998) in the nearby Saskatchewan Boreal Forest showed that canopy interception increased with LAI. Similarly, Strilesky *et al.* (2017) conducted a study on forest water use in the initial stages of oil sands reclamation (12-year record) and found that LAI increased every year, coinciding with change in vegetation dynamics and growth. The increasing trend observed in TF with increasing event size is consistent with findings of other tree and forest types (Gómez *et al.* 2002; Price & Carlyle-Moses, 2003; Ziegler *et al.* 2009; Lishman, 2015). Increases in TF with event size is likely a result of gradual saturation of the canopy, where for small events partitioning is dominated by free TF (Carlyle-Moses *et al.* 2004). A transition from free TF to canopy drip occurs as increasing rainfall inputs approach the foliage saturation storage capacity, promoting dripping from leaves and needles (Carlyle-Moses *et al.* 2014; Lishman, 2015). Additionally, the increased ability of coniferous trees to hold on to water droplets reduces TF in the form of canopy drip, leading to an overall decrease in TF compared to deciduous trees, which are capable of forming larger droplets (Quinonez-pinon, 2007).

Similar to TF, differences in INT between and within species is likely explained by differences in canopy densities (Barbier *et al.* 2009; Crockford & Richardson, 2000). In this study, INT was greatest for coniferous trees (*Picea mariana* and *Pinus banksiana*) and lower in broadleaf trees (*Populus tremuloides* and *Populus balsamifera*) (Table 5), which is in agreement with observations reported by Barbier *et al.* (2009) and Levia *et al.* (2011) where Boreal coniferous trees intercepted a greater percentage of total rainfall throughout the growing season. Coniferous trees generally produce a denser canopy resulting from wider crowns and therefore have higher INT capacities along with their larger surface area (Kermavnar & Vilhar, 2017). Results indicate that INT, as a percentage of total rainfall, decreased with increasing event size (Figure 11), which

is typical as the canopy reaches saturation storage capacity and becomes more efficient at transmitting TF and SF (Spencer & Van Meerveld, 2016; Carlyle-Moses & Price, 2006; Liang *et al.* 2009). As canopies approach their foliar storage capacities, they will ultimately contribute greater quantities to recharging soil moisture at the base of the tree (Keim *et al*. 2006; Levia *et al.* 2011). For smaller events (< 10 mm) with lower intensities (0.3 – 3 mm h^{-1}), *Populus tremuloides* and *Populus balsamifera* intercepted higher percentages, while during larger (> 10 mm) and more intense rainfall events (> 3 mm h^{-1}) *Picea mariana* and *Pinus banksiana* began to have greater INT abilities (Figure 11). Low INT in broadleaf trees is likely due to leaf structure, where leaves generally store thin layers of water at low intensities, while the clumping nature of needled trees create a larger surface area capable of intercepting a greater proportion of large rainfall events with higher intensities (Kleim *et al.* 2006; Levia *et al.* 2011). Furthermore, the high INT rates in coniferous tree species (Table 5) can be attributed to these young late successional trees having a large number of branches and dense foliage within a smaller trunk area (Crockford & Richardson, 2000). Therefore, spatial patterns in water inputs to the soil are likely due to differences in INT capabilities of different tree species. Regions of the NFW upland dominated by coniferous tree species may lead to higher INT rates and evaporation (Levia *et al.* 2011), therefore contributing less to the adjacent fen peatland.

During the non-growing season (October to April) a large proportion of precipitation occurs in the form of snowfall. In the winter, broadleaf deciduous trees lose their leaves considerably altering their INT capabilities and producing a higher net precipitation (Staelens *et al.* 2008; Levia & Frost, 2003). Although precipitation is minimal in the winter months, there will be higher direct snowfall accumulation around the trees, which during spring snowmelt will likely

contribute more to tree root water uptake in the early spring when demands are high and eventually made available during limiting moisture conditions (Levia *et al.* 2011; Ketcheson *et al.* 2016).

Although SF consisted of a small proportion of canopy water fluxes (Table 4-5), it is considered an important point source of water and nutrients to the base of the trees (Carlyle-Moses & Price, 2006; Levia & Herwitz, 2005). Not only are these concentrated inputs of water important for individual trees, SF has also been found to be an important supply to groundwater and recharge (Levia *et al.* 2011). Results of this study show that SF as a percentage of total rainfall was variable, depending mostly on tree type and size. Studies have established relationships between SF yield and tree height (Martinez-Meza & Whitford, 1996) and size (DBH) (Crockford & Richardson, 2000), with larger trees normally producing greater SF volumes. Ford & Deans (1979) attributed this relationship to the increased surface area of the tree trunk, enhancing its ability to capture incoming rainfall and generate SF. Differences among tree type were observed between coniferous and broadleaf tree species, where average SF was higher under coniferous (7.6%) than broadleaf trees (5.1%) (Table 5). This differs from what has been reported in other studies, where SF was generally greater below broadleaf trees than coniferous (Barbier *et al.* 2009; Spencer & Van Meerveld, 2016; Livesley *et al.* 2014). The relationship between tree size, height and SF production may be confounded when addressing coniferous species, as a result of greater bark roughness and storage capacity within larger trees of this type (Levia *et al.* 2011; Li *et al.* 2008; Siegert & Levia, 2014). However, when assessing SF at the individual species level results show that although substantial rainfall was intercepted by the canopy, *Picea* mariana trees were able to channel water efficiently to the base of the tree (Table 4) as SF despite being of coniferous genera and being the smallest species. Higher SF under *Picea mariana* is likely related to high average foliage densities and the geometric orientation of branches (Levia *et al.* 2011; Levia & Frost, 2003)

measured in the 2019 growing season (3.20 m^{-1}), which were noticeably higher than the other measured tree species. Whereas, crown structure of *Populus balsamifera* make them less favorable to produce large quantities of SF, as they have more sharply ascending branches with a rougher bark surfaces than *Populus tremuloides* (Peterson & Peterson, 1992).

Bark roughness was observed to have a strong control on a tree's ability to produce SF. Coniferous trees are characterized by rough bark surfaces, which are thicker and more absorbing (Crockford & Richardson, 2000; Siegert & Levia, 2014). These characteristics generally result in lower SF production, as the bark must be saturated before SF can commence (Crockford & Richardson, 2000). This was observed in *Pinus banksiana* trees as they yielded the lowest average SF as a percentage of total rainfall despite recording the highest average DBH and height. Results indicate that due to their rough bark texture, they require a larger rainfall event to saturate before channeling water to the base of the tree (Li *et al.* 2008; Sigert & Levia, 2014; Crockford & Richardson, 2000). Smooth bark surfaces, characteristic of *Populus tremuloides* and *Populus balsamifera*, yielded higher SF percentages than *Pinus banksiana* but smaller than what was measured for *Picea mariana*. Contrary to what was observed in this study, Price *et al.* (1997) assessed variability in canopy water fluxes of an old *Picea mariana* plantation and found that SF consisted of an even smaller proportion of total rainfall (0.95%) and attributed this small magnitude to canopy architecture, with branches sloping away from boles of the trees, and their relatively rough bark surfaces. Currently, *Picea mariana* branching architecture promotes larger SF production with vertical branches sloping towards the tree bole (André *et al.* 2008; Levia *et al.* 2011). Over time, as *Picea mariana* trees continue to grow taller, branches will begin to droop into plagiophile branching geometry reducing their ability to channel water to the base of the tree (Snelgrove *et al.* 2019) and ultimately reducing SF production (Levia *et al.* 2014). Therefore, at

NFW variations in SF production from dominant tree species can be expected as the site continues to grow, which may eventually impact soil water dynamics and recharge availability to the adjacent fen peatland (Carlyle-Moses & Price, 2006; Taniguchi *et al.* 1996).

When assessing average SF depth per event, there is a point at which SF plateaus, ranging between 8 to 12 mm for *Picea mariana*, *Pinus banksiana, Populus tremuloides* and *Populus balsamifera.* Studies assessing SF depth by event size have found that SF generally increases linearly with event size (Levia & Herwitz, 2005; Spencer & Van Meerveld, 2016; Siegert & Levia, 2014), however few studies have found that SF had a non-linear relationship with gross precipitation (Ahmed *et al.* 2017; Zhang *et al.* 2015). A consistency in a tree's ability to produce SF beyond this threshold may be explained by the intensity of the rainfall event causing preferential pathways to be overloaded and stimulating canopy drip and direct TF (Crockford & Richardson, 2000; Staelens *et al.* 2008). Additionally, SF production will depend on the storage capacity of the tree, which will determine the point at which INT transitions to channeling TF and SF (Crockford & Richardson, 2000). Carlyle-Moses & Price (2010) found that SF funnelling ratios could be used to determine the depth of rainfall required to meet the storage capacity of a tree canopy. Funnelling ratios demonstrate a tree's efficiency at generating SF and its use in rainfall partitioning research has increased (Carlyle-Moses & Price, 2006; Li *et al.* 2008; Spencer & Van Meerveld, 2016). Results show that funnelling ratios were variable between and within species, generally increasing with increasing rainfall until a threshold at which ratios began decreasing (Spencer & Van Meerveld, 2016; Mckee, 2011). The threshold is achieved when the canopy has reached complete saturation with any subsequent rainfall resulting in a decrease in funnelling ratios (Mckee, 2011). While ratios are smaller than what has been reported in current literature (Carlyle-Moses *et al.* 2010; Carlyle-Moses & Price, 2006; Li *et al.* 2008) they reveal the point of bark

saturation, which depends on bark texture of a specific tree and also displays the efficiency of each tree to generate SF (Marin *et al.* 2000). Results here show that *Picea mariana* are the most efficient at channelling SF, but also that they have a large bark water storage capacity (10 to 15 mm) (Figure 10). *Pinus banksiana, Populus tremuloides* and *Populus balsamifera* have a lower ability to generate SF while also having a lower storage water capacity due to a smooth bark texture (Barbier *et al* 2009; Crockford & Richardson, 2000). These characteristics are important when creating canopy water balance models, as many studies currently underestimate the canopy saturation point, which will have implication when estimating INT and TF.

5.3. Seasonal trends in transpiration of dominant tree species

In the sub-humid WBP, ET is the dominant hydrological flux, often exceeding precipitation and resulting in limiting moisture conditions (Strilesky *et al.* 2017, Sutton *et al.* 2019; Brown *et al.* 2010*,* Ketcheson *et al.* 2017). In the early developmental stages of the site, ET was generally low and dominated by surface evaporation. However, with canopy development, contributions of T from surface vegetation and growing tree communities start to increase and exert stronger controls on ET (Strilesky *et al.* 2017; Naeth *et al.* 2011; Nicholls *et al.* 2016). Vegetation plays an important role in controlling ET from forested uplands (Brown, 2010; Grelle *et al.* 1997), therefore the composition of vegetation at a site will govern exchanges of water and energy between the surface and atmosphere. The development in tree canopy will ultimately dictate the hydrological future of the system and determine the capability of the upland to supply groundwater to the adjacent fen peatland, while sustaining itself (Sutton *et al.* 2019; Rodriguez-Iturbe *et al.* 1999).

During the 2019 growing season, eddy covariance measurements highlighted the importance of ET water losses at the site, representing 82% of total growing season precipitation.

Total ET amounted to 236.9 mm, which is within the range of what has been observed in other studies addressing ET in the WBP (Amiro *et al.* 2006; Mkhabela *et al*. 2009; Kljun *et al.* 2006; Carey *et al.* 2008). ET rates at NFW are slightly lower than what was measured by Amiro *et al.* (2006) at a harvested and mature *Pinus banksiana* site, and higher than their burned mixed coniferous-deciduous stand. Levia *et al.* (2015) reviewed thirteen different Boreal Forest sites, in which greatest daily rates were measured at a deciduous *Populus tremuloides* forest in Canada. Canopy T was the main driver of ET losses from the system contributing 52% and reaching maximum values around 3.45 mm day^{-1}. While not measured directly, soil evaporation and evaporation of intercepted precipitation accounted for <50% of seasonal ET. Since the site consist of low-density scattered trees, we can assume that surface evaporation will make up a large proportion of remaining ET, while evaporation of intercepted water per unit area will be relatively small as a result of minimal canopy development. Although T makes up a large proportion and will continue to exert strong controls on ET with canopy development (Thompson *et al.* 2011), Farley *et al.* (2005) concluded that evaporation of intercepted precipitation can also increase substantially, especially in coniferous trees. Sparse canopies are characteristic of this region, making the development of understory vegetation possible and hydrologically significant (Levia *et al.* 2014). Understory vegetation is able to thrive in the early stages of forest re-vegetation due to the increased exposure to radiation and direct evaporation (Fatichi & Pappas, 2017). These conditions are short lived as with higher LAI, trees prompt changes in microclimate leading to shading and cooling at the surface, which ultimately reduce T of understory vegetation (Bayala & Wallace, 2015; Brown, 2010). Partitioning proportions will continue to evolve with canopy development at NFW, shifting towards higher contributions from T and evaporation of intercepted rainfall, which will minimize soil evaporation (Naeth *et al.* 2011, Fatichi & Pappas, 2017). The

ratio of T to ET is shown to be dependent on the growth stage of the forest stand and on LAI of the canopy (Wang *et al.* 2017; Hadiwijaya *et al.* 2020). The T/ET ratio at NFW was on the lower end than what has been reported in literature (Huang *et al.* 2015; Sarkkola *et al.* 2013; Cienciala *et al*. 1997; Wang *et al.* 2017; Kozii *et al.* 2019), which is likely due to the relatively young age of the stand, with characteristically small DBH and low LAI. However, results are within the range established by Zhou *et al.* (2016) using eddy covariance across different biomes.

Sap flow and eddy covariance measurements show similarities in their daily trends and their responses to meteorological conditions. Unexpected trends while comparing T and ET may arise due to differences in methods and their limitations. Measuring the systems response using multiple methods and comparing across methods is one of the best approaches to come to a better understanding of what the system is doing. Results suggest that variability in tree T is a result of numerous factors including VPD, Q^*, air temperature, and changes in water availability. To better understand the controls each variable has on T, measurements in the early growing season (DOY 145 to 173) were removed to avoid the period when leaves had not reached full expansion and T was relatively low. Results for this period show that VPD had strong relationships with T of *Picea mariana, Pinus banksiana* and *Populus tremuloides* throughout the growing season. Nonetheless, T generally showed an increasing response to VPD < 1 kPa after T began to plateau. This threshold is consistent with what has been reported in other studies in the region (Hogg & Hurdle, 1996; Hogg *et al.* 1997; Zhang *et al.* 1999), occurring due to trees closing their stomata to avoid major water losses and maintaining leaf water potentials above a critical threshold (Asbjornsen *et al.* 2011; Hogg & Hurdle, 1996). Pataki *et al.* (2000) even found a decreasing response of T to increasing VPD after reaching the threshold. The plateau and subsequent decrease in T at higher VPD indicates that stomatal closure controls T on an individual tree-level, and if thresholds are

exceeded it may result in xylem dysfunction (Bladon *et al.* 2006). When assessing individual species T responses to VPD, relationships indicate that *Populus balsamifera* were most sensitive to changes in VPD. This suggests that this species can conserve more water when facing limiting moisture conditions (Chen *et al.* 2014; Hamilton, 2019). The hysteresis behaviour in the relationship between *Populus balsamifera* T and environmental variables (Q* and VPD), may result due to the time-lag between these variables (VPD peaking latter in the day) or plant water status within the stem (Saugier *et al.* 1997; Oogathoo *et al.* 2020). Such responses to environmental variables have also been observed by trees in various ecosystems (Saugier *et al.* 1997; Oogathoo *et al.* 2020; Pappas *et al.* 2018). Results differ from those observed by Hamilton (2019), finding that VPD had significant controls on limiting T of a *Pinus banksiana* stand in the morning and restricting sap flow when VPD was low. Differences in the relationship between tree T and VPD were observed between coniferous and broadleaf trees following rainfall events. Weak relationships between coniferous tree T and VPD were observed when the canopy was wet, which is likely a result of water on the needles playing a role in regulating T rates (Hadiwijaya *et al.* 2020).

Previous work has shown that VPD had a stronger influence on sap fluxes but that Q^* also exerted strong controls (Li *et al.* 2016). However, VPD at NFW appeared to have a slightly stronger control on T rates of broadleaf tree species than Q*. Similar controls were observed for *Picea mariana, Pinus banksiana* and *Populus tremuloides,* as Q^* influences daily changes in T. The influences of Q^* on coniferous species were less apparent due to their low light saturation values and their dependence on VPD (Angstmann *et al.* 2013; Ewers *et al.* 2005). Additionally, David *et al.* (2004) found that the influence of radiation on generating sap flow becomes progressively less significant throughout the day, which indicates a temporal variation in

meteorological variables controls on tree water use throughout the day (Hamilton, 2019). Despite moderate relationships with VPD and Q^*, tree T responded to variations in meteorological conditions throughout the growing season. Other studies have also established relationships between tree T and VPD and Q^* (David *et al.* 2014; Li *et al.* 2016; Wang *et al.* 2017; Ewers *et al.* 2008; Ma *et al.* 2017; Kumagai *et al.* 2005). A notable period of discrepancy amongst T and ET occurs between DOY 194 and 205 where there is significantly lower T than ET during a time of optimal VPD, air temperature and Q^* conditions, which would favour higher water loss from tree communities. While, some of the discrepancy may result from systematic underestimation of T rates during this period, it appears to also occur during a time when soil moisture experiences sharp declines at all stations. Li *et al.* (2016) revealed that low incoming radiation limited tree T, however when radiation and evaporative demand were high tree T was mostly limited by soil moisture conditions.

5.4. Seasonal trends in water availability and tree water use

Spatial and temporal variability in water availability were evident in the upland throughout the growing season, and are governed by the relationships between soil, vegetation and atmosphere. More specifically, vegetation exerted strong controls on moisture dynamics, which feedback to influence vegetation growth over time. The variability in vegetation cover and water availability will promote fluctuations in T rates and more importantly, ET fluxes. Soil depth and soil texture will impact water movement and dictate available moisture for root water uptake. The importance of measuring species-specific T rates is further supported by the relationship between T and environmental variables, which can promote or suppress tree water use.

Few studies have established a relationship between VWC and canopy T, as a result of T dependence on meteorological variables but also the large spatial variation in soil moisture and

soil properties (Lagergren & Lindroth, 2002). Although data were collected for one growing season, soil moisture and tensiometer dynamics show the controls water availability have on tree T. Following initially high soil moisture contents and low soil water pressure in the early growing season, soil moisture declined in June and July in response to minimal precipitation. During this time, a link between soil water availability and tree T was observed as tensiometers responded to declining soil moisture with a decrease in soil water pressure and an overall decline in canopy T. Declines in tree T can be attributed to the limited ability of trees to extract water from the soil due to low soil water potentials. Changes in soil moisture content within the top 60 cm of the soil profile are likely a result of root water uptake by tree species. Changes will be dependent on tree type, as rooting depths may differ significantly. Rapid changes in soil water pressure at 50 cm, may be due to tensiometers being placed in coarse-grained, fast draining sandy soils with characteristically low water holding capacity. This was observed in tensiometers around *Populus tremuloides* and *Populus balsamifera* trees, which also have deep roots extending beyond the LFH and tailing sands interface. Additionally, for water to infiltrate to the tailing sand through the capillary barrier, it requires sufficient water content creating high pressures. Therefore, low soil water pressures measured within the sand layer may be caused by low soil water content within the LFH, limiting breakthrough the interface and enhancing drying in the tailing sand. Tensiometers placed at 30 cm were generally measuring changes in soil water pressure within the fine-grained LFH soil layer. Additionally, more notable changes in 30 cm tensiometers around *Pinus banksiana* and *Picea mariana* are likely a result of shallow roots characteristic of coniferous trees (Hamilton, 2019).

The relationship between T and soil moisture was also evident when assessing soil moisture dynamics at each station (130T, 220U and 320U), as they were responsive to rainfall events, which

eventually enhanced T. Rainfall reaching the surface, typically in the form of TF and SF in forested systems, strongly influence T and root water uptake of tree species while also contributing significantly to soil moisture conditions (Chen *et al.* 2014). However, Austin *et al.* (2004) and Ivans *et al.* (2006) found that small rainfall events saturating shallow soil layers may not necessarily contribute to T of deep rooting tree systems, in this case *Populus balsamifera* and *Populus tremuloides*. Therefore, larger events able to infiltrate deeper in the soil profile may be needed to sustain growth of these particular species. A time lag was observed in the response of T to rainfall events (1 to 2 days), likely coupled to the time it takes rainwater to infiltrate to tree specific rooting depths. Specifically, *Picea mariana* and *Pinus banksiana* responded more promptly than broadleaf tree species as a result of shallow roots. However, broadleaf trees are capable of utilizing a larger volume of soil for water uptake (Kropp *et al.* 2017). Bovard *et al.* (2005) determined that shallow-rooted species showed considerable reductions in sap fluxes in response to increasing VPD when surface soil moisture was depleted, whereas reductions in deep-rooted species were much slower. Tensiometer responses to small rainfall events at NFW support conclusions from these studies (Austin *et al.* 2004; Ivans *et al.* 2006) as greater responses to small rainfall events were observed at 30 cm, while 50 cm had greater responses to larger events which saturated the surface layers and promoted percolation to deeper depths within the soil profile. The influence of soil water on T was less apparent when water availability was not limiting in the rooting zone, and therefore varied in response to meteorological variables (Li *et al.* 2016). However, spatial variability in soil moisture was observed at the site with a shift from wetter conditions at the foot of the upland (station 130T) to successively drier conditions at 220U and 320U. The transitional shift in soil moisture at the site was also observed and modelled by Sutton

et al. (2019), which identified soil cover type and thickness as an important influence on soil moisture partitioning in the upland.

Spatial variability in soil moisture drives magnitude of tree water use creating tree spatial growth patterns due to species-specific tendencies (Leatherdale *et al.* 2012; Rodriguez-Iturbe *et al.* 1999). While it has been established that water availability has strong controls on tree T, responses differ between and within species. Measurements of species-specific sap flow of WBP trees and their respective contributions to T are limited in current literature and require increased attention to understand their role in the hydrologic cycle (Ford *et al.* 2007). Partitioning sap flow sensors per species allowed for the development of strong daily regressions of species-specific trends in sap flow throughout the growing season. Sap fluxes of both coniferous and broadleaf trees experienced diurnal fluctuations in response to changing VPD, Q^* and soil moisture. Diurnal patterns of sap flow were no longer evident on rainy days with low VPD and Q^*, creating low demands for canopy T. Diurnal fluctuations were consistent with observation made by Hogg & Hurdle (1997) at a Canadian boreal site dominated by *Populus tremuloides* and *Populus balsamifera*. Significant declines were observed in response to large precipitation events, as T is supressed by a wet canopy suggesting higher contributions from evaporation of intercepted rainfall (Hadiwijaya *et al.* 2020).

Coniferous trees, which occupied about 20% of the area showed lower average T rates than deciduous broadleaf species growing in wetter regions of the upland. The deciduous broadleaf stands, which occupy much of the remaining upland areas (80%), generally have a higher T rates, and provide less water for storage and runoff than the coniferous stands (Nijisse & Lattenmaier, 2002). Results are consistent with current literature assessing differences in T between coniferous and broadleaved trees (Strilesky *et al.* 2017; Amiro *et al.* 2006; Brown *et al*. 2014; Brümmer *et al*.

2012; Ewers *et al*. 2005). Sap fluxes of *Picea mariana* and *Pinus banksiana* remained consistent throughout the growing season. *Picea mariana* experienced significantly lower sap fluxes, likely due to its small size compared to the other species leading to differences in water transport capacity through the stem (Berry *et al.* 2018; Barbour & Whitehead, 2003). Several studies have shown that variations in sap fluxes are closely related to tree size (Loranty *et al.* 2006; Oren *et al.* 1999), which are ultimately dictated by competition for resources such as water and light (Hadiwijaya *et al.* 2020). Coniferous nature of *Picea mariana* and *Pinus banksiana* allow T to continue throughout what would be the senescence period for broadleaf trees and into the winter months. Low T and root water uptake from *Picea mariana* may compensate large INT rates to maintain sufficient moisture to sustain growth (Wang *et al*. 2017; Elliot *et al.* 1998). Due to shallow rooting depths, they typically spread laterally in the upper layers of the soil profile and root in regions with most optimal conditions for growth (Quiñonez-piñón, 2007; Verma *et al.* 2014). INT and subsequent evaporation from *Picea mariana* may make up a significant proportion of evaporative fluxes following rainfall events, similar to what was found by Farley *et al.* (2005) as they concluded that conifers can contribute substantially to overall ET. Sap fluxes of *Populus tremuloides* and *Populus balsamifera* started the season with very low diurnal fluctuations as leaves were in the development stages. On DOY 174, sap fluxes of broadleaf trees experienced a significant increase following consecutive precipitation events, which was also associated to greater T rates following spring leaf expansion. Temporal variations in sap fluxes and T by broadleaf trees throughout the growing season were also observed by Hogg & Hurdle (1997), as rates were consistent with changes in LAI. Decreased INT and T by broadleaf trees in the early and late stages of the growing season lead to effective saturation of the soil profile.

Populus tremuloides and *Populus balsamifera* have characteristically high-water use per unit leaf area, ultimately utilizing more water than coniferous stands (Strilesky *et al.* 2017; Huang *et al.* 2015; Barr *et al.* 2001; Elliot *et al.* 1998). Their high demand for water is dependent on a sufficient supply of moisture availability throughout the growing season to have successful growth (Errington & Pinno, 2015; Tremblay *et al.* 2019; Brown, 2010). These characteristics explain the success of *Populus tremuloides* and *Populus balsamifera* in the upland-fen transition zone, where VWC (station 130T) is consistently higher than what was observed moving further away from the fen peatland. Higher VWC at this station can be explained by a high-water table with associated high soil water pressures, creating ideal conditions for root water uptake and inducing tree T. Whereas, *Populus tremuloides* and *Populus balsamifera* were less successful in the drier regions of the upland around station 320U where moisture availability was more limiting and decreased soil water pressures limited root water uptake. Current literature shows that *Populus tremuloides* are important species in the WBP due to their overwhelming presence in natural systems, but also due to their ability to establish deep rooting systems (Cienciela *et al.* 1998; Blanken *et al*. 2001; Brown, 2010). The establishment of deep roots provides *Populus tremuloides* with the added capability of performing better during dry conditions by accessing water held by the capillary barrier and rooting at the interface between the tailing sands and LFH (Sutton *et al.* 2019). Additionally, it is equally important to understand their contributions when discussing the fate of the system in response to potential climate changes as their demands for water will increase with their increases in LAI over time (Hoffman & Jackson, 2000; Jackson *et al.* 2001; Vertessy, 2001), which will likely have implications for access to water by competing tree communities but also recharge inputs to the adjacent fen peatland (Strilesky *et al.* 2017; Farley *et al.* 2005; Wang *et al.* 2017).

Picea mariana and *Pinus banksiana* are less sensitive to water deficits and can successfully grow in drier conditions (Quiñonez-piñón, 2007), which explains their presence in drier regions of the upland around station 320U. Soil moisture was consistently lower than what was observed in regions closer to the fen peatland and experienced greater soil pressures. Furthermore, sap flow of trees in drier regions of the upland experienced much lower sap fluxes than ones in areas with higher water availability. The ability of *Picea mariana* to control water losses to the atmosphere and their small size relative to the other tree species explains their small contributions to T at the site. The controls of DBH have on magnitude of T, indicate that as these trees continue to grow their relative contributions will continue to flourish and potentially have a greater influence on water losses from the system.

5.5. Future implications and industry recommendations

Along with the many challenges faced in the construction of post-mined landscapes in the WBP, potential climate change poses considerable threats to ecosystems. Quantifying hydrological processes in the years following construction of the system provides a basis to understanding the interactions between soil, vegetation and atmospheric processes (Naeth *et al.* 2010; Leatherdale *et al.* 2012). Vegetation has strong controls on many processes in an ecosystem and their impacts will vary considerably with time since planting (Johnson & Miyanishi, 2008). Consistent monitoring of vegetation and hydrological dynamics in the upland are crucial to the success of the constructed system, as the upland plays a significant role in supplying moisture to the adjacent fen (Nicholls *et al.* 2016; Sutton *et al.* 2019). Figure 17 represents a conceptual diagram of the current hydrological processes in the upland of the NFW, as well as a diagram representing how they will change with time.

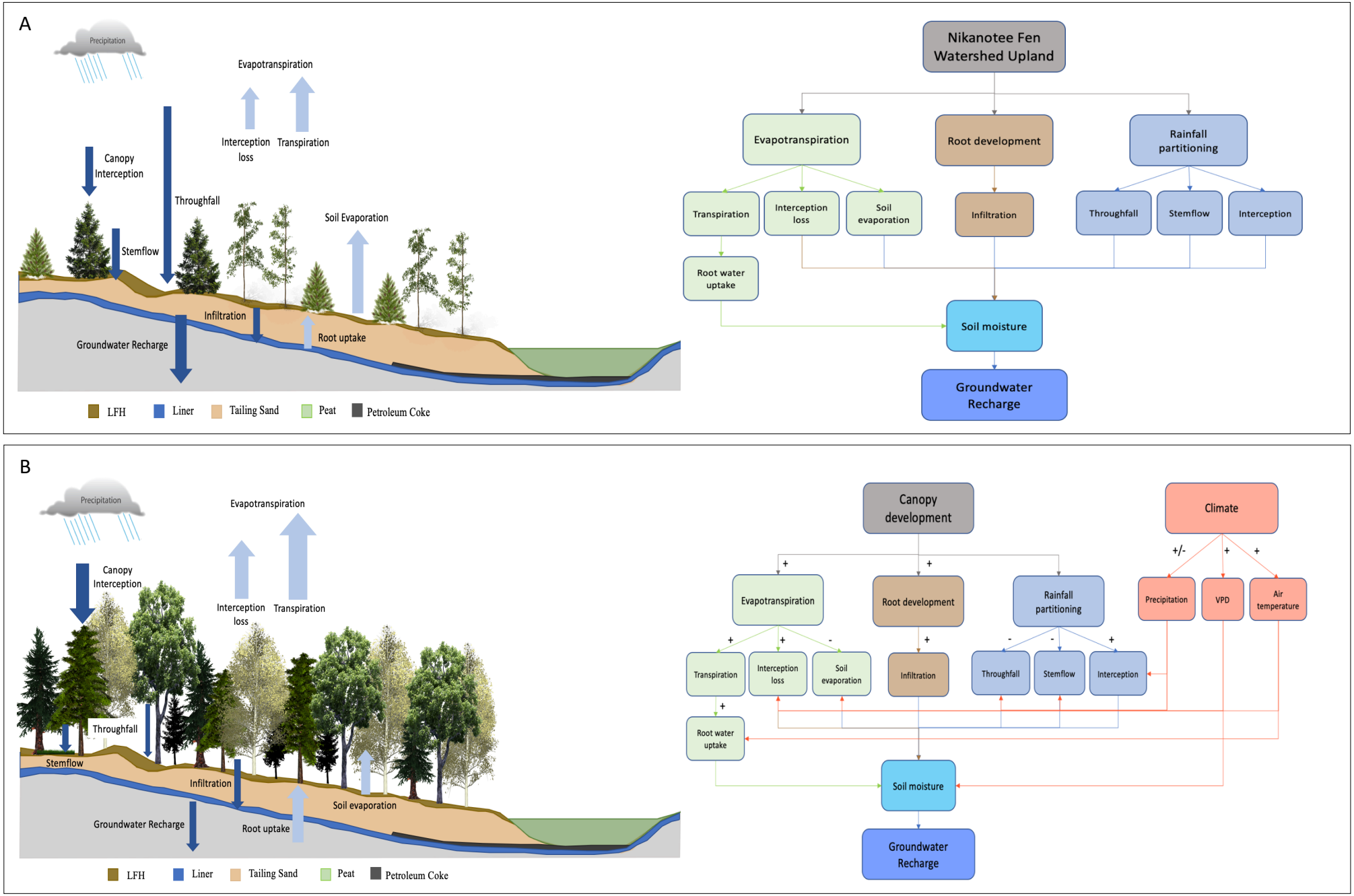

Figure 17: Conceptual diagram of (A) the current hydrological processes at the Nikanotee Fen Watershed (NFW), (B) changes in hydrological processes over time.

Development in vegetation, more specifically tree communities, will enhance root water uptake (Figure 17) and have a greater impact on the uplands ability to partition water towards recharging the fen. The extent to which root water uptake will affect soil water dynamics will depend on the success of vegetation communities and their respective abilities to partition water resources. Additionally, canopy development will increase canopy INT, which will reduce TF and SF contributions to near-surface soil moisture (Figure 17). Increases in INT will ultimately increase INT losses, and along with increases in T, will increase ET fluxes from the system (Figure 17). Increases in LAI, a dominant control on many hydrological processes interacting with vegetation, will enhance shading and decrease contributions from soil evaporation. Changes in these processes will have implications on moisture being partitioned to groundwater and directed towards the fen. Sutton *et al.* (2019) used modelling to determine whether the upland is capable of supplying sufficient recharge to the adjacent fen peatland by simulating groundwater recharge. This study found that 41 mm is required to offset evaporative losses from the fen peatland, and therefore the current configuration of the upland is capable of supporting moisture deficits (Sutton *et al.* 2019). The NFW provides a unique opportunity to assess the suitability of tree species in reclamation projects, and provide insight on the ability of specific trees to impact soil moisture dynamics.

Under the threat of climate change, selecting appropriate tree communities to use in reclamation becomes increasingly important with predicted increases in temperature and greater variability in precipitation events (Hidiwijawa *et al.* 2020; Pappas *et al.* 2018; Allen *et al.* 2015). Selection of tree species and are key drivers in the success of reclamation and rehabilitation of disturbed areas (Macdonald *et al.* 2012). Water and its availability to plants is a necessity for growth and to create a self-sustaining system following disturbances. More intense precipitation

events in the boreal region may enhance soil moisture stores due to reduced INT capabilities, conversely increases in temperature will enhance evaporative demand leading to significantly higher water losses from the system, ultimately in the form of ET (Pappas *et al.* 2018; Novick *et al.* 2016; Rigden & Salvucci, 2017). However, future climate projections also call for extended periods of minimal precipitation creating dry spells (Ruiz-Pérez & Vico, 2020), likely reducing the upland's ability to contribute to groundwater recharge and feed the adjacent peatland and further reducing water availability for root water uptake (Figure 17). Additionally, changes in temperature will prolong growing seasons creating more favorable conditions for photosynthesis (Kang *et al.* 2006; Jarvis & Lunder, 2000; Nemani *et al.* 2003).

In a region where ET typically exceeds P, selecting and planting trees capable of partitioning resources efficiently is essential to meet the goals set out for NFW and any reclaimed landscape to provide suitable soil water conditions while also developing a dense forest canopy. For example, *Pinus banksiana* may become an important species to use in reclamation efforts under a changing climate because of their ability to adapt to dry conditions and nutrient-poor soils for long periods (Moore *et al.* 2000). With shifts towards drier conditions, new reclamation strategies should consider the use of *Pinus banksiana* trees in upland designs as they possess water conserving strategies and have the potential to grow successfully despite limited moisture availability. Increasing proportions of coniferous trees within the WBP would promote lower T rates per unit leaf area as the stand ages compared to broadleaf trees (Ewer *et al.* 2005). These characteristics allow these species to reduce root water uptake and partition water resources efficiently, establishing a stable continuity between the upland and peatland system. Diversity in tree species is a good indicator of site productivity (Dhar *et al.* 2008), but can also increase the resiliency of the forest to combat climate change (Hof *et al.* 2017). The unpredictable nature of a

changing climate makes it difficult to anticipate the outcomes of plant succession and the future trajectory of the site. However, by planting a variety of tree species capable of responding to different potential scenarios of a changing climate, there will be species capable of exploiting the conditions available (Hof *et al.* 2017; Crowe & Parker, 2008). However, re-vegetation attempts of forest disturbances take numerous years to stabilize and have shown tendencies to create homogenized stand characteristics (stand age, diversity, structure) (Nyairo, 2003; Hanus *et al.* 2001).

Predicted changes in climate will affect vegetation composition and function, which will ultimately feedback to affect soil moisture regimes at the site. Development in vegetative cover will direct more radiation energy to plant T resulting in greater soil water uptake and less water available for percolation (Huang *et al.* 2015). Homogenization of tree population occurs as a result of rapid shifts in vegetation in response to a changing climate, creating dramatically different systems (Keenan, 2015). Additionally, Hadiwijaya *et al.* (2020) found that although ET is generally most sensitive to changes in precipitation patterns than temperature, we may see a shift in the distribution of coniferous trees as a result of climate change. In this case, we would see a greater distribution of deciduous broadleaf trees, which based on the results of this study were shown to have greater ET losses during the growing season. Evidence of post-disturbance transition to early-successional broadleaved stands have already been observed in the WBP (Searle & Chen, 2017; Stevens-Rumann *et al.* 2018). This will have implications for post-mined landscapes such as NFW, as *Picea mariana* and *Pinus banksiana* species may be outcompeted by broadleaf trees as a result of their abilities to penetrate deeper into the soil profile and access water that may not be available to species developing shallow root systems (coniferous trees) (Farrar, 2003; Quiñonez-piñón, 2007). Their ability to access deep water stores and take advantage of a

greater soil volume will eventually result in a reduction of soil water content and lead to further changes in spatial and temporal trends in vegetation and water availability throughout the growing season (Asbjornsen *et al*. 2011; Asbjornsen *et al.* 2008; Dalsgaard *et al*. 2011; Lu *et al*. 2011; Naeth *et al.* 2011; Schwinning, 2010). Meanwhile, broadleaf trees will have greater INT capacities when progressing towards canopy closure, likely reducing water reaching the surface and potentially reducing available water for T, while also reducing available water for recharge. Further research should look to address potential concerns of future conditions by continuously monitoring the success and development in tree communities, while also addressing their impending impacts on the hydrological cycle with time since construction at NFW.

Tree community development is not static, continuing to evolve many years following construction of the site (Dhar *et al.* 2018). Reclamation efforts need to take into consideration the inevitable changes that will occur in the WBP and address potential threats climate change may pose on tree succession and productivity. In landscapes involving upland-fen designs, selecting tree communities that will be able to withstand climate changes while continuing to provide sustainable moisture conditions and recharge will be critical in a dynamically changing climate region. Emphasis must be placed into including vegetation controls on moisture dynamics in future modeling scenarios. Continuous monitoring, instead of one-time measurements, of the combined processes of soil and vegetation dynamics will aid in the success of creating a self-sustaining and resilient system.

5.6. Project limitations

This study used a number of different methods to assess the role of trees on water partitioning. Limitations within the methodology and design of the study must be noted. Adequately representing sap flow stand heterogeneity was difficult due to limited cable lengths of the Flow32

sap flow monitoring system. Consequently, only trees within the range of cable lengths were instrumented, potentially overlooking diversity within the stand. Due to the inability to conduct destructive sampling of trees at the site, sapwood area was estimated by establishing linear regressions with DBH (Bond-Lamberty *et al.* 2002). Using an estimated value of sapwood area may not be representative of all trees and may raise uncertainty in scaling processes, as scaling is done using tree sapwood area. Additionally, uncertainty of scaling T to the stand level may have been reduced by instrumenting a larger number of trees. Instrumenting more than 4 trees would improve species-specific daily regressions to scale-up individual tree sap flow to the stand-level.

There are various errors associated with different measurement techniques, as different methods are used to compare throughout the study. Therefore, the potential differences in methods and their limitations may give rise to unexpected trends. Such trends were observed between ET and T rates, which may be attributed to gap-filling and correcting for energy balance closure on ET measurements from the EC system. These corrections can lead to over or underestimation of ET rates. Additionally, VWC was averaged over a 60 cm range within the soil profile to capture the entire rooting depth, which may lead to implications with respect to differences in moisture content at different depths. Averaging over such a wide depth raises uncertainty when assessing soil texture, as it may vary within that depth but also when comparing to soil water pressure measurements taken at 30 and 50 cm. Taking the average across 60 cm may not be representative of what the moisture content is at those specific depths, raising uncertainty in comparisons.

Data for this study were collected from small sample sizes for both rainfall partitioning and sap flow measurements. Due to logistical constraints, TF and SF were measured on 4 of each species, collecting measurements on average tree size based on tree surveys. Only representing a relatively small sub-group raises uncertainty in characterizing trends from specific trees.

Inaccurate measurement techniques have been at the forefront of difficulties faced in SF research (Levia & Frost, 2003). Currently, there lacks a standard procedure for SF measurements making it difficult to draw comparisons among studies and have a better understanding of the role SF plays in the hydrologic cycle (Germer *et al.* 2010; Levia & Frost, 2003). Furthermore, there is a lack in measurement of rainfall partitioning in juvenile and scattered trees following disturbances, especially on trees characteristic of the WBP region. Installation of SF collectors is quite difficult, requiring a significant amount of silicone to ensure a proper seal to the tree and avoid leaking. Therefore, removing collectors throughout the season for re-installation is not ideal and should be avoided. To avoid clogging, minimizing the distance of tape and screen between the trunk of the tree will reduce litter from potentially entering the funnel and tubing. However, litter may be carried with water along the stem making it difficult to avoid clogging and requiring frequent observation of the state of collectors. Overall, this method proved to be an efficient technique to measure SF on trees of small DBH and can be used on trees with varying bark textures, however SF measurements may still face potential uncertainties due to methodology. Future work should instrument a larger sample size to have a more comprehensive understanding of what trees are actually doing and reduce uncertainties, while keeping in consideration potential modifications to instrumentation design to avoid clogging and loss data points.

Using the systems response using multiple methods and comparing across methods is the best approach to come to a better understanding of what the ecosystem is actually doing – which is a strength of the work. Additionally, long-term monitoring is necessary when addressing tree water use and rainfall partitioning, as inevitable changes will occur with tree development.

Chapter 6: Summary and Conclusion

This study presented trends in species-specific T and rainfall partitioning over the course of the growing season at a post-mined oil sands site located in Fort McMurray, Alberta. Currently, wetland reclamation remains a novel strategy with the NFW being one of the first attempts in the WBP. Among the many challenges faced to date, the design and sustainability of these systems remains a central focus. The design incorporates uplands with the goal of supplying groundwater to the adjacent fen peatland, which will likely influence many components of the ecosystem, including vegetation growth and productivity. The vegetative state of the upland has progressed over the course of 6 years since construction, growing towards a denser forest canopy. Rapid re-establishment of vegetation communities can be attributed to considerable soil water conditions due to reduced canopy interception and limited tree transpiration (Bréda *et al.* 1994). While the goal of the target vegetation is to resemble natural WBP, it is also important that vegetation is suitable to achieve the desired outcomes. Progression in vegetation development will ultimately dictate partitioning of precipitation into interception, throughfall, stemflow, transpiration and recharge (Sutton *et al.* 2019). Furthermore, with the potential threats of climate change, understanding the likelihood of the upland to become a self-sustaining system while continuing to provide sufficient moisture to the adjacent fen is important.

The first objective of the study was to quantify rainfall partitioning components of throughfall, stemflow and interception of dominant tree species. It is important to note that the study took place during the growing season when rainfall is the predominant precipitation type, thus studies during the dormant season should be conducted to understand partitioning of snowfall. Vegetation structure and rainfall event characteristics were found to explain most of the variability in rainfall partitioning, which lead to interspecific and intraspecific differences in partitioning

abilities among species. Throughfall was the largest partitioning pathway, generally increasing with increasing event size for all tree species. Isolated and scattered trees characteristic of the site led to spatial variability in throughfall, ultimately resulting in significant volumes of water restoring soil moisture stores and recharging the adjacent fen peatland. Interception followed throughfall, increasing in response to increasing foliage density of individual trees. Results suggest that the dense foliage and large surface area of coniferous trees enables them to intercept a greater percentage of incoming precipitation. While, sparse and narrow features of juvenile broadleaf trees discourage high interception capabilities. While stemflow is a small input to surface soil moisture, it has hydrological and biogeochemical importance as a point source of water and nutrients for plant uptake.

The second objective was to assess trends in T of dominant tree species used in upland reclamation throughout the 2019 growing season. Contributions to ET fluxes are ultimately dictated by canopy LAI and will shift patterns as re-vegetation at the site occurs. While currently soil evaporation makes up a significant proportion of ET fluxes as a result of low-density canopy cover and scattered trees, it is expected that proportions will decrease as canopy continues to develop. Significant correlations were observed between ET measured from eddy covariance and stand T measured from sap flow, where deviations may likely be a result of underestimation of T. Results have confirmed the use of sap flow to assess tree water relations on small juvenile trees. T had the greatest contribution to ET fluxes throughout the growing season, varying spatially and temporally, while also varying within and between species. Though relationships weren't strong, daily variations in T responded to changes in meteorological conditions such as VPD, net radiation and air temperature. However, it was found that environmental variables influenced sap fluxes at different times throughout the day. Most noteworthy, *Populus balsamifera* were most sensitive to

variations in VPD emphasizing their abilities to close stomata in response to high evaporative demand and conserve water. VPD appeared to have stronger controls on T rates of coniferous trees, while net radiation had a greater influence on *Populus tremuloides*.

Transpiration, evaporation, interception, throughfall and stemflow are all essential factors to consider when assessing soil water dynamics in a system. Based on the results of this study, vegetation is the dominant control on partitioning of water resources following upland reclamation. Accordingly, emphasizing the importance of understanding how dominant tree species partition water resources in a managed system. Despite the young age of the stand, trends in tree water use indicate that tree species follow similar patterns to natural WBP systems and that water loss per species was minimized as a result of low LAI. Vegetation development was the main control on ET fluxes in the system and were for the most part dominated by contributions from broadleaf trees. Broadleaf, which constitute a majority of the tree community, currently contribute greatly to surface soil moisture as a result of high throughfall rates. However, throughfall rates at the site are subject to substantial changes as the canopy develops and canopy storage capacity is enhanced. Additionally, with predicted changes in climate regimes heightening evaporative demand, high water use characteristic of broadleaf trees will ultimately deplete soil water stores. Whereas, conifers were found to withstand a greater range of soil conditions and have greater control over water losses possibly suggesting a shift towards coniferous stands.

The complexity of interactions between soil, vegetation and atmosphere was observed in the feedbacks between these systems. A combination of vegetation and soil conditions are likely the explanation to spatial variability in soil moisture, which feedback to influence vegetation dynamics. Results suggest that trees responded more sensitively to fluctuations in soil moisture

over the course of the growing season. The spatial distribution in soil moisture regimes will determine the success of vegetation communities based on the trees respective abilities to withstand changes in moisture conditions. Soil moisture displayed a transitional pattern shifting from drier conditions in the upper slope regions of the upland to wetter conditions at the lower slope regions adjacent to the fen peatland. Specifically, broadleaf trees were most sensitive to changes in moisture availability due to their dependency on sufficient water supply, growing with greatest success in the upland-fen transitional zone. Coniferous trees were less sensitive to fluctuations in water availability explaining their success in the drier regions of the upland.

Results demonstrate the importance of tree resource partitioning for driving not only spatial patterns in moisture and nutrient availability, but landscape scale contributions to recharge following oil sands mining. This study provides a better understanding of the general pathway of plant community succession and the interactions between soil, vegetation and atmosphere in the early stages of landscape reclamation.

References

Aboal, J. R., Morales, D., Hernández, M., & Jiménez, M. S. (1999). The measurement and modelling of the variation of stemflow in a laurel forest in Tenerife, Canary Islands. *Journal of Hydrology*, *221*(3–4), 161–175. https://doi.org/10.1016/S0022-1694(99)00086-4.

Ahmed, A., Tomar, J. M. S., Mehta, H., Kaushal, R., Deb, D., Chaturvedi, O. P., & Mishra, P. K. (2017). Throughfall, stemflow and interception loss in grewia optiva and morus alba in North West Himalayas. *Tropical Ecology*, *58*(3), 507–514.

Alberta Environment (2010). Guidelines for Reclamation to Forest Vegetation in the Athabasca Oil Sands Region, 2nd Edition. Prepared by the Terrestrial Subgroup of the Reclamation Working Group of the Cumulative Environmental Management Association, Fort McMurray, AB.

Allen, R. G., Pereira, L. S., Raes, D., & Smith, M. S. (1998). Crop evapotranspiration – Guidelines for computing crop water requirements - FAO Irrigation and drainage paper 56. Irrig. Drain. 1–15. doi:10.1016/j.eja.2010.12.001.

Angstmann, J. L., Ewers, B. E., Barber, J., & Kwon, H. (2013). Testing transpiration controls by quantifying spatial variability along a boreal black spruce forest drainage gradient. *Ecohydrology*, *6*(5), 783–793. https://doi.org/10.1002/eco.1300.

Asbjornsen, H., Goldsmith, G. R., Alvarado-Barrientos, M. S., Rebel, K., Van Osch, F. P., Rietkerk, M., & Dawson, T. E. (2011). Ecohydrological advances and applications in plant-water relations research: A review. *Journal of Plant Ecology*, *4*(1–2), 3–22.

Aubinet, M., Vesala, T., & Papale, D. (2012). Eddy covariance: a practical guide to measurement and data analysis. Springer & Business Media

Audet, P., Pinno, B.D., Thiffault, E. (2015). Reclamation of boreal forest after oil sands mining: anticipating novel challenges in novel environments. Can. J. For. Res. 45, 364–371. doi:dx.doi.org/10.1139/cjfr-2014-0330.

Austin, A. T., Yahdjian, L., Stark, J. M., Belnap, J., Porporato, A., Norton, U., & Schaeffer, S. M. (2004). Water pulses and biogeochemical cycles in arid and semiarid ecosystems. *Oecologia*, *141*(2), 221–235. https://doi.org/10.1007/s00442-004-1519-1.

Barbier, S., Balandier, P., & Gosselin, F. (2009). Influence of several tree traits on rainfall partitioning in temperate and boreal forests: a review. *Annals of Forest Science*, *66*(6), 602–602. https://doi.org/10.1051/forest/2009041.

Barr, A. G., Morgenstern, K., Black, T.A., McCaughey, J.H., and Nesic, Z. (2006), Surface energy balance closure by the eddy-covariance method above three boreal forest stands and implications for the measurement of CO2 flux, Agric. For. Meteorol., 140, 322–337, doi:10.1016/j.agrfor- met.2006.08.007.

Benegas Negri, L. A. (2018). The role of scattered trees in soil water dynamics of pastures and agricultural lands in the Central American Tropics. PhD. Thesis. Department of Forest Ecology and Management, PhD. Swedish University of Agricultural Sciences.

Benyon, R. G., & Doody, T. M. (2015). Comparison of interception, forest floor evaporation and transpiration in Pinus radiata and Eucalyptus globulus plantations. *Hydrological Processes*, *29*(6), 1173–1187. https://doi.org/10.1002/hyp.10237.

Bladon, K. D., Silins, U., Landhausser, S. M. & Lieffers, V. J. (2006). Differential transpiration by three boreal tree species in response to increased evaporative demand after variable retention harvesting. Agric. For. Meteorol. 138: 104?119.

Bond-Lamberty, B., Wang, C., & Gower, S. T. (2002). Aboveground and belowground biomass and sapwood area allometric equations for six boreal tree species of northern Manitoba. *Canadian Journal of Forest Research*, *32*(8), 1441–1450. https://doi.org/10.1139/x02-063.

Bovard, B. D., Curtis, P. S., Vogel, C. S., Su, H. B., & Schmid, H. P. (2005). Environmental controls on sap flow in a northern hardwood forest. *Tree Physiology*, *25*(1), 31–38.

Brown, S.M., Petrone, R.M., Mendoza, C., & Devito, K.J. (2010). Surface vegetation controls on evapotranspiration from a sub-humid Western Boreal Plain wetland. Hydrol. Process. 24, 1072–1085. doi:10.1002/hyp.7569.

Burba, G., Schmidt, A., Scott, R. L., Nakai, T., Kathilankal, J., Fratini, G., Velgersdyk, M. (2012). Calculating CO2 and H2O eddy covariance fluxes from an enclosed gas analyzer using an instantaneous mixing ratio. Global Change Biology, 18, 385-399.

Burgess, S. S. O., Adams, M. A., Turner, N. C., Beverly, C. R., Ong, C. K., Khan, A. A. H., & Bleby, T. M. (2001). An improved heat pulse method to measure low and reverse rates of sap flow in woody plants. *Tree Physiology*, *21*(9), 589–598.

Carey, S.K., (2008). Growing season energy and water exchange from an oil sands overburden reclamation soil cover, Fort McMurray, Alberta, Canada 2857, 2847–2857. doi:10.1002/hyp.

Carlyle-Moses, D. E., Iida, S., Germer, S., Llorens, P., Michalzik, B., Nanko, K., & Levia, D. F. (2018). Expressing stemflow commensurate with its ecohydrological importance. *Advances in Water Resources*, *121*(July), 472–479. https://doi.org/10.1016/j.advwatres.2018.08.015.

Carrera-Hernández, J. J., Mendoza, C. A., Devito, K. J., Petrone, R. M., & Smerdon, B. D. (2011). Reclamation for aspen revegetation in the Athabasca oil sands: Understanding soil water dynamics through unsaturated flow modelling. *Canadian Journal of Soil Science*, *92*(1), 103–116. https://doi.org/10.4141/cjss2010-035.

Cumulative Environmental Management Association (CEMA), (2006). Land capability classification system for forest ecosystems in the oil sands. CEMA, Fort McMurray, AB, Canada.

Cermak, J., & Nadezdhina, N. (1998). Sapwood as the scaling parameter: defining according to xylem water content or radial pattern of sap flow?. Ann. For. Sci., 55, P.509-521.

Čermák, J., Kučera, J., & Nadezhdina, N. (2004). Sap flow measurements with some thermodynamic methods, flow integration within trees and scaling up from sample trees to entire forest stands. *Trees - Structure and Function*, *18*(5), 529–546. https://doi.org/10.1007/s00468-004-0339-6.

Chen, J.M., Rich, P.M., Gower, S.T., Norman, J.M., & Plummer, S. (1997). Leaf area index of boreal forest: Theory, techniques, and measurements. Journal of Geophysical Research. 102:24, P.29429-29443.

Chen, L., Zhang, Z., Zha, T., Mo, K., Zhang, Y., & Fang, X. (2014). Soil water affects transpiration response to rainfall and vapor pressure deficit in poplar plantation. *New Forests*, *45*(2), 235–250. https://doi.org/10.1007/s11056-014-9405-0.

Cienciala, E., Running, S. W., Lindroth, A., Grelle, A., & Ryan, M. G,. (1998). Analysis of carbon and water fluxes from the NOPEX boreal forest: comparison of measurements with FOREST-BGC simulations. Journal of Hydrology 212-213: 62–78.

Clulow, A. D., Everson, C. S., Mengistu, M. G., Jarmain, C., Jewitt, G. P. W., Price, J. S., & Grundling, P. L., 2012. Measurement and modelling of evaporation from a coastal wetland in Maputaland, South Africa. Hydrology and Earth System Sciences, 16(9), 3233.

Clulow, AD, Everson, CS., Mengistu, MG., Price, JS., Nickless, A., and Jewitt, GPW., 2014. Extending periodic eddy covariance latent heat fluxes through tree sapflow measurements to estimate long-term total evaporation in a peat swamp forest. Hydrol. Earth Syst. Sci. Discuss., 18, 13607-13661.

Crockford, R. H., & Richardson, D. P. (2000). Partitioning of rainfall into throughfall, stemfow and interception: effect of forest type, ground cover and climate. *Hydrolo*, 2903–2920.

Daly, C.A., Price, J.S., Rezanezhad, F., Pouliot, R., Rochefort, L., & Graf, M., (2012). Initiatives in oil sand reclamation: Considerations for building a fen peatland in a post-mined oil sands landscape. In: Restoration and Reclamation of Boreal Ecosystems - Attaining Sustainable Development. Vitt D, Bhatti JS (eds.) Cambridge University Press, pp: 179-201.

David, T.S., Ferreira, M. I., Cohen, S., Pereira, J. S., & David, J. S. (2004). Constraints on transpiration from an evergreen oak tree in southern Portugal. Agricultural and Forest Meteorology. 122(3): 193-205.

Depante, M., Petrone, R. M., Devito, K. J., Kettridge, N., Macrae, M. L., Mendoza, C., & Waddington, J. M. (2018). Potential influence of nutrient availability along a hillslope: Peatland gradient on aspen recovery following fire. *Ecohydrology*, *11*(5), 1–13. https://doi.org/10.1002/eco.1955.

Devito, K., Creed, I., Gan, T., Mendoza, C., Petrone, R., Silins, U., & Smerdon, B., (2005). A framework for broad-scale classification of hydrologic response units on the Boreal Plain: is topography the last thing to consider? Hydrol. Process. 19, 1705–1714. doi:10.1002/hyp.5881.

Dhar, A., Comeau, P. G., Karst, J., Pinno, B. D., Chang, S. X., Naeth, A. M., & Bampfylde, C. (2018). Plant community development following reclamation of oil sands mine sites in the boreal forest: A review. *Environmental Reviews*, *26*(3), 286–298. https://doi.org/10.1139/er-2017-0091.

Dimitrov, D.D., Bhatti, J.S., & Grant, R.F., (2014). The transition zones (ecotone) between boreal forests and peatlands: Ecological controls on ecosystem productivity along a transition zone between upland black spruce forest and a poor forested fen in central Saskatchewan. Ecol. Modell. 291, 96–108. doi:10.1016/j.ecolmodel.2014.07.020.

D'Odorico, P., Caylor, K., Okin, G. S., & Scanlon, T. M. (2007). On soil moisture-vegetation feedbacks and their possible effects on the dynamics of dryland ecosystems. *Journal of Geophysical Research: Biogeosciences*, *112*(4), 1–10. https://doi.org/10.1029/2006JG000379.

Dynamax Inc. (2007). Flow 32-1K Sap Flow System with CR1000 Data Logger Manual. Dynamax Inc, Houston, TX.

Dynamax Inc. (2007b). Dynagage sap flow sensor user manual. Dynamax Inc, Houston, TX.

Elliot-Frisk, D. L. (1988). The boreal forest. In Barbour, M. G. and Billings, W. D., editors, North American Terrestrial Vegetation, chapter 2, pages 33–62. Cambridge University Press, New York, first edition.

Elliott, J. A., Toth, B. M., Granger, R. J., & Pomeroy, J. W. (1998). Soil moisture storage in mature and replanted sub-humid boreal forest stands. *Canadian Journal of Soil Science*, *78*(1), 17–27. https://doi.org/10.4141/S97-021.

Environment Canada. (2015). Canadian Climate Normals 1981-2010 Station Data [WWW Document]. URL http://climate.weather.gc.ca/climate_normals/results_1981_2010_e.html?stnID=2519&autofwd=1 (accessed 2.10.19).

Errington, R.C., & Pinno, B.D., (2015a). Early successional plant community dynamics on a reclaimed oil sands mine in comparison with natural boreal forest communities. Écoscience 22, 133–144. doi:10.1080/11956860.2016.1169385.

Ewers, B. E., Gower, S. T., Bond-Lamberty, B., & Wang, C. K. (2005). Effects of stand age and tree species on canopy transpiration and average stomatal conductance of boreal forests. *Plant, Cell and Environment*, *28*(5), 660–678. https://doi.org/10.1111/j.1365-3040.2005.01312.x.

Ewers, B.E., Mackay, D.S., Tang, J., Bolstad, P.V., & Samanta, S. (2008). Intercomparison of sugar maple (Acer saccharum March.) stand transpiration responses to environmental conditions for the Western Great Lakes Region of the United States. Journal of Agricultural Forest Meteorology, 128, P.231-246.

Farley, K. A., Jobbágy, E. G., & Jackson, R. B. (2005). Effects of afforestation on water yield: A global synthesis with implications for policy. *Global Change Biology*, *11*(10), 1565–1576. https://doi.org/10.1111/j.1365-2486.2005.01011.x.

Farrar, J. L. (2003). Trees in Canada. Fitzhenry & Whiteside Limited, Markham, Ontario, eight edition.

Fatichi, S., & Pappas, C. (2017). Constrained variability of modeled T:ET ratio across biomes. *Geophysical Research Letters*, *44*(13), 6795–6803. https://doi.org/10.1002/2017GL074041.

Ferone, J.M., & Devito, K.J. (2004). Shallow groundwater-surface water interactions in pond-peatland complexes along a Boreal Plains topographic gradient. J. Hydrol. 292, 75–95. doi:10.1016/j.jhydrol.2003.12.032.

Foken, T., & Leclerc, M. Y. (2004). Methods and limitations in validation of footprint models. Agriculture and Forest Meteorology, 127(3-4), 223-234.

Ford, C.R., Hubbard, R.M., Kloeppel, B.D., & Vose, J.M. (2007). A comparison of sap flux-based evapotranspiration estimates with catchment-scale water balance. Journal of Agricultural Forest Meteorology, 145, P.176-185.

Freeze RA, Cherry JA. (1979). Groundwater. Prentice-Hall.

Frerichs, L. A., Bork, E. W., Osko, T. J., & Naeth, M. A. (2017). Effects of boreal well site reclamation practices on long-term planted spruce and deciduous tree regeneration. *Forests*, *8*(6). https://doi.org/10.3390/f8060201.

Gabrielli, E. C. (2016). Partitioning Evapotranspiration in Forested Peatlands within the Western Boreal Plain, Fort McMurray, Alberta, Canada, 133.

Germer, S., Werther, L., & Elsenbeer, H. (2010). Have we underestimated stemflow? Lessons from an open tropical rainforest. *Journal of Hydrology*, *395*(3–4), 169–179. https://doi.org/10.1016/j.jhydrol.2010.10.022.

Gingras-Hill, T., Petrone, R. M., Nwaishi, F. C., & Price, J. S. (2018). Ecohydrological functioning of an upland undergoing reclamation on post - mining landscape of the Athabasca oil sands region, Canada, (September 2017), 1–12. https://doi.org/10.1002/eco.1941.

Grelle, A., Lundberg, A., Lindroth, A., Moren, A. S., Cienciala, E. (1997). Evaporation components of a boreal forest: variations during the growing season. Journal of Hydrology 197: 70–87.

Grime, V. L., Morison, J. I. L., & Simmonds, L. P. (1995). Including the heat storage term in sap flow measurements with the stem heat balance method. *Agricultural and Forest Meteorology*, *74*, 1–25.

Groot, A., & King, K. M. (1992). Measurement of sap flow by the heat balance method: numerical analysis and application to coniferous seedlings. *Agricultural and Forest Meteorology*, *59*(3–4), 289–308. https://doi.org/10.1016/0168-1923(92)90098-O.

Hadiwijaya, B., Pepin, S., Isabelle, P. E., & Nadeau, D. F. (2020). The dynamics of transpiration to evapotranspiration ratio under wet and dry canopy conditions in a humid boreal forest. *Forests*, *11*(2), 1–25. https://doi.org/10.3390/f11020237.

Hamilton, I., (2015). The interactions of Jack Pine trees (*Pinus banksiana*) and water, M.Sc. Thesis. Department of Soil Science, M.Sc. University of Saskatchewan.

Herwitz, S. R. (1986). Infiltration-excess caused by Stemflow in a cyclone-prone tropical rainforest. *Earth Surface Processes and Landforms*, *11*(4), 401–412. https://doi.org/10.1002/esp.3290110406.

Hogg, E. H. (1994). Climate and the southern limit of the western Canadian boreal forest. Canadian Journal of Forest Research 24: 1835–1845.

Hogg, E. H., Black, T. A., Den Hartog, G., Neumann, H. H., Zimmermann, R., Hurdle, P. A., & Oren, R. (1997). A comparison of sap flow and eddy fluxes of water vapor from a boreal deciduous forest. *Journal of Geophysical Research Atmospheres*, *102*(24), 28929–28937. https://doi.org/10.1029/96jd03881.

Hogg, E. H., & Hurdle, P. A. (1997). Sap flow in trembling aspen: Implications for stomatal responses to vapor pressure deficit. *Tree Physiology*, *17*(8–9), 501–509. https://doi.org/10.1093/treephys/17.8-9.501.

Huang, M., Barbour, S.L., & Carey, S.K., (2015). The impact of reclamation cover depth on the performance of reclaimed shale overburden at an oil sands mine in Northern Alberta. Canada. Hydrological Processes 29 (12), 2840–2854.

Huang, M., Barbour, S.L., Elshorbagy, A., Zettl, J., & Si, B.C., (2013). Effects of Variably Layered Coarse Textured Soils on Plant Available Water and Forest Productivity. Procedia Environ. Sci. 19, 148–157. doi:10.1016/j.proenv.2013.06.017.

Huang, M., Lee Barbour, S., Elshorbagy, A., Zettl, J.D., & Cheng Si, B., (2011). Infiltration and drainage processes in multi-layered coarse soils. Can. J. Soil Sci. 91, 169–183. doi:10.4141/cjss09118.

Irving, H. (2020). *The Impact of LFH Mineral Mix on the Function of Reclaimed Landscapes in the Athabasca Oil Sands Region, Alberta, Canada*.

Ivans, S., Hipps, L., Leffler, A. J., & Ivans, C. Y., (2006) Response of water vapor and CO2 fluxes in semiarid lands to seasonal and intermittent precipitation pulses. J Hydrometeorology 7(5):995–1010.

Jain, M., Kuriakose, G., & Balakrishnan, R. (2010). Evaluation of methods to estimate foliage density in the understorey of a tropical evergreen forest. *Current Science*, *98*(4), 508–515.

Jean, S. A., Pinno, B. D., & Nielsen, S. E. (2019). Trembling aspen root suckering and stump sprouting response to above ground disturbance on a reclaimed boreal oil sands site in Alberta, Canada. *New Forests*, *50*(5), 771–784. https://doi.org/10.1007/s11056-018-09698-2.

Johnson, E. A, & Miyanishi, K., (2008). Creating new landscapes and ecosystems: the Alberta Oil Sands. Ann. N. Y. Acad. Sci. 1134, 120–45. doi:10.1196/annals.1439.007.

Kaimal, J. C., & Finnigan, J. J. (1994). Atmospheric boundary layer flows: their structure and management. New York: Oxford University Press.

Kang, S., Kimball, J. S., & Running, S. W. (2006). Simulating effects of fire disturbance and climate change on boreal forest productivity and evapotranspiration. *Science of the Total Environment*, *362*(1–3), 85–102. https://doi.org/10.1016/j.scitotenv.2005.11.014.

Kermavnar, J., & Vilhar, U. (2017). Canopy precipitation interception in urban forests in relation to stand structure. *Urban Ecosystems*, *20*(6), 1373–1387. https://doi.org/10.1007/s11252-017-0689-7.

Kessel, E., (2016). The hydrogeochemisty of a constructed fen peatland in a post-mined landscape in the Athabasca Oil Sands Region, Alberta, Canada, M.Sc. Thesis. Department of Geography and Environmental Management, M.Sc. University of Waterloo.

Ketcheson, S., (2015). Hydrology of a Constructed Fen Watershed in a Post-Mined Landscape in the Athabasca Oil. PhD dissertation. University of Waterloo.

Ketcheson, S., & Price, J., (2016). A comparison of the hydrological role of two reclaimed slopes of different age in the Athabasca Oil Sands Region, Alberta, Canada. Can. Geotech. J. 14, cgj- 2015-0391. doi:10.1139/cgj-2015-0391.

Ketcheson, S.J., Price, J.S., Carey, S.K., Petrone, R.M., Mendoza, C.A., & Devito, K.J., (2016). Constructing fen peatlands in post-mining oil sands landscapes: Challenges and opportunities from a hydrological perspective. Earth-Science Rev. 161, 130–139. doi:10.1016/j.earscirev.2016.08.007.

Ketcheson, S.J., Price, J.S., Sutton, O., Sutherland, G., Kessel, E., & Petrone, R.M., (2017). The hydrological functioning of a constructed fen wetland watershed. Sci. Total Environ. 603, 593–605.

Kljun, N., Calanca, P., Rotach, M., & Schmid, H. (2004). A simple parameterisation for flux footprint predictions. *Boundary-Layer Meteorol*, 112: 503–523. doi:10.1023/B:BOUN.0000030653. 71031.96.

Kumagai, T., Nagasawa, H., Mabuchi, T., Ohsaki, S., Kubota, K., Kogi, K., Utsumi, Y., Koga, S., & Otsuki, K., (2005). Sources of error in estimating stand transpiration using allometric relationships between stem diameter and sapwood area for Cryptomeria japonica and Chamaecyparis obtusa. For. Ecol. Manage. 206, 191-195.

Lagergren, F., & Lindroth, A. (2002). Transpiration response to soil moisture in pine and spruce trees in Sweden. *Agricultural and Forest Meteorology*, *112*(2), 67–85.

Langs, L. E. (2019). Quantifying coniferous subalpine tree transpiration and source water under seasonal and hydrological stress in the Canadian Rocky. M.Sc. Thesis. Department of Geography and Environmental Management, M.Sc. University of Waterloo.

Leatherdale, J., Chanasyk, D.S., & Quideau, S., (2012). Soil water regimes of reclaimed upland slopes in the oil sands region of Alberta. Can. J. Soil Sci. 92, 117–129. doi:10.4141/cjss2010-027.

Leuning, R., & Judd, M. J. (1996). The relative merits of open- And closed-path analysers for measurement of eddy fluxes. *Global Change Biology*, *2*(3), 241–253.

Levia, D. F., & Frost, E. (2003). A review and evaluation of stemflow literature in the hydrologic and biogeochemical cycles of forested and agricultural ecosystems. *Journal of Hydrology*, *274*, 1–29.

Levia, D. F., & Herwitz, S. R. (2005). Interspecific variation of bark water storage capacity of three deciduous tree species in relation to stemflow yield and solute flux to forest soils. *Catena*, *64*(1), 117–137. https://doi.org/10.1016/j.catena.2005.08.001.

LI-COR. (2012). LAI-2200 Plant Canopy Analyzer: Instruction Manual. https://doi.org/10.5749/minnesota/9780816692019.003.0001

Lishman, C. E. (2015). Rainfall Redistribution by the Canopy of a Juvenile Lodgepole Pine Stand. M.Sc. Thesis. Department of Geography and Environmental Studies, M.Sc. Thompson Rivers University.

Livesley, S. J., Baudinette, B., & Glover, D. (2014). Rainfall interception and stem flow by eucalypt street trees - The impacts of canopy density and bark type. *Urban Forestry and Urban Greening*, *13*(1), 192–197. https://doi.org/10.1016/j.ufug.2013.09.001.

Loranty, M. M., Mackay, D. S., Ewers, B. E., Adelman, J. D., & Kruger, E. L. (2008). Environmental drivers of spatial variation in whole-tree transpiration in an aspen-dominated upland-to-wetland forest gradient. *Water Resources Research*, *44*(2), 1–15.

Macdonlad, E., Quideau, S., & Lanhausser, S. (2012). Rebuilding boreal forest after industrial disturbances. In Restoration and Reclamation of boreal ecosystems: attaining sustainable development. Edited by D.H. Vitt and J.S. Bhatti. Campridge University Press, Cambridge, UK. p. 123-160.

Macdonald, S.E., Landhäusser, S.M., Skousen, J., Franklin, J., Frouz, J., Hall, S., Jacobs, D.F., & Quideau, S., (2015a). Forest restoration following surface mining disturbance: challenges and solutions, New Forests. doi:10.1007/s11056-015-9506-4.

Macdonald, S.E., Snively, A.E.K., Fair, J.M., & Landhäusser, S.M., (2015b). Early trajectories of forest understory development on reclamation sites: influence of forest floor placement and a cover crop. Restor. Ecol. 23, 698–706. doi:10.1111/rec.12217.

Mackenzie, D., (2011). Best Management Practices for Conservation of Reclamation Materials in the Mineable Oil Sands Region of Alberta. Prepared for the Terrestrial Subgroup, Best Management Practices Task Group of the Reclamation working group of the Cumulative Environmental Management Association, Fort McMurray, AB.

MacKenzie, D.D., & Naeth, M.A., (2007). Assisted natural recovery using a forest soil propagule bank in the Athabasca oil sands. Seeds Biology, Development and Ecology, pp. 374–382.

Mackenzie, D.D., & Naeth, M.A., (2010). The role of the forest soil propagule bank in assisted natural recovery after oil sands mining. Restor. Ecol. 18, 418–427. doi:10.1111/j.1526-100X.2008.00500.x.

Marin, C. T., Bouten, W., & Sevink, J. (2000). Gross rainfall and its partitioning into throughfall, stemflow and evaporation of intercepted water in four forest ecosystems in western Amazonia. *Journal of Hydrology*, *237*(1–2), 40–57.

Mckee, A. J., (2008). The quantitative importance of stemflow: An evaluation of past research and results from a study in Lodgepole pine (*Pinus contorta var. latifolia*) stands in southern British Columbia, M.Sc. Thesis. Department of Geography, M.Sc. Thompson Rivers University.

Millennium EMS Solutions Ltd. (2011). Laricina Germain Project Expansion Vegetation, Wetlands, and Plant Biodiversity Assessment.

Mkhabela, M. S., Amiro, B. D., Barr, A. G., Black, T. A., Hawthorne, I., Kidston, J., & Zha, T. (2009). Comparison of carbon dynamics and water use efficiency following fire and harvesting in Canadian boreal forests. Agricultural and Forest Meteorology, 149(5), 783–794. https://doi.org/ 10.1016/j.agrformet.2008.10.025.

Moore, K. E., Fitzjarrald, D. R., Sakai, R. K., & Freedman, J. M. (2000). Growing season water balance at a Boreal jack pine forest. *Water Resources Research*, *36*(2), 483–493.

Moreno-de Las Heras, M., Merino-Martín, L., & Nicolau, J.M., (2009). Effect of vegetation cover on the hydrology of reclaimed mining soils under Mediterranean- Continental climate. Catena 77 (1), 39–47.

Naeth, M.A., Chanasyk, D.S., & Burgers, T.D., (2011). Vegetation and soil water interactions on a tailings sand storage facility in the Athabasca oil sands region of Alberta Canada. Phys. Chem. Earth 36, 19–30. doi:10.1016/j.pce.2010.10.003.

Nicholls, E. M., Carey, S. K., Humphreys, E. R., Clark, M. G., & Drewitt, G. B. (2016). Multi-year water balance assessment of a newly constructed wetland, Fort McMurray, Alberta. *Hydrological Processes*, *30*(16), 2739–2753. https://doi.org/10.1002/hyp.10881.

Novick, K. A., Ficklin, D. L., Stoy, P. C., Williams, C. A., Bohrer, G., Oishi, A. C., & Phillips, R. P. (2016). The increasing importance of atmospheric demand for ecosystem water and carbon fluxes. *Nature Climate Change*, *6*(11), 1023–1027. https://doi.org/10.1038/nclimate3114.

Oogathoo, S., Houle, D., Duchesne, L., & Kneeshaw, D. (2020). Vapour pressure deficit and solar radiation are the major drivers of transpiration of balsam fir and black spruce tree species in humid boreal regions, even during a short-term drought. *Agricultural and Forest Meteorology*, *291*, 108063. https://doi.org/10.1016/j.agrformet.2020.108063

Pappas, C., Matheny, A. M., Baltzer, J. L., Barr, A. G., Black, T. A., Bohrer, G., & Stephens, J. (2018). Boreal tree hydrodynamics: Asynchronous, diverging, yet complementary. *Tree Physiology*, *38*(7), 953–964. https://doi.org/10.1093/treephys/tpy043.

Pataki, D. E., Oren, R., & Smith, W. K. (2000). Sap flux of co-occurring species in a western subalpine forest during seasonal soil drought. *Ecology*, *81*(9), 2557–2566. https://doi.org/10.1890/0012-9658(2000)081[2557:SFOCOS]2.0.CO;2.

Peterson, E. B., & Peterson, N. M. (1992). Ecology, management, and use of aspen and balsam poplar in the prairie provinces, Canada. *Forestry Canada, Northwest Region, Forestry Centre*, 1–252.

Petrone, R. M., Chasmer, L., Hopkinson, C., Silins, U., Landhäusser, S. M., Kljun, N., & Devito, K. J. (2015). Effects of harvesting and drought on CO2 and H2o fluxes in an aspen-dominated western boreal plain forest: Early chronosequence recovery. *Canadian Journal of Forest Research*, *45*(1), 87–100. https://doi.org/10.1139/cjfr-2014-0253.

Petrone, R. M., Silins, U., & Devito, K. J. (2007). Dynamics of evapotranspiration from a riparian pond complex in the Western Boreal Forest, Alberta, Canada. *Hydrological Processes*, 21, 1391–1401. https://doi.org/10.1002/hyp.

Petrone, R. M., Waddington, J. M., & Price, J. S. (2001). Ecosystem scale evapotranspiration and net CO2 exchange from a restored peatland. *Hydrological Processes*, *15*(14), 2839–2845.

Pinno, B., & Hawkes, V. (2015). Temporal Trends of Ecosystem Development on Different Site Types in Reclaimed Boreal Forests. Forests 6, 2109–2124. doi:10.3390/f6062109.

Pinno, B.D., Errington, R.C., (2015). Maximizing natural trembling aspen seedling establishment on a reclaimed boreal oil sands site. Ecol. Restor. 33, 43–50. doi:10.3368/er.33.1.43.

Price, A. G., Dunham, K., Carleton, T., & Band, L. (1997). Variability of water fluxes through the black spruce (Picea mariana) canopy and feather moss (Pleurozium schreberi) carpet in the boreal forest of Northern Manitoba. *Journal of Hydrology*, *196*(1–4), 310–323.

Price, J.S., McLaren, R.G., & Rudolph, D.L. (2010). Landscape restoration after oil sands mining: conceptual design and hydrological modelling for fen reconstruction. Int. J. Mining, Reclam. Environ. 24, 109–123. doi:10.1080/17480930902955724.

Pu, R. (2017). Hyperspectral remote sensing: Fundamentals and practices. Hyperspectral Remote Sensing: Fundamentals and Practices. https://doi.org/10.1201/9781315120607.

Quiñonez-piñón, M. (2007). Improved Techniques for Measuring and Estimating Scaling Factors Used to Aggregate Forest Transpiration, PhD. Dissertation. Department of Geomatics Engineering, PhD. University of Calgary.

Quinty, F., & Rochefort, L. (2003). Peatland restoration guide, 2nd edn. Canadian Sphagnum Peat Moss Association, New Brunswick Department of Natural Resources and Energy, Quebec, Canada. www.peatmoss.com.

Rigden, A., & Salvucci, G. (2016). Stomatal response to humidity and CO 2 implicated in recent decline in U.S. evaporation. *Global Change Biology*, *23*. https://doi.org/10.1111/gcb.13439.

Rodriguez-Iturbe, I., D'Odorico, P., Porporato, A., & Ridolfi, L. (1999). On the spatial and temporal links between vegetation, climate, and soil moisture. *Water Resources*, *35*(12), 3709–3722.

Rooney, R.C., Bayley, S.E., & Schindler, D.W. (2012). Oil sands mining and reclamation cause massive loss of peatland and stored carbon. Proc. Natl. Acad. Sci. U. S. A. 109, 4933–7. doi:10.1073/pnas.1117693108.

Rowland, S.M., Prescott, C.E., Grayston, S.J., Quideau, S. A, & Bradfield, G.E., (2009). Recreating a functioning forest soil in reclaimed oil sands in northern alberta: an approach for measuring success in ecological restoration. J. Environ. Qual. 38, 1580–90. doi:10.2134/jeq2008.0317.

Ruiz-Pérez, G., & Vico, G. (2020). Effects of Temperature and Water Availability on Northern European Boreal Forests. *Frontiers in Forests and Global Change*, *3*, 1–18.

Sakuratani, T. (1981). A heat balance method for measuring water flux in the stem of intact plants. Journal of Agricultural Meteorology, 37, P.9-17.

Santos, F. L., Valverde, P. C., Reis, J. L., Ramos, A. F., & Castanheira, N. L. (2012). Sap flow scaling and crop coefficient of dry-farmed olive orchards converted to irrigation. *Acta Horticulturae*, *949*, 231–236. https://doi.org/10.17660/ActaHortic.2012.949.33.

Sarkkola, S., Nieminen, M., Koivusalo, H., Laurén, A., Ahti, E., Launiainen, S., & Hökkä, H. (2013). Domination of growing-season evapotranspiration over runoff makes ditch network maintenance in mature peatland forests questionable. *Mires and Peat*, *11*, 1–11.

Saugier, B., Granier, A., Pontailler, J. Y., Dufrene, E., & Baldocchi, D. D. (1997). Transpiration of a boreal pine forest measured by branch bag, sap flow and micrometeorological methods. *Tree Physiology*, *17*(8–9), 511–519.

Searle EB, Chen HYH (2017) Persistent and pervasive compositional shifts of western boreal forest plots in Canada. Global Change Biology 23: 857–866.

Schooling, J. T., & Carlyle-Moses, D. E. (2015). The influence of rainfall depth class and deciduous tree traits on stemflow production in an urban park. *Urban Ecosystems*, *18*(4), 1261–1284.

Siegert, C. M., & Levia, D. F. (2014). Seasonal and meteorological effects on differential stemflow funneling ratios for two deciduous tree species. *Journal of Hydrology*, *519*(PA), 446–454.

Sims, R.A., Kershaw, H.M., and G.M. Wickware. (1990). Autecology of major tree species in north central region of Ontario. Technical Report 48, Northwestern Ontario Forest Technology Development Unit, Ontario Ministry of Natural Resources, Thunder Bay, Ontario. 126 pp.

Smith, D. M., & Allen, S. J. (1996). Measurement of sap flow in plant stems. *Journal of Experimental Botany*, *47*(12), 1833–1844. https://doi.org/10.1093/jxb/47.12.1833

Snelgrove, J. R., Buttle, J. M., & Tetzlaff, D. (2019). Importance of rainfall partitioning in a northern mixed forest canopy for soil water isotopic signatures in ecohydrological studies. *Hydrological Processes*, *34*(2), 284–302. https://doi.org/10.1002/hyp.13584.

Staelens, J., Schrijver, A., Verheyen, K., & Verhoest, N. (2008). Rainfall partitioning into throughfall, stemflow, and interception within a single beech (Fagus sylvatica L.) canopy: influence of foliation, rain event characteristics, and meteorology. *Hydrological Processes*, *22*, 33–45. https://doi.org/10.1002/hyp.

Stefani, F., Isabel, N., Morency, M. J., Lamothe, M., Nadeau, S., Lachance, D., & Séguin, A. (2018). The impact of reconstructed soils following oil sands exploitation on aspen and its associated belowground microbiome. *Scientific Reports*, *8*(1), 2761.

Stevens-Rumann CS, Kemp KB, Higuera PE, Harvey BJ, Rother MT, Donato DC, et al. (2018) Evidence for declining forest resilience to wildfires under climate change. Ecology Letters 21:243–252.

Strilesky, S. L., Humphreys, E. R., & Carey, S. K. (2017). Forest water use in the initial stages of reclamation in the Athabasca Oil Sands Region. *Hydrological Processes*, *31*(15), 2781–2792.

Su, L., Xie, Z., Xu, W., & Zhao, C. (2019). Variability of throughfall quantity in a mixed evergreen-deciduous broadleaved forest in central China. *Journal of Hydrology and Hydromechanics*, *67*(3), 225–231. https://doi.org/10.2478/johh-2019-0008.

Sutton, O. F., & Price, J. S. (2019). Soil moisture dynamics modelling of a reclaimed upland in the early post-construction period. *Science of the Total Environment*, 134628.

Sutton, O. F., & Price, J. S. (2020). Modelling the hydrologic effects of vegetation growth on the long-term trajectory of a reclamation watershed. *Science of the Total Environment*, *734*, 139323.

Swaffer, B. A., Holland, K. L., Doody, T. M., & Hutson, J. (2014). Rainfall partitioning, tree form and measurement scale: A comparison of two co-occurring, morphologically distinct tree species in a semi-arid environment. *Ecohydrology*, *7*(5), 1331–1344.

Tremblay, P. Y., Thiffault, E., & Pinno, B. D. (2019). *Effects of land reclamation practices on the productivity of young trembling aspen and white spruce on a reclaimed oil sands mining site in northern Alberta*. *New Forests* (Vol. 50). Springer Netherlands.

Viereck, L. A., & Johnston, W. F., (1990). Picea mariana (Mill-) B.S.P. In Silvics of North America. Vol. 1. conifers. R.M. Burns and B.H. Honkala (Eds.). USDA Forest Service, Agriculture Handbook 654. pp. 227 -237.

Vitt, D. H., & Bhatti, J. (2012). The changing boreal forest: incorporating ecological theory into restoration planning. Restoration and Reclamation of Boreal Ecosystems: Attaining Sustainable Development (eds D.H. Vitt & J. Bhatti), pp. 3–12. Cambridge University Press, Cambridge, UK.

Wang, C., Fu, B., Zhang, L., & Xu, Z. (2019). Soil moisture–plant interactions: an ecohydrological review. *Journal of Soils and Sediments*, *19*(1), 1–9. https://doi.org/10.1007/s11368-018-2167-0.

Wang, H., Tetzlaff, D., Dick, J. J., & Soulsby, C. (2017). Assessing the environmental controls on Scots pine transpiration and the implications for water partitioning in a boreal headwater catchment. *Agricultural and Forest Meteorology*, *240–241*, 58–66.

Webb, E. K., Pearman, G. I., & Leuning, R. (1980). Correction of flux measurements for density effects due to heat and water vapour transfer. *Quarterly Journal of the Royal Meteorological Society*, *106*(447), 85–100.

Whitford, W., Anderson, J., & Rice, P. (1997). Stemflow contribution to the 'fertile island' effect in creosotebush, Larrea tridentata. *Journal of Arid Environments*, *35*, 451–457.

Wilson, K.B., Hanson, P.J., Mulholland, P.J., Baldocchi, D.D., & Wullschleger, S.D. (2001). A comparison of methods for determining forest evapotranspiration and its components: sap-flow, soil water budget, eddy covariance and catchment water balance. Journal of Agricultural Forest Meteorology, 106, P.153-168.

Wolken, J. M., Landhäusser, S. M., Lieffers, V. J., & Dyck, M. F. (2010). Differences in initial root development and soil conditions affect establishment of trembling aspen and balsam poplar seedlings. *Botany*, *88*(3), 275–285. https://doi.org/10.1139/B10-016.

Wu, S., (2015). Soil and vegetation properties on reclaimed oil sands in Alberta, Canada: a synthetic review. The faculty of Forestry. University of British Columbia.

Zhang, Y., Wang, X., Hu, R., Pan, Y., & Paradeloc, M. (2015). Rainfall partitioning into throughfall, stemflow and interception loss by two xerophytic shrubs within a rain-fed re-vegetated desert ecosystem, northwestern China. *JOURNAL OF HYDROLOGY*, *527*, 1084–1095.